USDOT Tier 1
University Transportation Center
on Improving Rail Transportation Infrastructure
Sustainability and Durability

Final Report UD-4

ANALYSIS OF WHEEL WEAR AND FORECASTING OF WHEEL LIFE FOR TRANSIT RAIL OPERATIONS

By

Kyle Ebersole, MCE
Graduate Research Assistant
Department of Civil Engineering, University of Delaware
ebersole@udel.edu

Allan Zarembski, PhD, PE, FASME, Hon. Mbr. AREMA
Professor and Director of Railroad Engineering and Safety Program
Department of Civil Engineering, University of Delaware
dramz@udel.edu

and

Joseph Palese, MCE, MBA
Senior Scientist
Department of Civil Engineering, University of Delaware
palesezt@udel.edu

March 27, 2019

Grant Number: 69A3551747132

DISCLAIMER

The contents of this report reflect the views of the authors, who are responsible for the facts and the accuracy of the information presented herein. This document is disseminated in the interest of information exchange. The report is funded, partially or entirely, by a grant from the U.S. Department of Transportation's University Transportation Centers Program. However, the U.S. Government assumes no liability for the contents or use thereof.

ABSTRACT

As transit vehicle wheels accrue mileage, they experience flange and tread wear based on the contact between the railhead and wheel-running surface. When wheels wear excessively, the likelihood of accidents and derailments increases. Thus, regular maintenance is performed on the wheels, until they require replacement. One common maintenance practice is truing; using a specially designed cutting machine to bring a wheel back to an acceptable profile. This process removes metal from the wheel and is often based on wheel flange thickness standards (and sometimes wheel flange angle). Wheel replacement is usually driven by rim thickness, which is continuously reduced by wear, as well as metal removal during truing. This research study used wheel wear data provided by the New York City Transit Authority (NYCTA) to analyze wheel wear trends and forecast wheel maintenance (truing based on flange thickness) and wheel life (replacement based on rim thickness). Using automatic wheel-scanning technology, NYCTA was able to collect wheel profile measurements for nearly 4,000 wheels in its fleet over a two year period, measured weekly. The resulting wheel measurement data was analyzed using advanced stochastic techniques to determine relationships for the changes in flange thickness over time for each wheel in the fleet. Flange thickness wear rate relationships for each wheel were then used to forecast the time it would take for a wheel to reach the flange thickness maintenance threshold as defined by NYCTA standards. Furthermore, a subpopulation of wheels that exhibited very high rates of wear were classified as “bad actors”, and identified for further investigation to understand the cause of accelerated wear. This allows for identification and addressing of causal factors that relate to accelerated wear, such as angle of attack and L/V ratio. NYCTA has recently started capturing such data that relates truck performance, which in turn, can be related to rate of wear.

TABLE OF CONTENTS

LIST OF FIGURES

LIST OF TABLES

EXECUTIVE SUMMARY

Over time, transit vehicle wheels begin to experience flange and tread wear based on the contact between the railhead and wheel-running surface. When wheels continue to wear excessively, the likelihood of accidents and derailments vastly increases. Thus, regular maintenance is performed on the wheels, until they require replacement. One common maintenance practice is truing; using a specially designed cutting machine to bring a wheel back to an acceptable profile. This process removes metal from the wheel and is often based on wheel flange thickness standards (and sometimes wheel flange angle). Wheel replacement is usually driven by rim thickness, which is continuously reduced by wear, as well as metal removal during truing.

This research effort utilized various data streams made available from a recent project carried out by the New York City Transit Authority (NYCTA). Wheel profile measurements, L/V measurements, and truck performance parameters were some of the more insightful data streams used. This research primarily used wheel profile measurements (obtained from the KLD Automatic WheelScan installed on NYCTA 7 Line) and NYCTA truing standards to analyze flange wear. Currently, NYCTA is truing primarily to maintain flange thickness. According to NYCTA standards, truing occurs when the flange thickness approaches an "8" on the AAR finger gauge, or 24.2 mm. A new or recently trued wheel will read "0" on the AAR finger gauge, corresponding to a flange thickness of 32.1 mm. The negative result of truing is that the rim thickness decreases. When a wheel is trued, the rim thickness decreases anywhere from 5 to 10 mm as a function of the truing process. Eventually, there comes a point where the rim thickness can no longer be decreased, and thus, a new wheel needs to be installed. According to NYCTA, the rim thickness is not allowed to drop below 22.2 mm. Therefore, there are a finite number of times a given wheel can be trued. These standards were used in order to analyze flange wear and predict future maintenance events.

Nonlinear regression techniques were used in order to predict the rate of flange wear for each wheel in the NYCTA 7 Line fleet. Upon investigation of the data, it was discovered that the wearing of wheels behaved in a nonlinear and exponential manner. Thus, exponential regression was used in order to obtain a flange thickness wear rate parameter for every wheel. Based on the behavior of the wheel wear data and the results of the analysis, an exponential fit appears to be an appropriate method for calculating the wear rate of these particular wheels at this time.

With a flange wear rate obtained for every wheel in the fleet, predictions could be made as to when the next maintenance event would occur. With the last recorded flange thickness measurement known for every wheel, a simple forecast could be made as to when the wheel will reach a flange thickness of 24.2 mm; the NYCTA maintenance limit. When forecasts were made for every wheel in the fleet, it was discovered that NYCTA may be truing their wheels too early. Rather than allowing the wheels to wear until the threshold, they are being trued before reaching their actual maintenance limit. This is a more conservative and safety-oriented approach. The operational and economic effects of altering these practices should be examined.

It was also discovered that within the overall population of wheels, there appears to be three different sub-populations based on their actual wear performance. There is a large group of wheels that are behaving as expected. Next, there is a slightly smaller group of wheels that are behaving better than expected. These subpopulations of wheels are exhibiting a very low rate of flange wear,

and as such, can be classified as “good actors”. Lastly, there is a small group of wheels that are behaving worse than expected. This subpopulation of wheels is exhibiting a very high rate of flange wear, and as such, can be classified as “bad actors”. It is of practical significance to be able to identify and understand these bad actor wheels, so that they may be more regularly inspected and maintained. Thus, a logistic regression model was developed in order to predict which wheels in the fleet will act as bad actors. The wheel’s wear rate, last flange thickness measurement, average L/V ratio, average angle of attack, average tracking position, and average speed were used to build such a model. The model correctly identified 83.1 % of the “bad acting” wheels and 93.3 % of the “good acting” wheels. Overall, the logistic regression model operated at an accuracy of 92.1 %.

Lastly, a relation between flange wear rate and L/V ratio was discovered. More specifically, such a relationship was found for those wheels with excessive wear rates. For those wheels with wear rates less than -0.007 $days^{-1}$, it was found that there are two distinct types of behavior. There are some wheels in the fleet whose high rate of flange wear is largely dependent on a high L/V ratio. On the other hand, there are other wheels in the fleet whose high rate of flange wear is largely independent of a high L/V ratio. Another unknown variable is likely controlling these excessive rates of wear.

In all, the results of this research effort can lead to opportunities for future work. For example, further analyses should be conducted in order to better understand those wheels with excessive wear rates. In addition, the developed logistic regression model can continue to be improved, and higher-order regression techniques could be implemented to solve for flange wear rate. However, this research effort was successful in proving that big data analysis techniques can be used in order to provide in-depth analyses of basic engineering data.

INTRODUCTION

Introduction to Wheel Wear

In the railroad industry, a railway's maintenance and safety standards often govern the manner in which the line operates. In other words, engineering decisions are made to ensure that maintenance and safety standards are upheld. This is especially true when dealing with transit rail operations; if maintenance and safety standards are not followed, human lives are put at risk. One area that is of particular interest to transit rail operations is wheel wear. As transit vehicle wheels accrue mileage, they experience wear based on the contact between the railhead and wheel-running surfaces. If this wear is not properly monitored, these wheels can begin to wear excessively over time. This greatly increases the likelihood of accidents and derailments, as the wheel profile no longer conforms with the railhead profile. This presents a danger as thin flanges, hollowed treads, and excessive flange angles can lead to fracture and cause wheel climb. Therefore, it is crucial that wheel wear is monitored to ensure that maintenance and safety limits are not exceeded.

Introduction to the Project

A recent project undertaken by New York City Transit Authority's (NYCTA) titled "Integrated Wheel/Rail Characterization and Safety" was funded under the auspices of the Federal Transit Administration and US Department of Transportation. The goal of this study was to implement a comprehensive wheel, track, and truck measurement and analytics system. More specifically, the NYCTA aimed to enhance operational safety and system resiliency, reduce energy usage, planned capital costs, and cost of asset ownership, and improve overall passenger experience and customer service. As part of the work, several automated inspection systems were installed on the NYCTA 7 Line, and multiple levels of data analytics implemented. As a result of this project, a large amount of wheel condition and maintenance data were collected that leant itself to a detailed stochastic analysis of wheel condition, degradation, and maintenance performance. The focus of this research is a comprehensive analysis of the rate of wear of the NYCTA transit vehicle wheels, and assessment of current maintenance performance. Wheel tread and flange measurements (conducted approximately weekly), collected as part of this activity by the recently installed KLD Automatic WheelScan system, were made available together with NYCTA furnished information about the truing maintenance and replacement of the wheels. This allowed for the rate of wheel wear to be thoroughly analyzed and assessed.

As previously mentioned, due to the continuous nature of transit rail operations, wheels will begin to wear excessively over time. Thus, regular maintenance is performed on the wheels, until they require replacement. One of the most common maintenance practices used to address wheel wear, particularly wheel flange wear as most commonly experienced by NYCT, is truing. Thus, this analysis looked at current NYCTA standards for wheel wear, to include when the wheel is to be trued and when it is to be replaced. Truing is the act of bringing a wheel back to an acceptable wheel profile as defined by standards. This is done through the use of specially designed cutting machines known as wheel truing machines, which cut and reshape up to four wheels (one truck) at a time. Currently, NYCTA is truing primarily to maintain flange thickness. According to NYCTA standards, truing occurs when the flange thickness approaches an "8" on the AAR finger gauge, or 24.2 mm. A new or recently trued wheel will read "0" on the AAR finger gauge,

corresponding to a flange thickness of 32.1 mm. Wheel tread defects and flats are milled away as necessary, depending on the defect. Therefore, the "cut depth" of each truing cycle varies. The negative result of truing is that the rim thickness decreases. When a wheel is trued, the rim thickness decreases anywhere from 5 to 10 mm as a function of the truing process. Eventually, there comes a point where the rim thickness can no longer be decreased, and thus, a new wheel needs to be installed. According to NYCTA, the rim thickness is not allowed to drop below 22.2 mm. Therefore, there are a finite number of times a given wheel can be trued.

Introduction to the Research Objectives

The overall objective of this study was to analyze the wear patterns of transit vehicle wheels in order to better understand their behavior and life cycle. This was done by analyzing the wear rates of the NYCTA transit vehicle wheels, project that rate of wear to calculate a remaining wheel life, and identify wheels that have excessively high rates of wheel wear. It should be noted that NYCTA wheel wear is predominantly flange wear and as such, flange wear is the primary analysis parameter used here. The analysis used wheel flange data as measured by the KLD Automatic WheelScan system to calculate the wear rate of each wheel on every vehicle in the fleet. The calculation of these wear rates allows for a projection to when the next maintenance event will occur. In other words, it is possible to forecast the time until a given wheel will have a flange thickness of 24.2 mm, the NYCTA maintenance limit. Ultimately, these forecasts allow for an assessment of the performance of NYCTA's vehicle fleet from a wheel wear perspective, and can be used to optimize current maintenance practices. In addition, advanced statistical techniques such as logistic regression were used in order to identify and predict which wheels in the fleet will perform poorly in terms of projected life. Such wheels can be classified as "bad actors", and are important to identify so that they may be more regularly inspected, maintained, and replaced. Lastly, an initial exploratory data analysis (EDA) was performed in order to provide a preliminary assessment of the data and identify potential relationships within the dataset.

BACKGROUND

Railroad Wheels

There are many components required for effective and safe railroad operations. and. The track, ties, and ballast must be able to support and distribute the heavy loads exerted by cars. The signal systems must be operational, and the employees must be qualified and able to operate the trains. However, one of the most important components used in the railroad industry is the wheel. Over time, the rail wheel has changed little in size or shape, but has been upgraded in order to meet the demands of today's railway operations. Improvements made to the wheel have allowed for increased safety, reduced maintenance, increased mileage, higher travel speeds, and greater tonnage capacity. Yet, despite all of these advancements, the wheel still serves the same three core functions. First, the wheel must be able to support the car on the track and allow it to move. Second, the wheel must be able to effectively guide and control the motion of the car to follow the rails. Last, the wheel must be able to act as a braking surface for which the brake shoes act upon (Railway Education Bureau, 2015). Figure 1 presents a cutaway of a standard wheel.

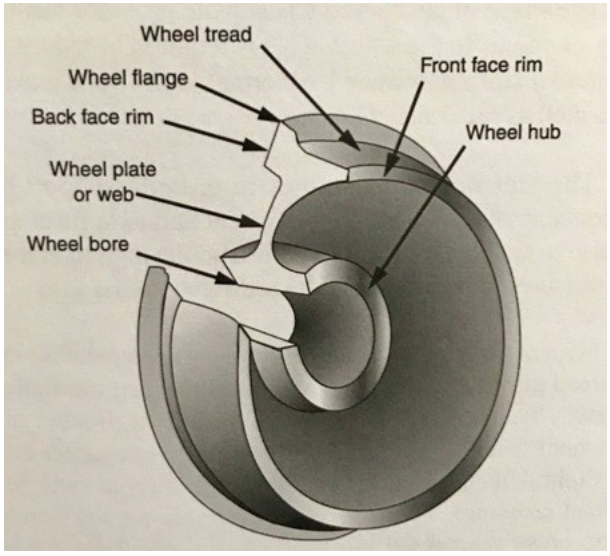

Figure 1 Standard railroad wheel (railway education bureau, 2015).

If a railroad wheel fails to meet one of the three aforementioned core functions, safety is greatly compromised. Each and every train is dependent upon the integrity of each individual wheel within that train. Traveling on wheels with defects or wheels that have been excessively worn greatly increases the likelihood of serious accidents and derailments; which in turn cause economic losses, injuries, and deaths. All operating railroads place great emphasis on wheel durability under heavy load conditions and high wear resistance. In addition, railroads implement a vast network of wheel inspection, maintenance, and replacement standards, to ensure that safety and efficiency can be maximized. Wheels that are excessively worn or defective must be identified and removed from service in order to maintain safety (Railway Education Bureau, 2015). Therefore, in order to best maintain wheels and maximize safety, the fundamentals of wheel wear need to be understood.

Wheel Wear

One of the most fundamental issues facing the rail industry today is wheel wear. Wheels wear as a result of friction between the wheel and rail during operation. Moreover, wheels wear as a function of the contact forces and creep forces associated with the longitudinal and lateral motion of the wheelset. As a consequence, wheels tend to wear in two distinct locations: the flange and the tread. The rate of wear at these two locations depends on vehicle design, wheel service profile, track profile, the status of the contacting surfaces, and the inherent properties of the wheel and rail. (Braghin, et al., 2009). As wear increases over time, the wheel profile changes depending on the severity of the load environment. These changes in wheel profile greatly impact the dynamic characteristics of railway vehicles. For example, the stability of vehicles with worn wheels is greatly compromised as the wheel profile and rail head profile no longer conform with one another. This situation can lead to increased dynamic loads and excessive wear, which can result in accidents and derailments. In addition, in the passenger rail realm, increased vibration and noise levels can be attributed to worn wheels, which ultimately decrease passenger comfort (Braghin, et al., 2009). The difference between in a new wheel and a worn wheel is shown in Figure 2.

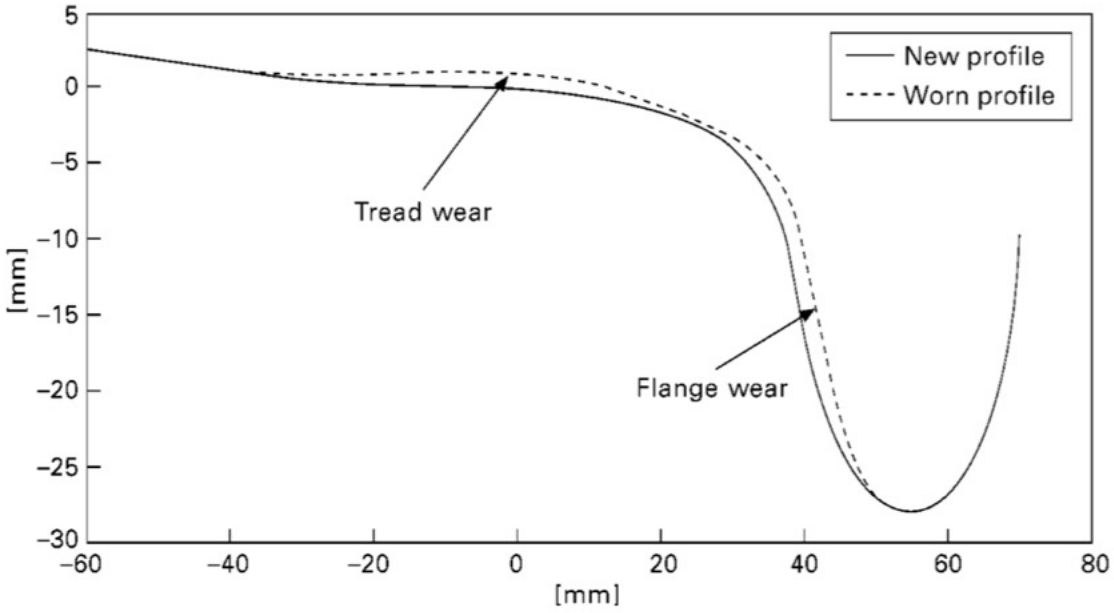

Figure 2 New wheel profile vs worn wheel profile (Braghin, et al., 2009).

Nonetheless, when wheels wear, the flange becomes thinner and the tread becomes hollower. In particular, a worn or thin flange is extremely dangerous, as it can result in total flange fracture. A worn flange also results in an excessive flange angle, which promotes wheel climb. Figure 3 presents the breakdown of train accidents classified by wheel defect type. As can be seen, worn or thin flanges is the most frequent wheel defect that causes accidents (IHHA, 2001). Thus, it is crucial that the wearing behavior and patterns for wheel flanges are better analyzed and understood, in hopes of reducing the accidents associated with them.

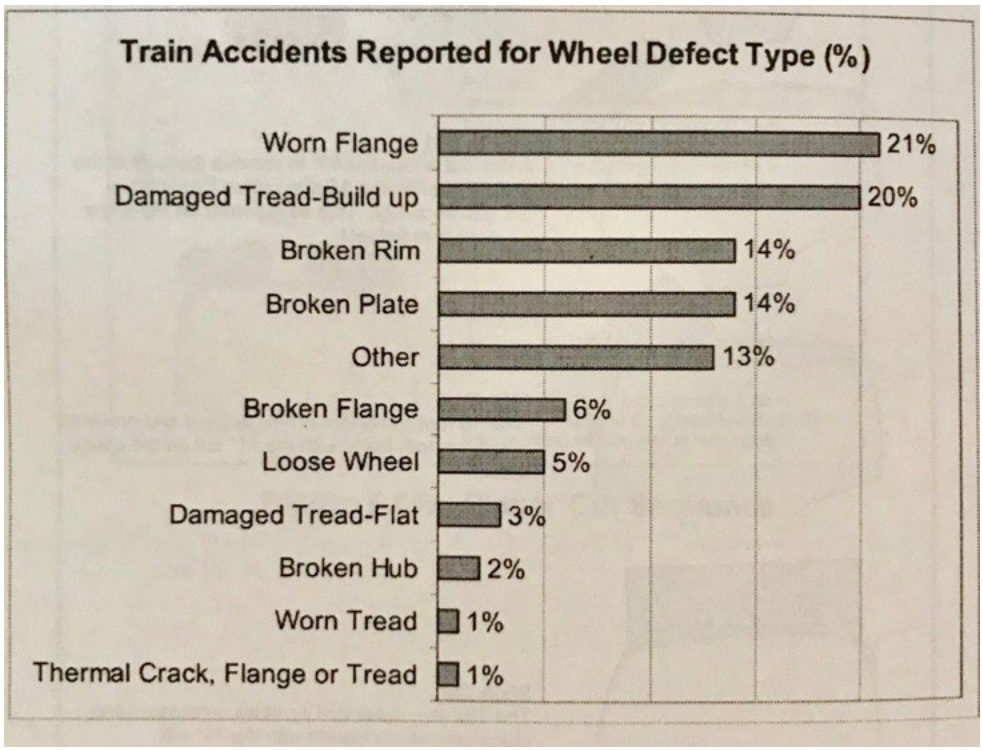

Figure 3 Breakdown of total train accidents classified by wheel defect type (IHHA 2001).

Essentially, the life cycle of a railway wheel is governed by wheel wear (Braghin, et al., 2006). Wheel life can be extended through the use of truing; a maintenance practice that reshapes a worn wheel to its original profile. This is a common practice that most railroads use in order to combat the aforementioned issue of worn or thin flanges. However, constant reshaping and reprofiling can negatively impact the physical characteristics and metallurgical properties of the wheel itself (Pradhan, et al., 2018). Therefore, it is of great practical significance to be able to analyze and predict wheel profile degradation due to wear. Doing so would allow decisions to be made as to when wheels should be maintained (e.g. by truing), when wheels should be replaced, and how maintenance practices could be altered to limit the effects of worn wheels. By optimizing the wheel and rail profiles with respect to wear, the dynamics between the wheel and rail can be better controlled (Braghin, et al., 2006). A great deal of work has been done in the field of predicting wheel wear, and a few examples will be discussed in the coming sections.

However, creating a model to predict wheel wear is not a trivial feat. The load environment that occurs at the interface between the rail head and the wheel running surface is quite complex. The wheel's running surface is constantly exposed to high normal and tangential contact forces and stresses. As stated earlier, wheels wear as a function of the contact forces and creep forces associated with the longitudinal and lateral motion of the wheelset. The creep forces are mainly caused by friction during braking and acceleration, truck hunting, track defects, temperature changes, and the load implications of traveling through sharp curves (Pradhan, et al., 2018). The contact forces between the wheel and the rail are constantly changing, as the point of contact can

move. The magnitude and orientation of these contact forces vary as the wheels travel through curves, crossing, and track surface defects. As wheels travel down the track, the contact patch moves along the wheel tread, and in some cases can extend to the flange. There may also be a small amount of localized slipping that occurs at the interface between the wheel surface and the rail head. The amount of slipping depends on the geometry of the contact patch, the coefficient of friction between the wheel and rail, and the exerted normal and lateral forces (Braghin, et al. 2006). A flowchart describing the wheel wear process in shown in Figure 4. In addition, Figure 5 shows a schematic representation of the contact patch between the wheel and the rail.

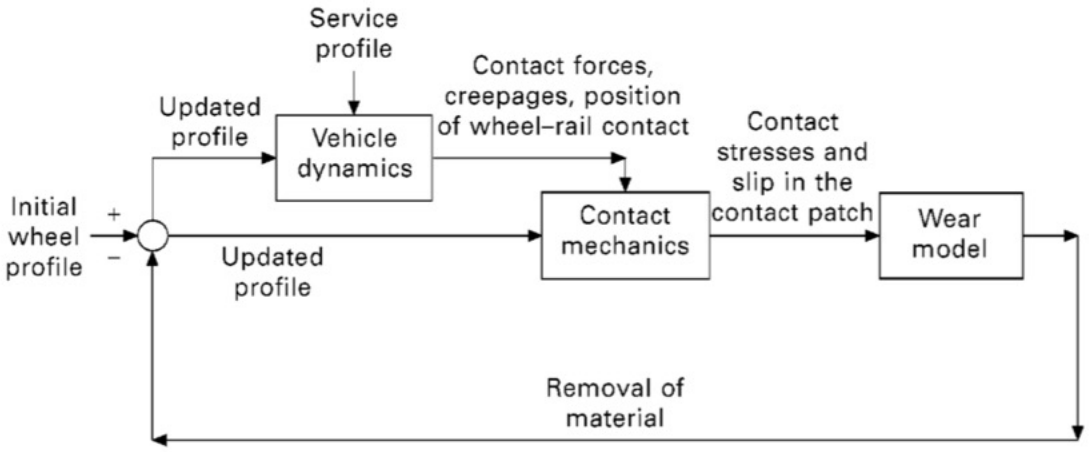

Figure 4 Wheel Wear Flowchart (Braghin, et al., 2009).

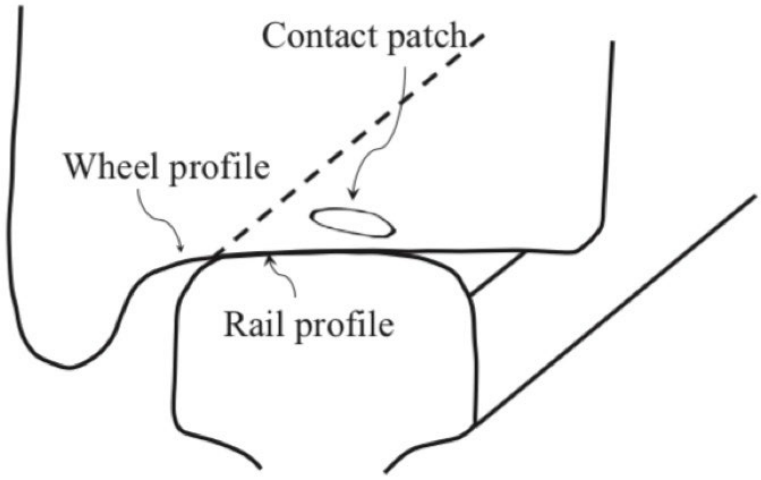

Figure 5 Wheel/Rail contact interface (Ayasse and Chollet, 2006).

The flowchart presented in Figure 4 provides a general idea as to how wheels wear over time. It begins with an initial wheel profile, and considers how vehicle dynamics cause dynamic variations of wheel loads. Next, the effects of the various creepage and frictional forces, as well as the

migration and slipping of the contact patch, are considered. This information gives way to the determination of the shape, location, and size of the contact patch, as well as the distribution of the normal and tangential stresses within that patch. Finally, the normal and tangential stresses cause metal to be worn away in the tread and flange, and ultimately cause the aforementioned modification of wheel profile and causes maintenance process to form a natural loop. Unfortunately, the components that make up the loop are non-linear. This makes it difficult to predict how the process will evolve with time, and how the change of a single parameter, such as initial wheel profile, will impact the progression of wear (Braghin, et al., 2009).

Wheel/Rail Contact

As discussed, rail wheel wear is a function of the contact stresses and slippage between the wheel and rail surfaces. However, studying the mechanics of wheel/rail contact is quite complex. The interface at which the wheel and rail come in contact with one another can be thought of as a small horizontal patch. At this patch, there is a great deal of concentrated stress due to the contact between the two bodies. The center of this patch is also the point at which the tangential forces are applied. In order to understand the dynamic behavior of a wheelset, and better understand how wear is affected, these forces must be known (Ayasse and Chollet, 2006). There are two primary means in which this can be accomplished: the "normal problem" and the "tangential problem". When looking at the normal problem, the contact patch and stress distributions are obtained as a function of both the geometry of the wheel and rail profiles and the resulting normal force reactions. When looking at the tangential problem, contact stresses and slippage are defined as a function of the normal pressures, the resulting frictional forces, and the creepage forces (Braghin et al., 2009).

The primary means as to which the normal problem of wheel/rail contact is defined is through Hertzian contact theory. In 1882, German physicist Heinrich Hertz was able to demonstrate the various pressures, stresses, and deformations that occur when two or more curved elastic bodies contact each other (Oldknow, 2017). Hertz assumed that when two elastic bodies are pressed together, there would be elastic behavior, a large curvature radius compared to the contact patch size, and constant curvatures inside the contact patch. If all of these assumptions held true, then it can be stated that when two elastic bodies are pressed together, the resulting contact patch will be a flat ellipse. Furthermore, the resulting contact pressures will be parabolic. The geometry of the contact patch and the maximum value of the contact pressure depend on the curvature of and the normal force reaction between the wheel and rail surfaces. Also, they are typically expressed by analytical formulas that are based on elliptic integrals. This is one of the main reasons why Hertzian contact theory is the most computationally efficient solution to the normal problem (Braghin et al., 2009). Hertzian contact theory in the general and railroad-specific cases can be seen in Figure 6 (Ayasse and Chollet, 2006). A visual representation of the parabolic distribution of contact pressures can be seen in Figure 7 (Braghin, et al., 2009).

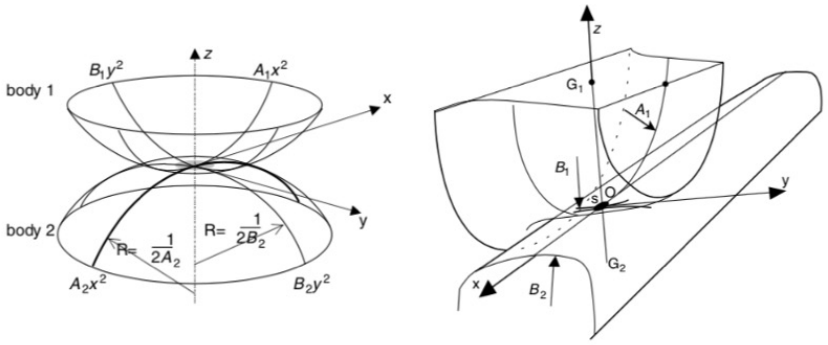

Figure 6 General (left) and railroad-specific (right) Hertzian contact (Ayasse and Chollet, 2006).

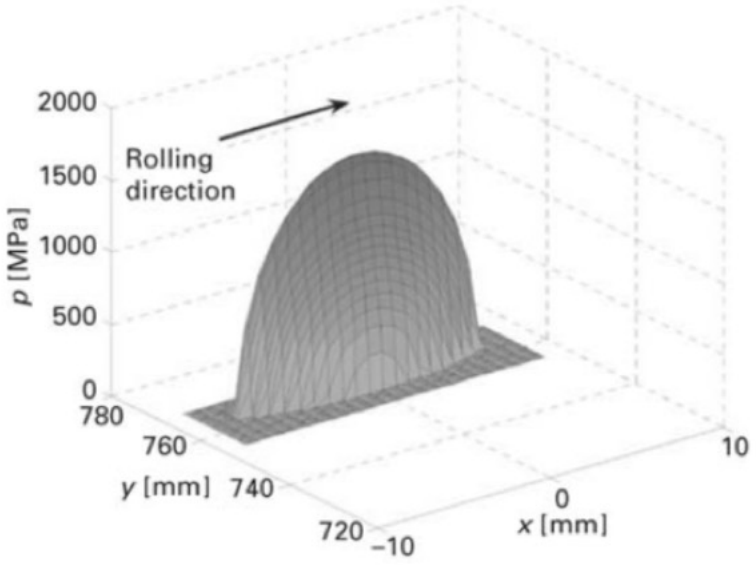

Figure 7 Parabolic contact pressure distribution according to Hertzian contact theory (Braghin et al., 2009).

However, the assumption of constant curvature inside the contact patch does not hold true when considering the contact of worn wheels and rails. Wear tends to modify the profile of wheels and rails, causing them to be nonconformal. In this case, the Hertzian contact theory is not appropriate, and more complex techniques are needed to solve the normal problem. The most accurate way of doing this was presented by Kalker in 1990. He makes use of the initial assumptions made by Hertz, but adds that the two contacting surfaces have a transversal profile curvature that is constant in the longitudinal direction. This is acceptable in the rail world, since the longitudinal curvature of the wheel is constant and the rail surface has no curvature in the longitudinal direction. When the wheel and rail come in contact, the normal pressure at the interface is computed as a function of the elastic displacements of the two bodies. Thus, the contact patch geometry and the normal pressure magnitude can be approximated. Kalker's approach is more attractive when considering

the contact of worn wheels and rails. It allows for the repeated calculation of contact conditions, simulating the modification of the wheel profile over time (Braghin et al., 2009).

Kalker's work also gave way to the primary means as to which the tangential problem of wheel/rail contact is defined. Essentially, the tangential problem deals with determining the tractions and the slippages that occur within the contact patch. Kalker divided the contact patch into longitudinal regions. For each region, constant deformation is assumed and calculated based on the resulting normal force reactions and creep forces. The tangential contact stresses can then be calculated along each region of the contact patch, assuming stress is proportional to the deformation. This process was originally used for Hertzian contact applications, where tables of friction and flexibility coefficients can be chosen to match the real-world behavior of the wheel and rail (Braghin et al., 2009).

METHODOLOGY

Instrumentation

As previously mentioned, the overarching goal of the NYCTA's Integrated Wheel/Rail Characterization and Safety project was to prove that it is both technically feasible and cost effective to implement and operate an advanced and automated data collection, measurement, and analytics system. These analytics could then be used to foster the decision-making process that is associated with wheel, track, and equipment maintenance. Thus, a number of advanced instrumentation and measurement systems were installed and used throughout this project. To narrow their scope, NYCTA chose the 7 Line as its study line. The 7 Line is one of the longest and most heavily traveled lines in New York City, as it runs from Times Square to Queens. A map of the 7 Line can be seen in Figure 8 NYCTA 7 Line Map. Systems installed on the 7 Line include the KLD Automatic WheelScan, NRC-C Instrumented Wheelsets (IWS), WID TBOGI, ISI L/V measurement system, Data Collection Consist (DCC), NYCTA Track Geometry Car (TGC), and Automated Equipment Identification (AEI). Each of these systems collects specific data types and has significant applications to maintenance and analysis. Thus, the wayside (track) mounted measurement systems, such as the WheelScan, TBOGI, and L/V systems collected data on each wheel and/or axle that passed over it. Conversely, the vehicle mounted measurement systems, such as the DCC, IWS, and TGC collected data on the track and the interaction of the specific vehicle with the track. Finally, the AEI system allowed for the ready identification of individual cars for analysis and correlation of results. This information is summarized in Table 1. However, for the scope of this thesis, the data provided by the Automatic WheelScan, TBOGI, and L/V Measurement System were primarily used.

Figure 8 NYCTA 7 Line map (NYCTA).

Table 1 Data Sources

Source	Data Acquired	Instrumentation Used
NYCTA	Track geometry	Track Geometry Car
KLD Labs	Wheel profile measurements	Automatic WheelScan
NRC - C	Dynamic forces	Instrumented Wheelset
Dayton T. Brown	Acceleration, noise, vibration, energy	Data Collection Consist
Plasser American	RFID tags, contact analytics	Data Collection Consist
WID	Angle of attack	T-BOGI
ISI	L/V ratio	L/V Measurement System

KLD Automatic WheelScan

One of the key new wayside instrumentation packages installed for this project was the Automatic WheelScan, provided by KLD Labs at the NYCTA car wash at Corona Yard, Queens, NY. The WheelScan is designed to monitor wheel profile and record digitized wheel condition data for each wheel that passes over it. For every wheel in the NYCTA 7 Line Fleet, the flange thickness, flange angle, flange height, rim thickness, wheel diameter, back of flange reading, and back to back gauge are measured. This, in turn, allows for accurate and timely monitoring of wheel profile conditions, based on NYCTA standards for wheel safety, maintenance, and replacement. In addition, this data allows for calculation of wheel wear rates and forecasting of projected wheel lives. This in turn allows for a more in-depth understanding and evaluation of current wheel maintenance procedures. The KLD Automatic WheelScan is shown in Figure 9.

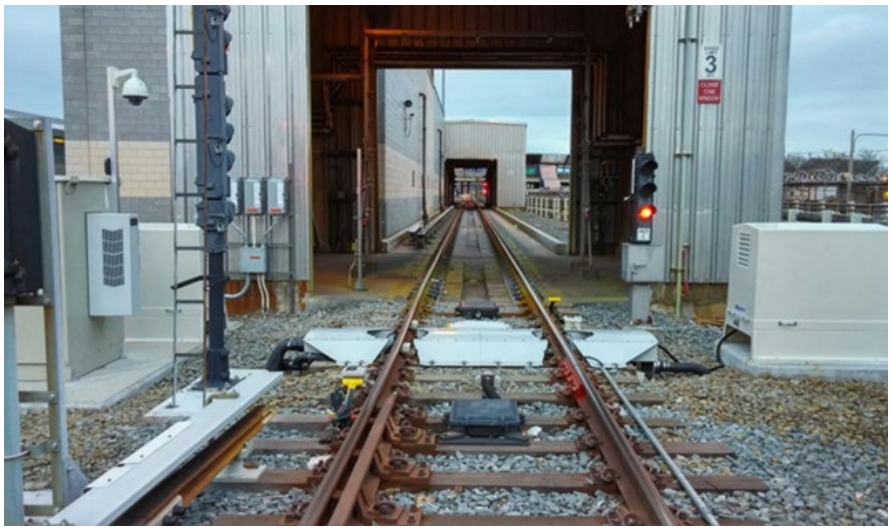

Figure 9 KLD automatic WheelScan located at the Corona Yard Car Wash (NYCTA).

ISI L/V Measurement System

Another newly installed wayside system was the L/V Measurement System, as provided by ISI. This wayside device was also located in a 3.2-degree left-hand curve just north of 103rd Street station, approximately 300 feet away from the TBOGI. As the name implies, this system measured

lateral and vertical wheel/rail forces and calculated associated L/V ratios for every vehicle that passed over it, which included the entire 7 Line fleet. Excessively high L/V ratios are a cause for concern, as wheel climb derailments could occur. Thus, using the L/V system allows for better monitoring of wheel and rail performance, and identifies specific axles or bogies that may be at risk of derailment. In addition, the system allows for better monitoring of truck performance, and how it is affected by track maintenance activities like re-profiling, grinding, and lubrication. The ISI L/V Measurement System is shown in Figure 10.

Figure 10 ISI L/V measurement system located north of 103rd street station (NYCTA).

WID TBOGI

A companion wayside measurement system, also installed as part of this project was the TBOGI, as provided by WID, and located at the exit of a 3.2-degree curve just north of 103rd Street station. This wayside device was designed to measure key truck (bogie) characteristics and performance. Thus, for every truck that passes over the TBOGI, a set of key truck performance parameters are measured or calculated; most notably angle of attack and tracking position, but also inter-axle misalignment, rotation, shift, and tracking error. These parameters are used to help to identify bad acting trucks, to include any truck with curving performance issues, such as skewed axles, misaligned axles, or improper tracking. If left unattended, these issues can result in unsafe lateral load or L/V levels, as well as accelerated wheel and rail wear. In addition, these measurements can help characterize the wheel/rail interface, wheel and rail wear rates, and rolling resistance. The WID TBOGI is shown in Figure 11.

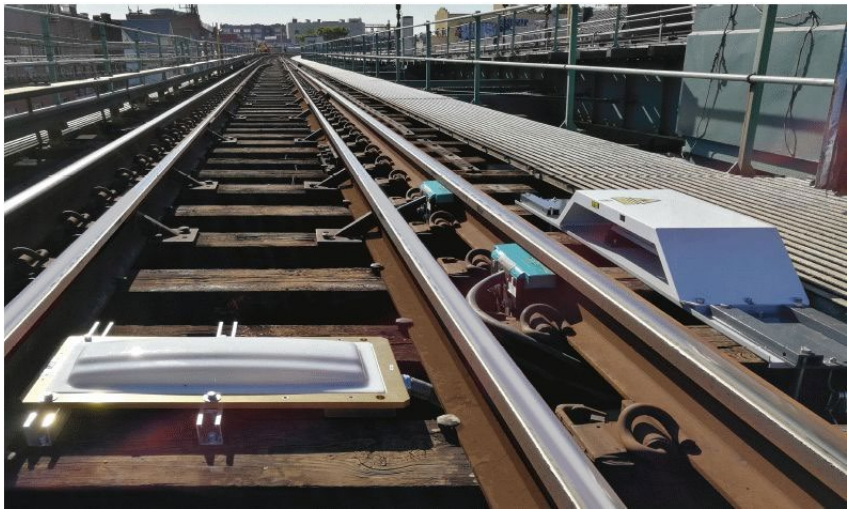

Figure 11 WID TBOGI site located north of 103rd Street station (NYCTA).

Explanation of the Dataset

The NYCTA 7 Line fleet consisted of nearly 500 cars and 4,000 wheels, each of which was measured each time it passed the WheelScan. This resulted in each wheel being measured at least once a week. Furthermore, thanks to AEI, each car was equipped with an RFID tag, so individual wheels and their associated wear data could be identified. The data that was used for this research spanned from June 1, 2017 to April 30, 2018. In all, there were over 140,000 data points recorded by the WheelScan, where one point is a complete set of wheel profile measurements.

The TBOGI and L/V Measurement System produced a much greater amount of data. As these systems are installed in track, data is recorded every time a wheel passes them. Thus, thousands of data points were made available each day. Unfortunately, these systems were not operational until January 19, 2018. Therefore, the data that was used for this research spanned from January 19, 2018 to February 19, 2018. In all, there were over 1,000,000 total data points recorded by the L/V Measurement System and 250,000 recorded by the TBOGI. Note that the difference in data volume is due to the fact that the L/V Measurement System measures every wheel, while the TBOGI measures every truck.

In order to utilize the data that was made available by the aforementioned instrumentation systems, a working database needed to be created. Microsoft Access was used to organize and store the large amount of data. Code was written in VBA that allowed for data files to be easily read, formatted, and imported into the Microsoft Access database. Upon completion of the database, the data was able to be used for further analyses.

Exploratory Data Analysis

As is with most research efforts, the first step of this study was to understand the data that was provided and its general stochastic parameters. Therefore, an Exploratory Data Analysis (EDA) was conducted. EDA is a standard data analytics approach that is used to provide a preliminary assessment of the data and identify any potential relationships within the dataset (Attoh-Okine,

2017). Typical techniques used in EDA include creating histograms, scatterplots, and box and whisker plots of the data, as well as generating descriptive statistics. Various aspects of EDA were implemented in order to understand the WheelScan, L/V Measurement System, and TBOGI data.

Exploratory Data Analysis of the WheelScan Data

The data provided from the WheelScan was the initial focus of this thesis. As mentioned, the WheelScan is designed to monitor wheel profile and record wheel profile data for each wheel that passes over it. For every wheel in the fleet, the flange thickness, flange angle, flange height, rim thickness, wheel diameter, back of flange reading, and back to back gauge are measured. Furthermore, it is known that NYCTA maintains wheels based on flange thickness. Yet, other parameters recorded by the WheelScan, such as rim thickness, flange height, and flange angle are used for maintenance and replacement decisions. Therefore, these four parameters were deemed to be the most important when conducting a wheel wear analysis, and as such, were investigated with various EDA techniques. Figure 12 defines these various wheel profile measurements.

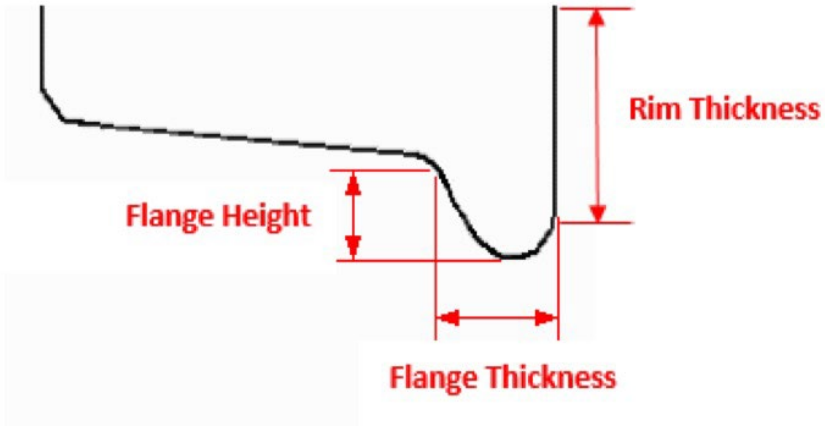

Figure 12 Wheel profile measurements.

The initial EDA included but was not limited to summaries of descriptive statistics, histograms, and box-and-whisker plots. Of particular interest were the histograms of flange thickness, flange height, flange angle, and rim thickness shown in Figure 13. The x-axis displays the measurement of each parameter; rim thickness, flange thickness, and flange height are measured in millimeters, while flange angle is measured in degrees. The y-axis displays the frequency of the observations. The blue lines on these plots represent the value of a new or recently trued wheel. Values beyond these lines can be attributed to measurement errors or errors in fabrication or maintenance. The red lines on these plots represent the maintenance limits set forth by the NYCTA. It is important to note that the rim thickness maintenance limit is 22.2 mm, but no wheel in the fleet has yet to reach a rim thickness that low. Wheels are typically replaced before this point is reached. Lastly, NYCTA has not reported a maintenance limit for flange height.

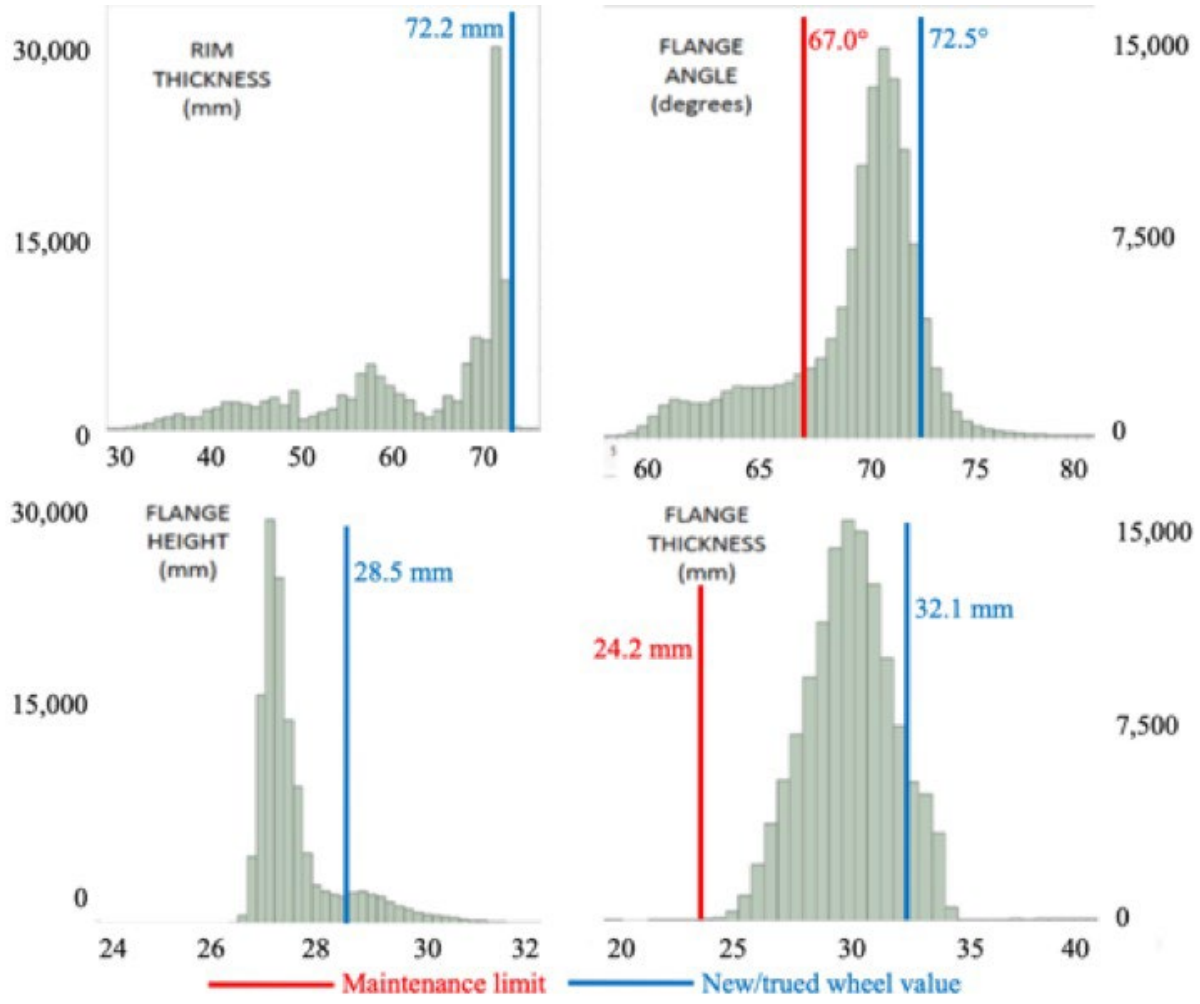

Figure 13 Histograms of wheel profile measurements.

Various observations can be made from the distributions above. First of all, the distributions of flange angle, flange height, and flange thickness all appear to be generally normal. Flange angle and flange height are slightly skewed, but not drastically. These distributions allow for the conclusion to be made that wheels were regularly maintained. Had the distributions been more spread out, such a conclusion may not have been supported. More specifically, the histogram of rim thickness was particularly insightful, as shown in Figure 14, which shows three distinct distributions. At any point in time, a wheel can fall into one of three groups, based upon its rim thickness. This can be attributed to maintenance practices. Recall that every time a wheel is trued, its rim thickness is decreased in order to restore an acceptable profile. Thus, it appears that there is a large population of new wheels that have not yet been trued, along with two smaller populations of wheels which have been trued once or twice.

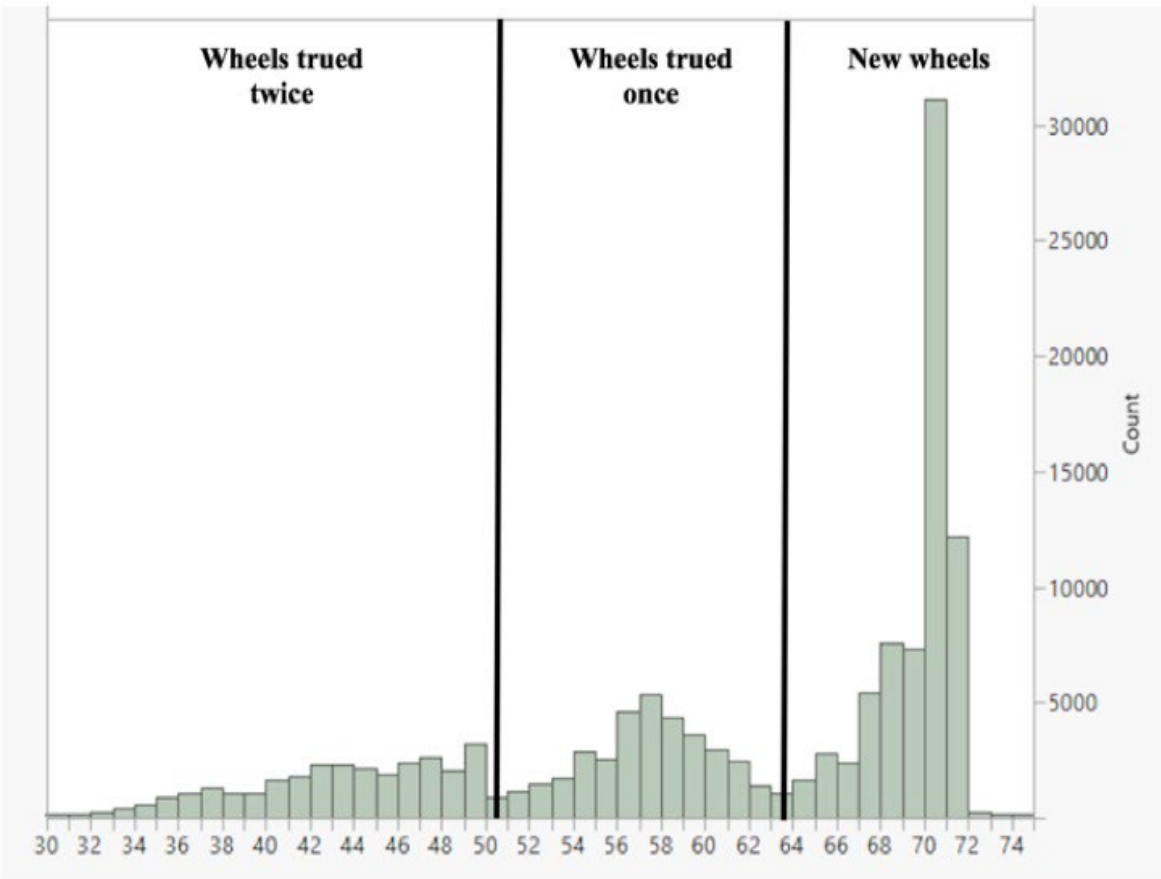

Figure 14 Histogram of rim thickness (mm) depicting truing cycles.

While the previous figure indicates that wheels are being trued at regular intervals, further investigation was conducted to verify this observation. In order to do this, plots of wheel measurements against time were generated, including flange thickness, rim thickness, and flange height. When truing occurs, a sudden drop in rim thickness is observed, accompanied by an increase in flange thickness. Moreover, the value of flange height stays relatively constant. Figure 15 is an example of one of these plots, for the left wheel on the first axle of car 7228.

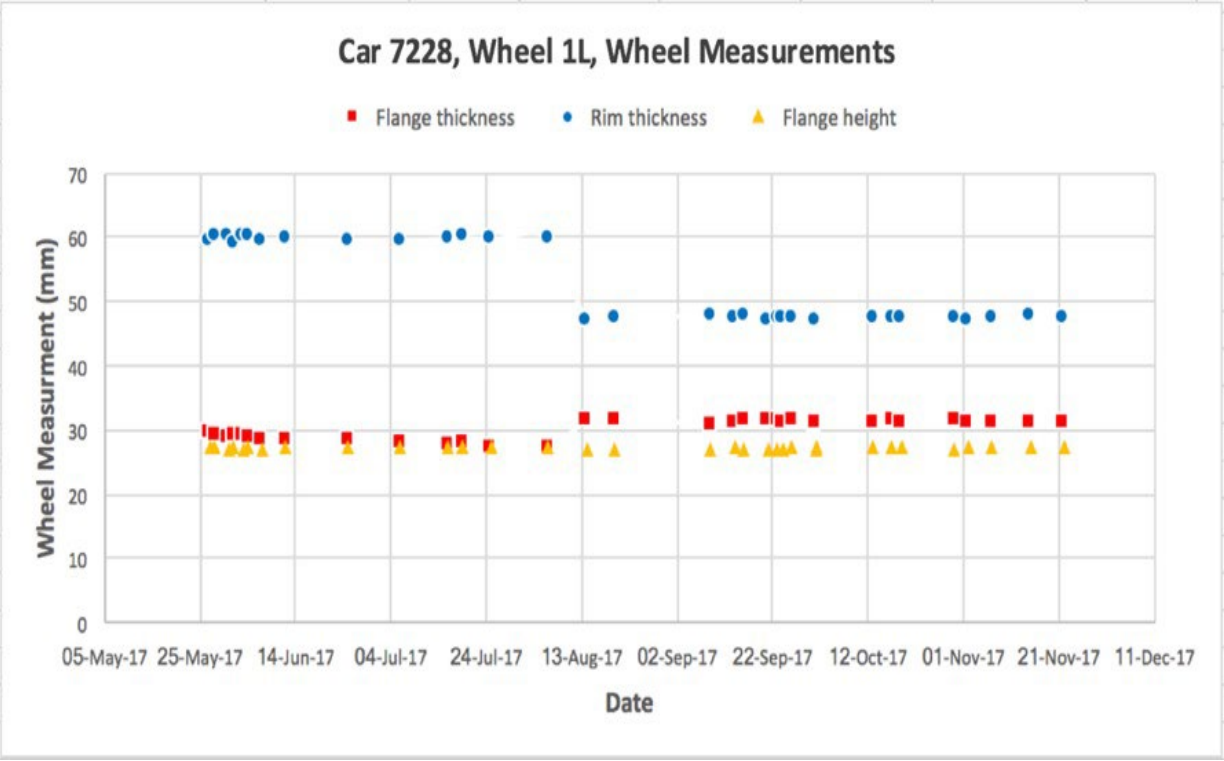

Figure 15 Plot of wheel measurements for Car 7228, Axle 1, left wheel.

From the above figure, it is clear that truing occurred between July 24, 2017 and August 13, 2017. At this point, there is an approximate 12 mm drop in rim thickness accompanied by a slight increase in flange thickness. However, it is important to note that the flange thickness measurement was not at the 24.2 mm threshold at the time of truing. Rather, the flange thickness was approximately 28 mm at the time of truing. This is due to NYCTA's maintenance practices. NYCTA practice is to true the entire truck when the flange thickness of one wheel on the truck approaches the 24.2 mm limit. Therefore, on Car 7228, this wheel did not trigger the truing decision for this truck. On car 7228, wheel 2L (Axle 2, left wheel) reached a flange thickness value of 25.56 mm, which prompted the entire truck to be trued. Thus, it appears that there may be wheels that are being trued too early. This idea will be further evaluated in the coming chapters.

Similar wheel wear plots were created for a number of the most frequently measured cars. The behavior shown in Figure 15 was consistently observed, indicating truing was regularly occurring. Since the truing process is primarily governed by the flange thickness measurement, the flange thickness wear rate is of great interest. If the flange thickness wear rate is known, then it can be used in order to predict when the next maintenance event will occur.

Exploratory Data Analysis of the L/V Measurement System Data

It was decided that in addition to the WheelScan data, L/V data would be used in order to form conclusions about the wearing of the wheels on the 7 Line. The higher the L/V ratio on a given wheel, the higher the lateral force will be, and thus the more that wheel will be expected to wear.

As discussed, ISI has instrumented a portion of the NYCT Flushing line to measure the L/V ratio on every passing wheel. Each wheel can be identified to a single car thanks to RFID tags. The device has been installed on a 3.2 degree curve, with a positive L/V value indicating a gage spreading force. Furthermore, due to issues associated with matching the data from L/V Measurement System to the car RFID tags, usable data was not available until January 2018. However, the measurement system recorded every single wheel that passed over it in a given day. Thus, each day anywhere from 30,000 to 40,000 new data points were obtained. At the time of analysis, there are over 1,000,000 data points in the L/V ratio database. Figures 16 and 17 present a histogram and cumulative distribution plot of all recorded L/V ratios.

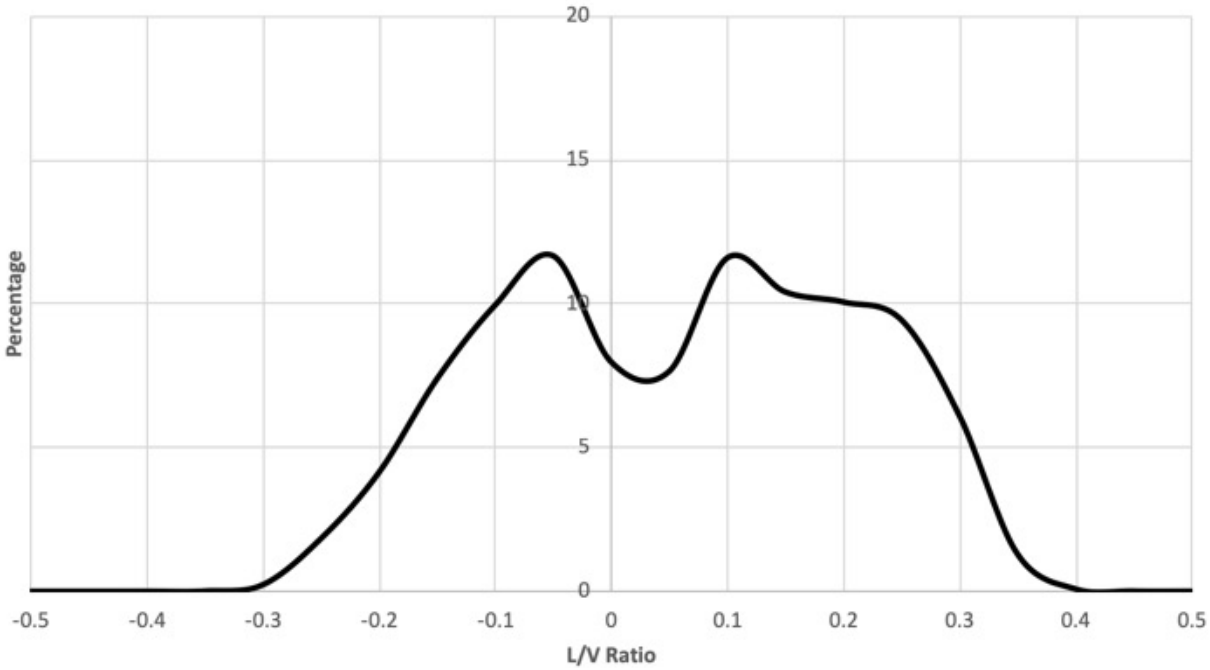

Figure 16 Histogram of L/V ratio.

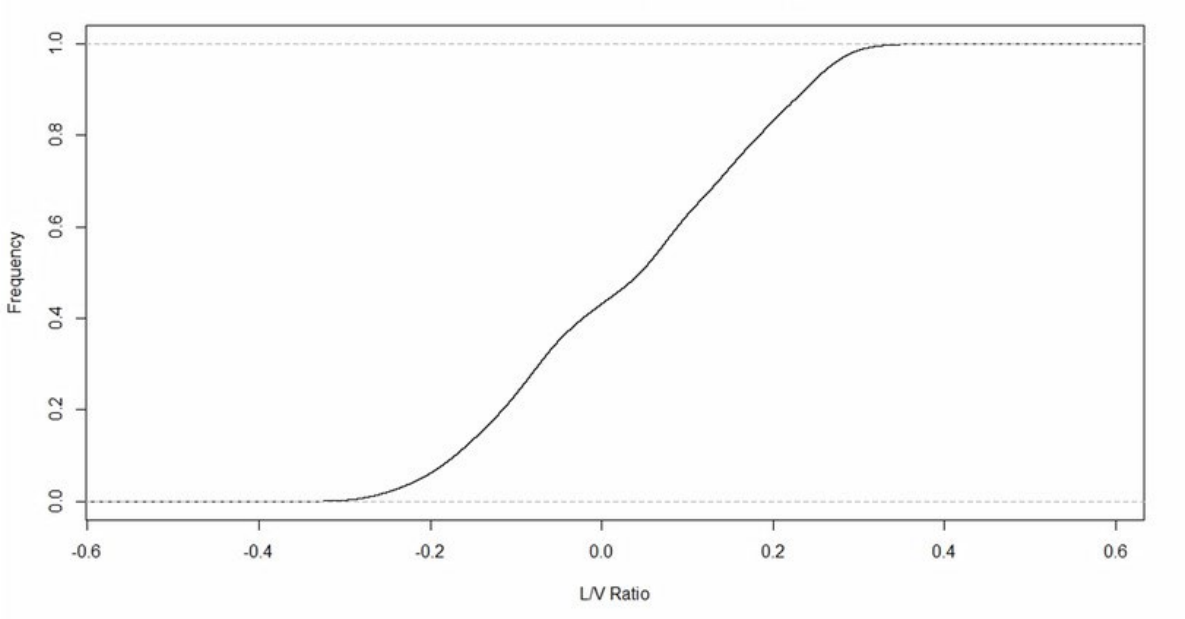

Figure 17 Cumulative distribution plot of L/V ratio.

As shown in Figure 16, there are two clear distributions within the L/V dataset. There is one distribution containing all the positive L/V values, while the other contains all the negative L/V values. This split in the distribution causes the mean to be nearly zero, at 0.033. Based on the anticipated behavior of the wheels, this is expected. Because of equilibrium, there should be an equal amount of positive (gage spreading) and negative (gage narrowing) lateral forces. This is also shown in Figure 17. Nearly 50% of the L/V ratios are less than zero. Similarly, nearly 50% of the L/V are greater than zero. However, if each distribution is looked at independently, it appears as if their means would be closer to 0.1 and -0.1. These are relatively small L/V ratios, which is due to the fact that the measurement system was placed in a relatively shallow curve. Had the system been installed in a sharper curve, the measured L/V ratios may have been of a greater magnitude. However, when a distribution of L/V ratios by wheel position is generated, some more insightful conclusions can be drawn. Figure 18 shows such distributions, where the measured L/V ratios are plotted according to wheel position.

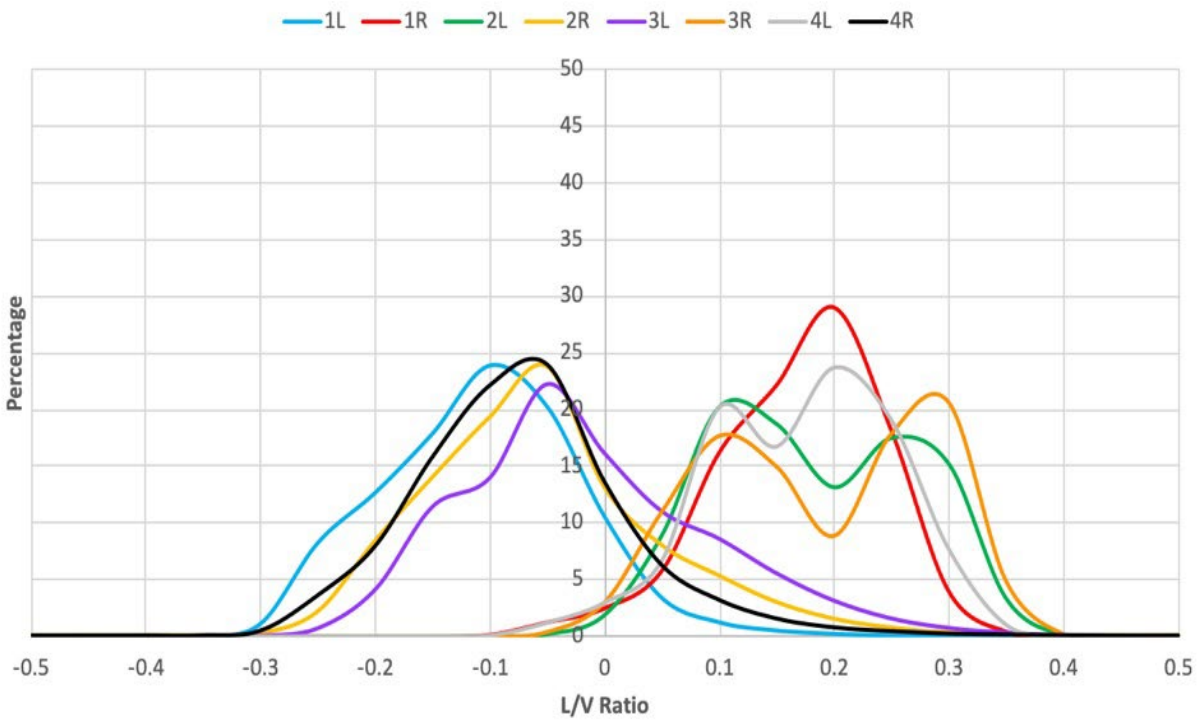

Figure 18 Histogram of L/V ratio by wheel position.

Figure 18 shows that the two aforementioned L/V ratio distributions can be attributed to the position of the wheel being measured. The population of positive L/V ratios are being seen on leading axle, right-side wheels (1R and 3R) and trailing axle, left-side wheels (2L and 4L). Conversely, the population of negative L/V ratios are being seen on leading axle, left-side wheels (1L and 3L) and trailing axle, right side wheels (2R and 4R). Being that the L/V measurement system is installed on a 3.2 degree, left-hand curve, this behavior is expected. As the car travels through the curve, the wheels in the 1R and 3R position will flange up against the high rail, leading to the generation of high positive (gage spreading) lateral forces. Meanwhile, the wheels in the 1L and 3L position will generate forces towards the center of the track, resulting in negative L/V ratios. This confirms that the data is behaving as expected, and can thus be deemed reliable. It can also be seen that there are slightly higher positive L/V ratios that negative. These are wheels that are excessively flanging and generating higher lateral forces. In turn, it is believed that these wheels are much more likely to be wearing more severly than the rest of the population. In order to further investigate this belief, relationships between wheel wear rate and L/V ratio were examined, and will be discussed in later sections.

Exploratory Data Analysis of the TBOGI Data

In addition to the WheelScan and L/V data, TBOGI data would also be used in order to form conclusions about the wearing of the wheels on the 7 Line. The TBOGI measures a variety of parameters, such as angle of attack, tracking position, inter-axle misalignment, rotation, shift, tracking error, and speed. Angle of attack was the most interesting parameter here, as it can be used to identify misbehaving trucks and axles. Essentially, the higher the angle of attack is, the more a wheel will be expected to wear. WID has instrumented a portion of the NYCT Flushing

line with their TBOGI system. This will take measurements of the aforementioned parameters of every passing axle. The device has been installed on a 3.2 degree curve, approximately 300 feet from the L/V Measurement System. Figure 19 defines each parameter measured by the TBOGI, with a positive sign convention shown. Angle of attack, inter-axle misalignment, and rotation are measured in milliradians, and the other parameters are measured in millimeters.

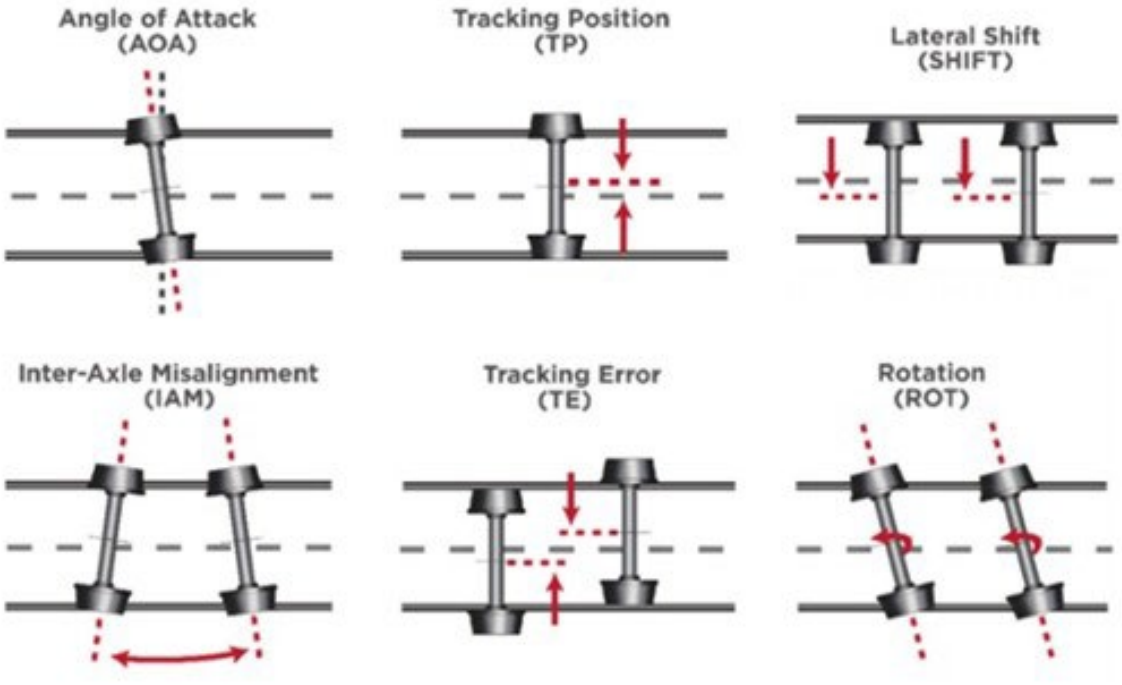

Figure 19 Parameters measured by the TBOGI (NYCTA).

Similar to the issues encountered with the L/V data, the TBOGI was not useable until January 2018. Prior, the RFID tag reader was not functioning properly, meaning that data could not be matched up to individual cars. However, the system records every single truck that passes over it in a day. At the time of analysis there are over 250,000 data points in the TBOGI database.

From an engineering perspective, it was thought that angle of attack, tracking position, and speed would have the greatest impact on the wearing of wheels. The greater the angle of attack is, the greater the lateral force between the wheel and rail will be. Similarly, the faster an axle is traveling, the higher the generated forces will be. In addition, the greater the tracking position (the more off center an axle is), the more likely severe wheel flanging is to occur. In all cases, there should be a direct correlation to wear. Increased lateral forces and increased wheel flanging are typical causes of accelerated wear. Thus, these parameters were deemed to be most influential in this study. However, this does not mean that the other variables are unimportant. Rather, it means that angle of attack, tracking position, and speed are more significant for this work. Figure 20 below presents a histogram of all recorded angle of attack values.

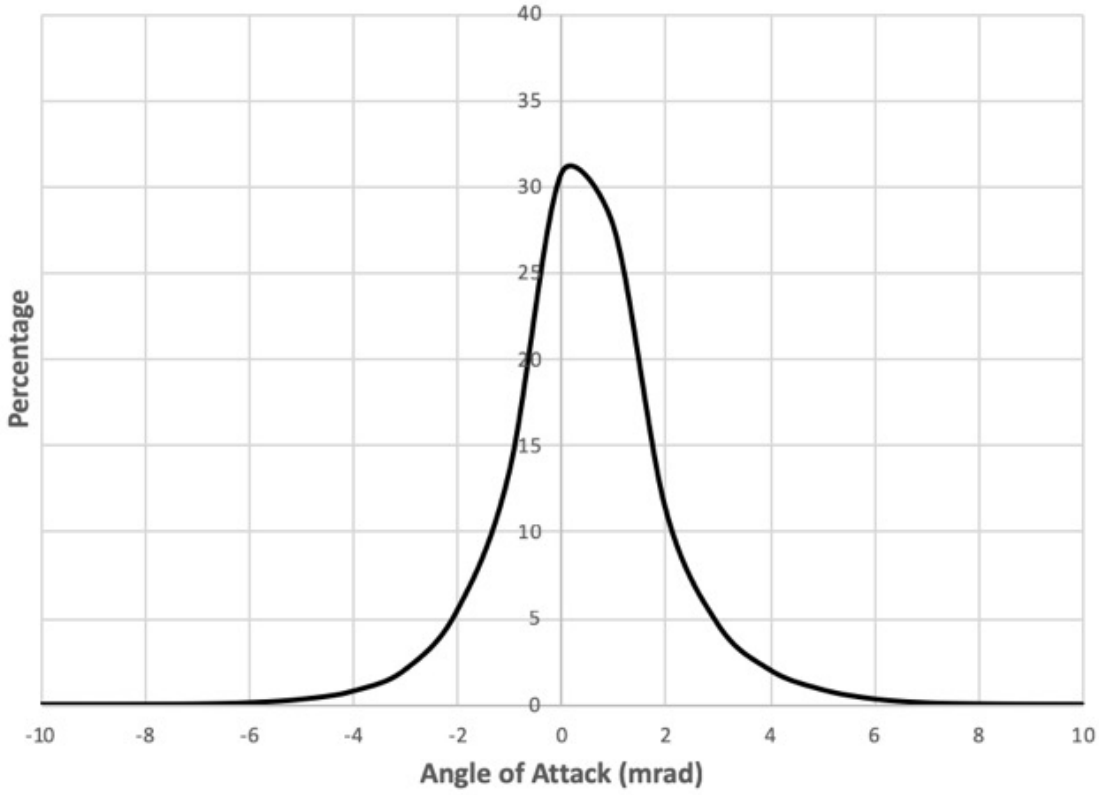

Figure 20 Histogram of angle of attack (mrad).

As shown, the angle of attack measurements is normally distributed and the mean is nearly zero. However, a large spread is seen in the data. Angle of attacks have been recorded anywhere between -10 mrad to 10 mrad. While these values are small in magnitude, the difference in behavior between an axle with a 0 mrad angle of attack and an axle with a 10 mrad angle of attack is significant. When the data is separated by axle, as in Figure 21, it can be seen that the lead axle angle of attack trend in the positive direction, while the trail axle angle of attack trends in the negative direction. Based on the fact that the TBOGI was placed in a left-hand curve, this type of behavior is anticipated. The same plots were created for tracking position, as shown in Figures 22 and 23, and the same statements can be made. Again, the mean is nearly zero, but there are some more extreme values that can lead to poor axle and truck behavior. However, when the data is separated by axle in Figure 23, the two distributions are nearly identical.

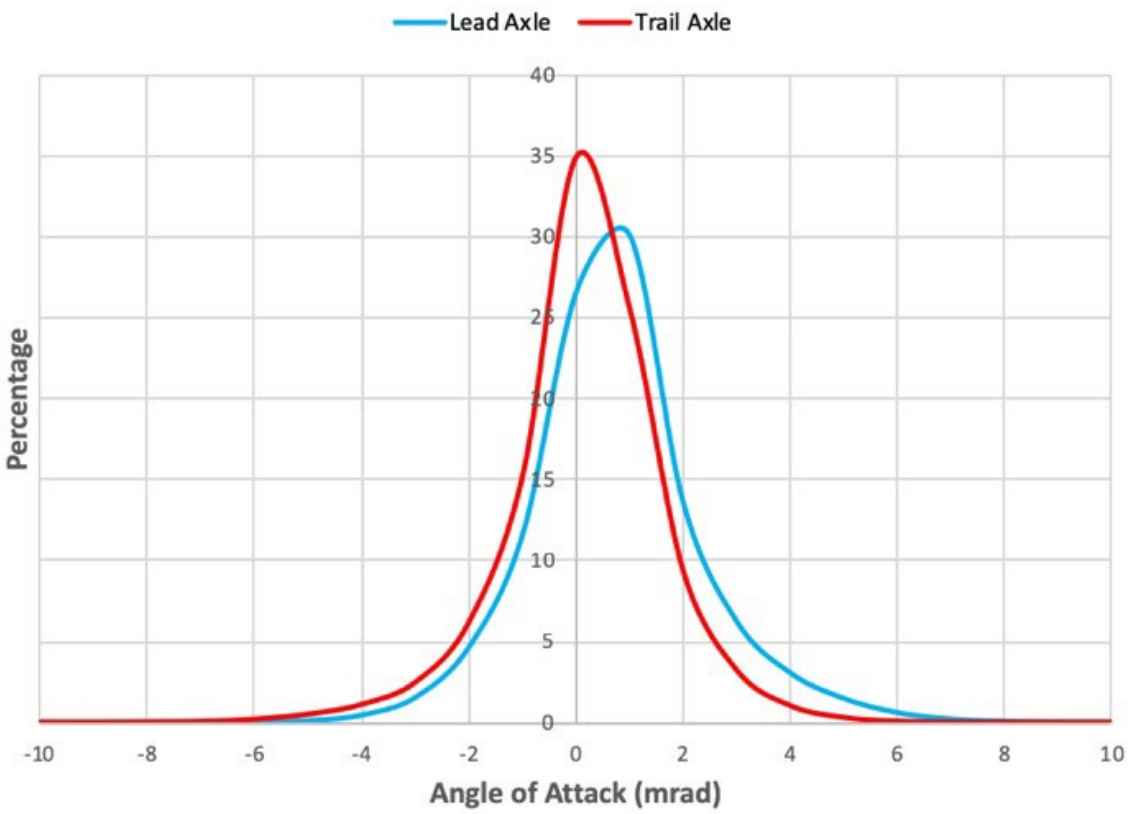

Figure 21 Histogram of angle of attack by axle position.

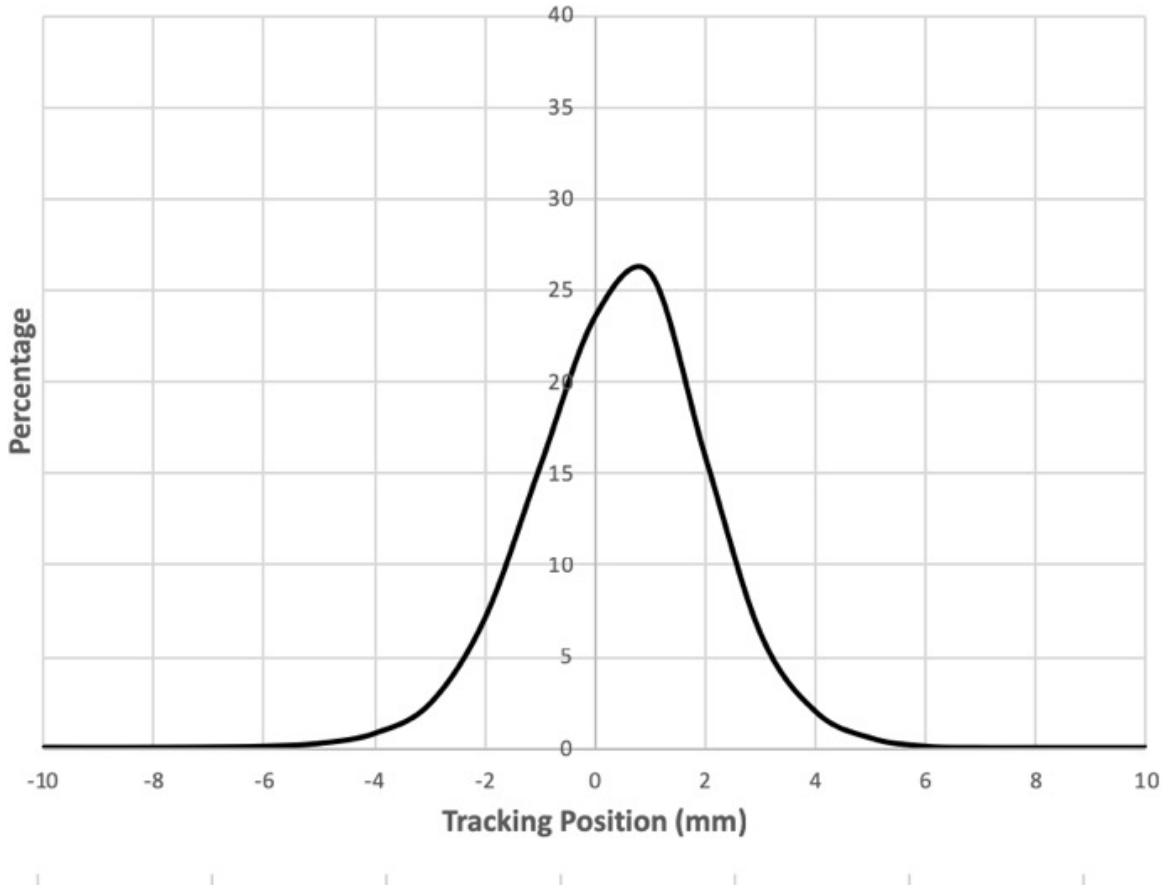

Figure 22 Histogram of tracking position (mm).

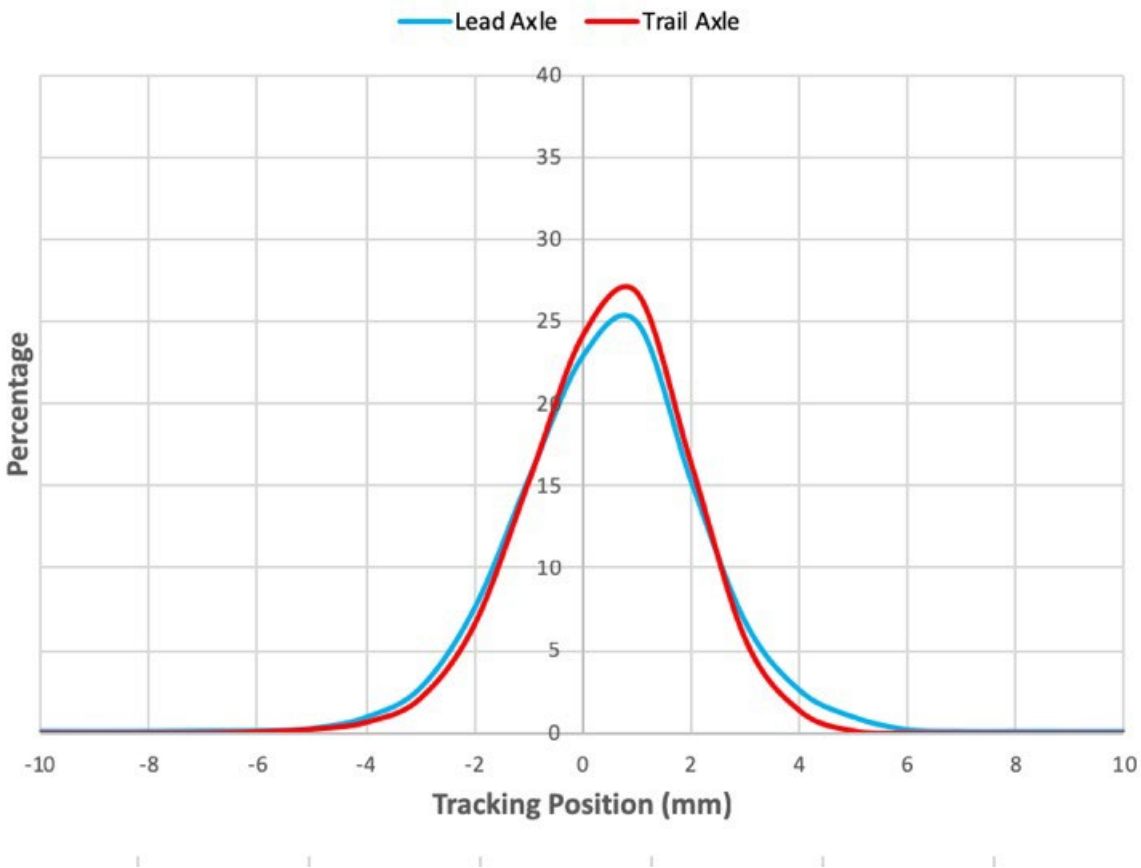

Figure 23 Histogram of tracking position by axle position.

Figure 24 shows a histogram of speed. The TBOGI system measures the speed of every truck that passes over it, rather than every axle. Unlike previous distributions, speed does not appear to be normally distributed about its mean. Rather, the distribution is heavily skewed to the right side. A large cluster of trucks passing over the TBOGI are travelling between 45 – 60 km/hr. A slightly smaller cluster of trucks are traveling below 45 km/hr. And, there is a significantly small cluster of trucks that appear to be travelling over 60 km/hr. NYCT states that balance speed on this section of the track is 56 km/hr. With a mean speed of 44.927 km/hr, the trains on this line are travelling significantly under balance speed on average. This would lead to less lateral force generation, and in turn, less wheel wear, than if the trains were consistently traveling at the same speed. However, it needs to be noted that these are speed measurements at one point along the line. The speeds at this location are not indicative of the speeds along the rest of the line, which must be considered as this study progresses.

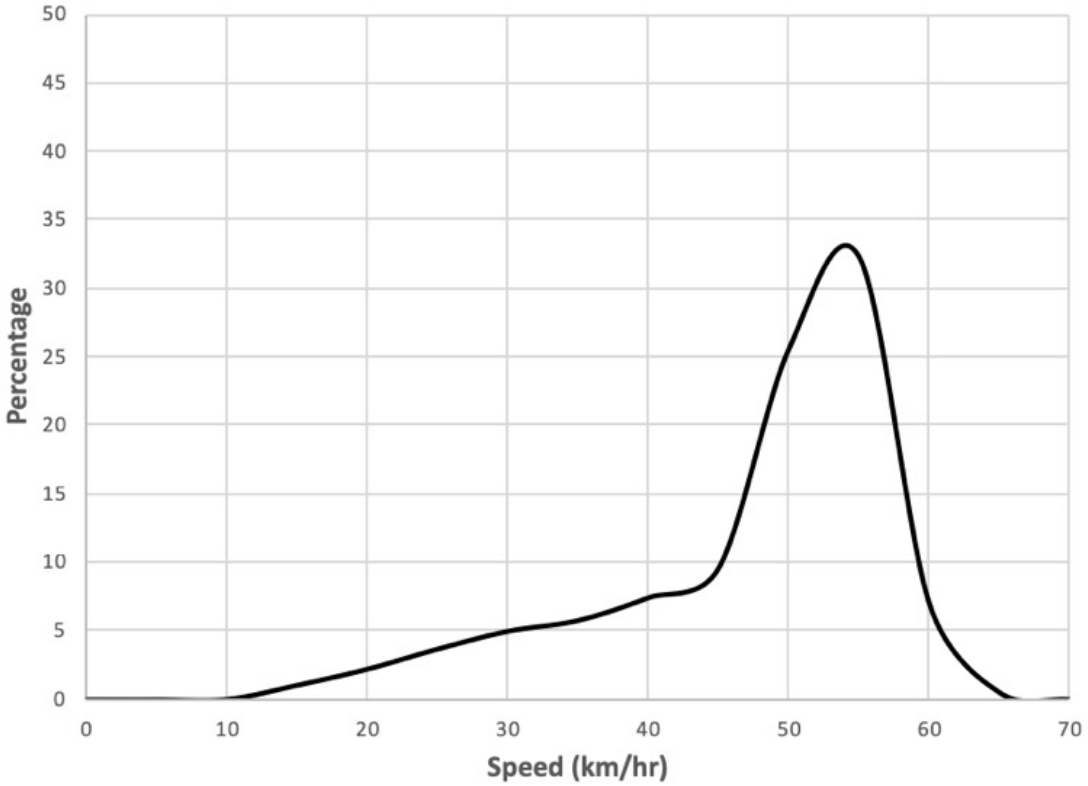

Figure 24 Histogram of speed (km/hr).

Although the three aforementioned parameters were thought to be most influential in a wheel wear analysis, histograms of the others were created. The following figures present distributions of inter-axle misalignment, tracking error, rotation, and lateral shift.

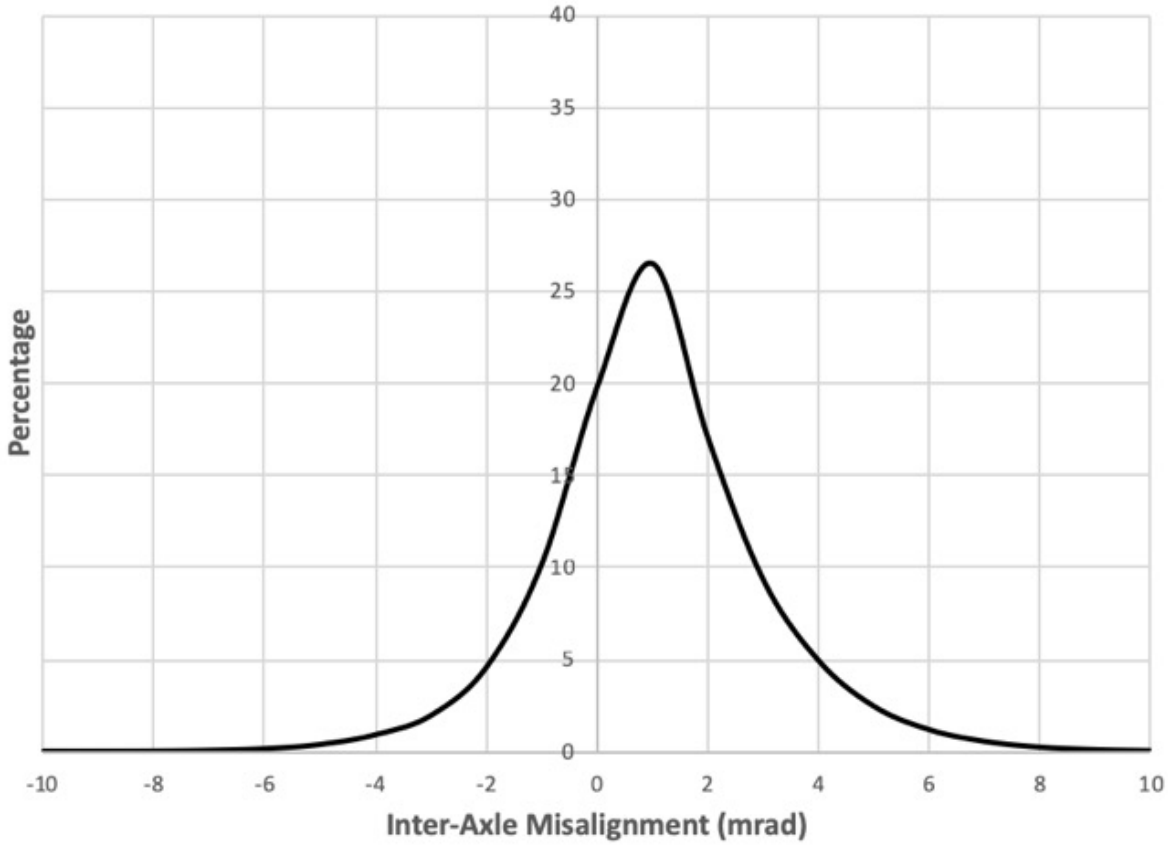

Figure 25 Histogram of inter-axle misalignment (mrad).

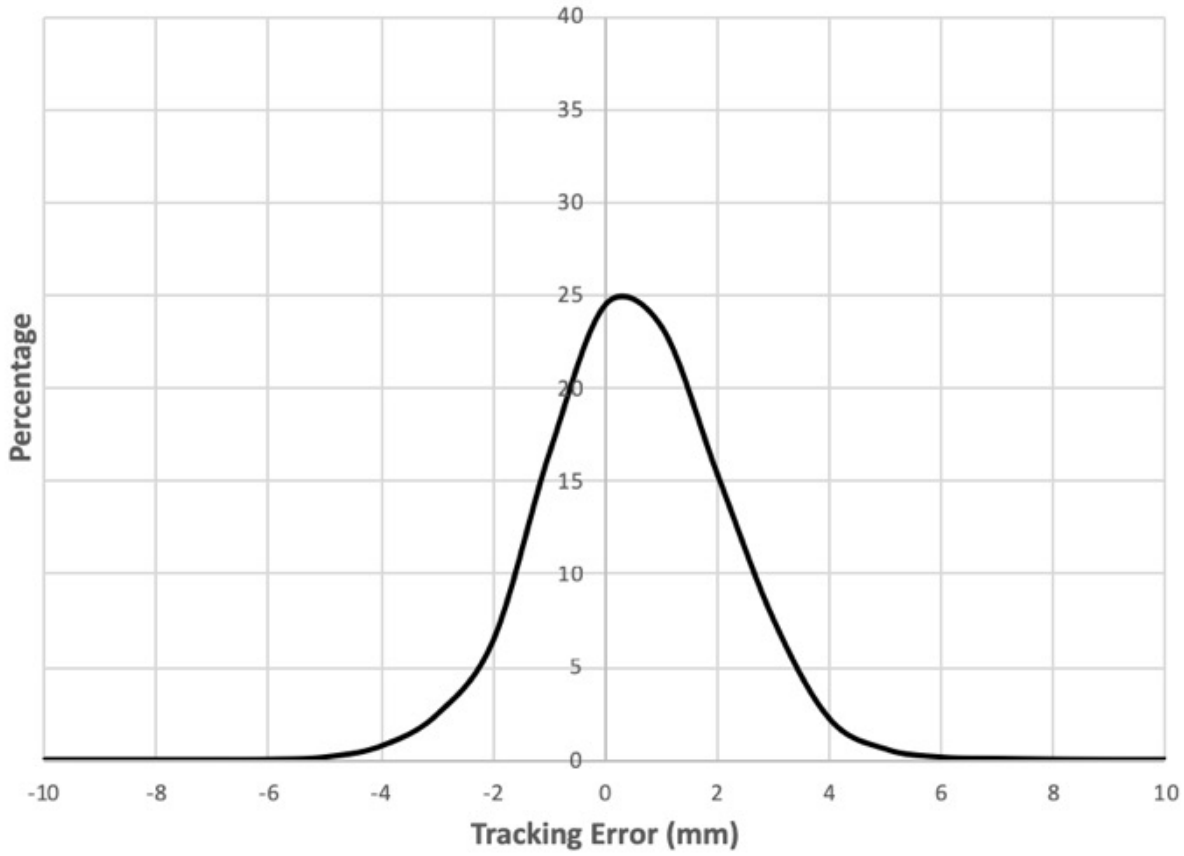

Figure 26 Histogram of tracking error (mm).

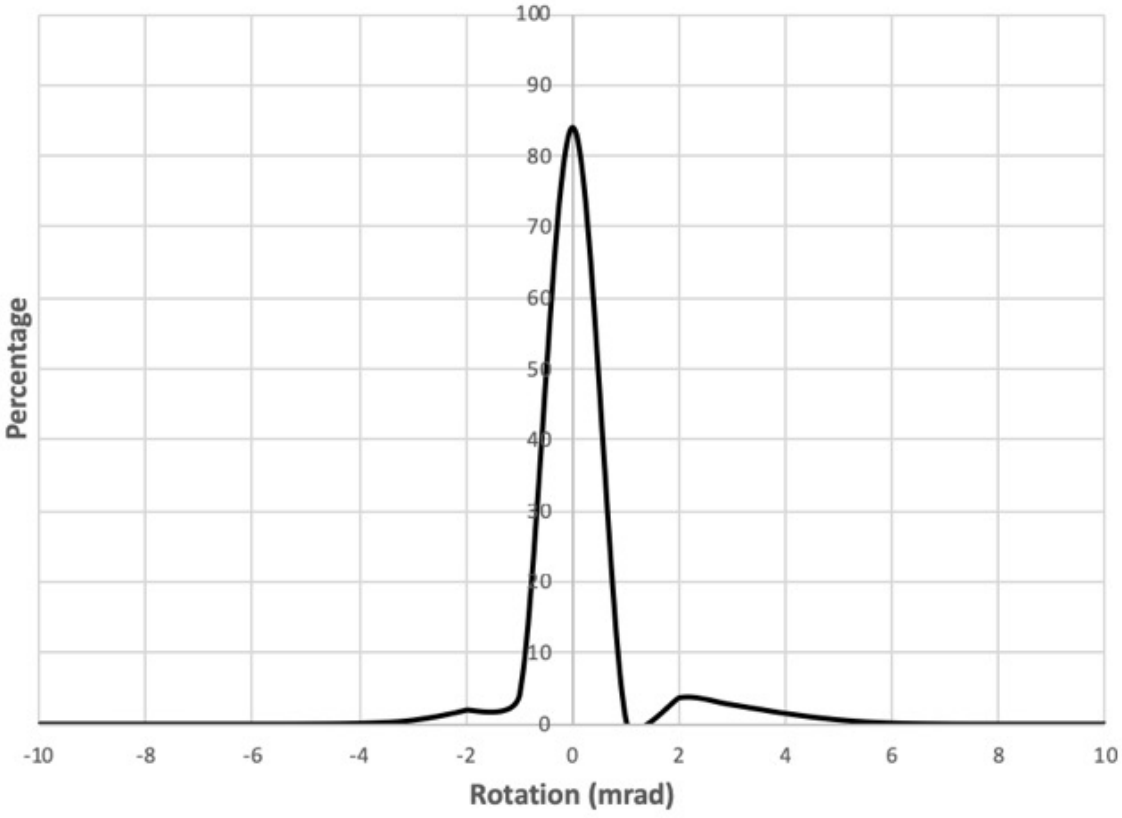

Figure 27 Histogram of rotation (mrad).

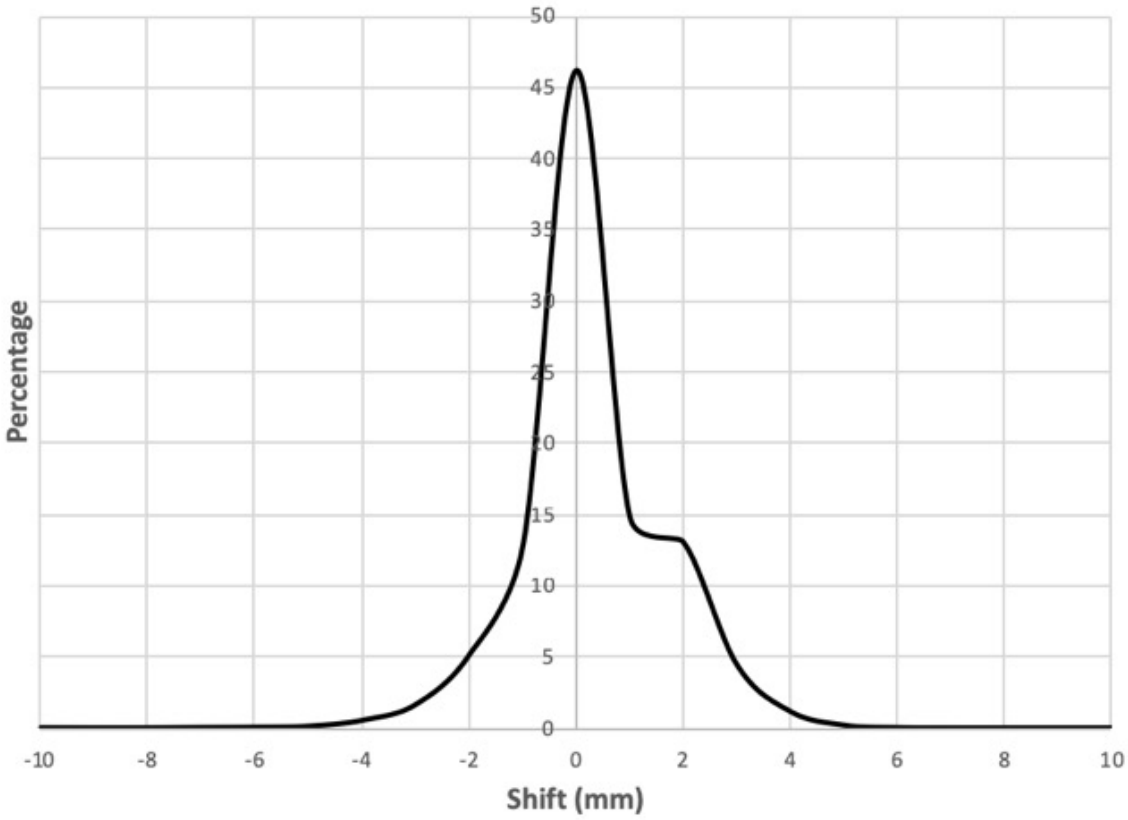

Figure 28 Histogram of shift (mm).

From the previously shown distributions, each variable is normally distributed about their means. Furthermore, the mean value of each variable is nearly zero. This could lead to the assumption that all axles and trucks are behaving properly. However, as shown by the spreads of the distributions, this is not the case. For example, the inter-axle misalignment measurement spans from -10 mrad to 10 mrad. In fact, during NYCTA's study, it was cited that for the given speed of travel, the measured inter-axle misalignments were alarmingly higher than expected. Thus, it appears that there are some trucks behaving poorly.

Data Preparation

With various the various Exploratory Data Analyses completed, the various streams of data were better understood. Moreover, the trends and behaviors seen in the data lined up with prior expectations, leading to the assumption that the data collected was reliable. As mentioned earlier, the overall objective of this study was to analyze the wear patterns of transit vehicle wheels in order to better understand their behavior and life cycle. Therefore, the data needed to be prepared in a way that would allow for a population of wheel wear rates to be obtained and analyzed. Furthermore, in hopes of findings relationships between wheel wear and the other available data sources, the L/V Measurement System and TBOGI data needed to be adjusted accordingly. The following sections provide a narrative on how this was accomplished.

Calculation of Wheel Wear Rates

With all of the KLD WheelScan data combined into a database, wheel wear rates could be calculated. However, the data needed to be cleaned prior to performing this analysis. Prior to receiving the data, KLD had performed their own analysis in order to filter out any bad data points. These bad points could be due to errors in the image scanning system or faulty calculations. Thus, any bad data point received a data quality index value of "0". Conversely, all good data points received a data quality index value of "1". Therefore, any points with a "0" data quality were discarded. Furthermore, KLD stated that this filtering process was not put in place until June 1, 2017. Thus, all data before June 1, 2017 had not been analyzed and filtered. Therefore, the decision was made to ignore all data before June 1, 2017, since there was a great deal of uncertainty associated with it. Lastly, all data from January 2018 had not been correctly tagged with the RFID scanner. Therefore, it is not possible match this data with the appropriate car numbers. However, the RFID scanner was fixed as of February 7, 2018. Thus, in order to establish degradation rates and maintenance performance, the wheel wear measurements were collated for each wheel for the data collected from June 1, 2017 to December 31, 2017 and February 7, 2018 to April 30, 2018.

Confident that any bad data points had been removed, the next step was to parse out the data based on when a maintenance event happened. In this dataset, there are essentially three events that can take place: a wheel can be trued, a wheel can be replaced, or a wheel can have no maintenance performed. In order to obtain accurate results, it is necessary to calculate only the wear rates for the duration of each event. For example, in Figure 15, two wear rates would be calculated: one before truing and one after truing. Conversely, for those wheels that had not been trued or replaced yet, only one wear rate would be calculated. Thus, a series of rules and checks were put in place to determine if and when a maintenance event occurred.

Code was then written in VBA that would calculate the wear rate of every wheel in the 7 Line fleet, based upon their flange thickness measurements over time. As discussed, NYCTA wheel wear is predominantly flange wear and as such, flange wear is the primary analysis parameter used. In addition, NYCTA truing practices are governed by a wheel's flange thickness measurements. Therefore, in order to eventually accurately predict when a wheel will need to be maintained or replaced, a wear rate based upon flange thickness needed to be calculated. Originally, standard linear regression was used to calculate wear rate. The flange thickness measurements for each wheel were regressed linearly over time in order to generate the following equation:

$$y = mx + b \tag{1}$$

Where

y = flange thickness (mm)
m = flange thickness wear rate (mm/day)
x = time (days)
b = constant (mm)

Initially, this approach provided an adequate representative of the fleet's wheel wear. However, upon further investigation of the data, it was realized that linear regression would not be acceptable. The flange thickness of a new or recently trued wheel exhibited a sharp and rapid

wearing in period, whereby the flange would wear at a higher rate early on and eventually settle into a steady wear rate. Typically, this type of behavior appears to be an exponential decay. This is illustrated in Figure 29, where it can be seen that the flange thickness appears to decay exponentially over time, rather than at a constant linear rate. This is clearly shown by the first series of data, from June to December. This type of behavior was also cited by multiple parties involved in NYCTA's Integrated Wheel/Rail Characterization and Safety Project (NYCTA 2019). In their discussion on wheel wear, they too noticed the aforementioned wearing in period, and suggested that a nonlinear or exponential fit of the data would be most appropriate and representative of the behavior of these particular wheels. Thus, simple linear regression would not accurately portray the wheel's behavior. Instead, a nonlinear regression analysis technique would be needed.

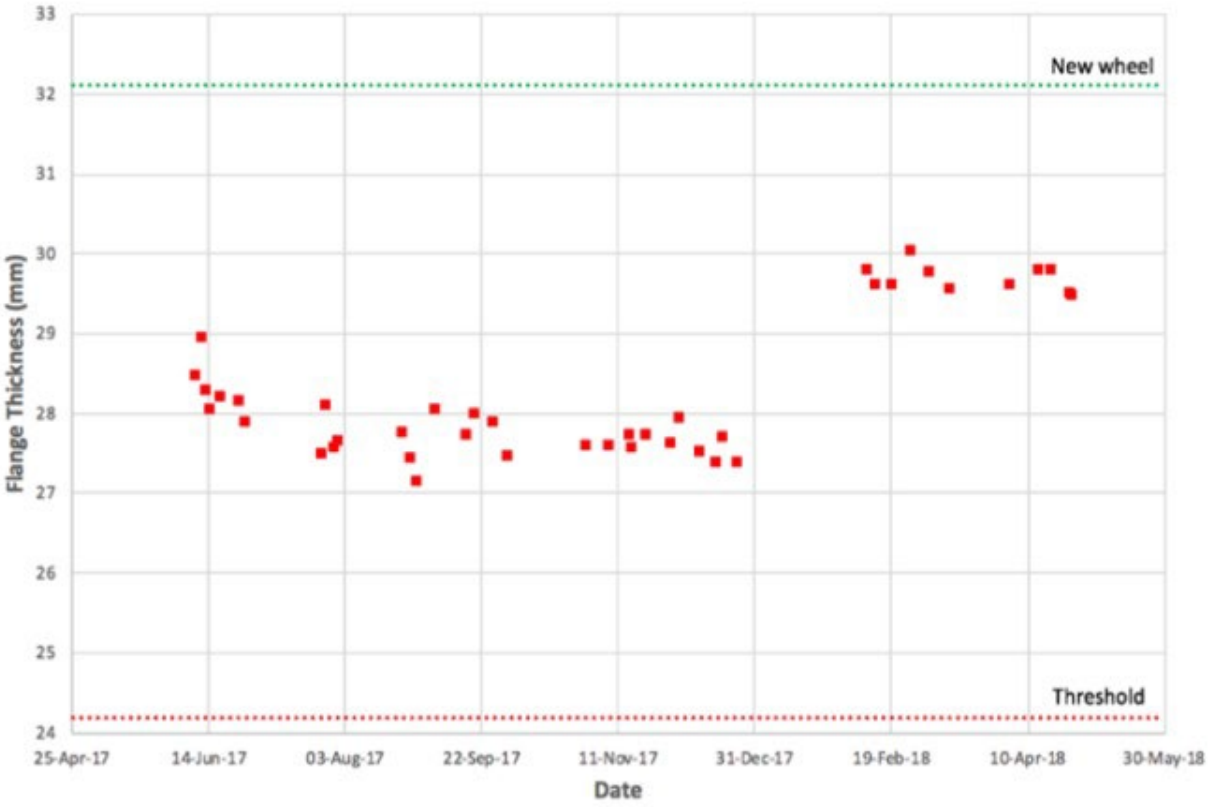

Figure 29 Plot of flange thickness measurements depicting exponential decay for Car 7502, Axle 1, right wheel.

The resulting analysis utilized an exponential decay function derived through nonlinear regression for each event of every wheel in the population. The code that was originally written was adjusted to regress the flange thickness nonlinearly over time, rather than linearly. For reference, the code that was written to perform this analysis can be found in Appendix A. Equation 2 represents the exponential decay function that was derived through nonlinear regression for each event of every wheel in the population.

$$y = Ae^{kx} \tag{2}$$

Where

y = flange thickness (mm)
A = constant (mm)
e = 2.71828 (mathematical constant)
k = flange thickness wear rate (1/days)
x = time (days)

Using Equation 2, the A and k parameters were calculated for each event of every wheel in the population. In addition, an R^2 value was calculated to indicate how well the nonlinear regression fit the data. As an example, Figure 30 shows how the data in Figure 29 was fit to this function. At first glance it appears as if the fit is linear. This is deceiving, because the data range is so narrow. It is difficult to fully visualize an exponential curve when the data lies within a 2 mm range. In addition, any scatter that is observed in the data can be attributed to the measurement system having the capability of measuring flange thickness with a tolerance of +/- 0.5mm. This inherent field accuracy tolerance affects the overall fit of the exponential function.

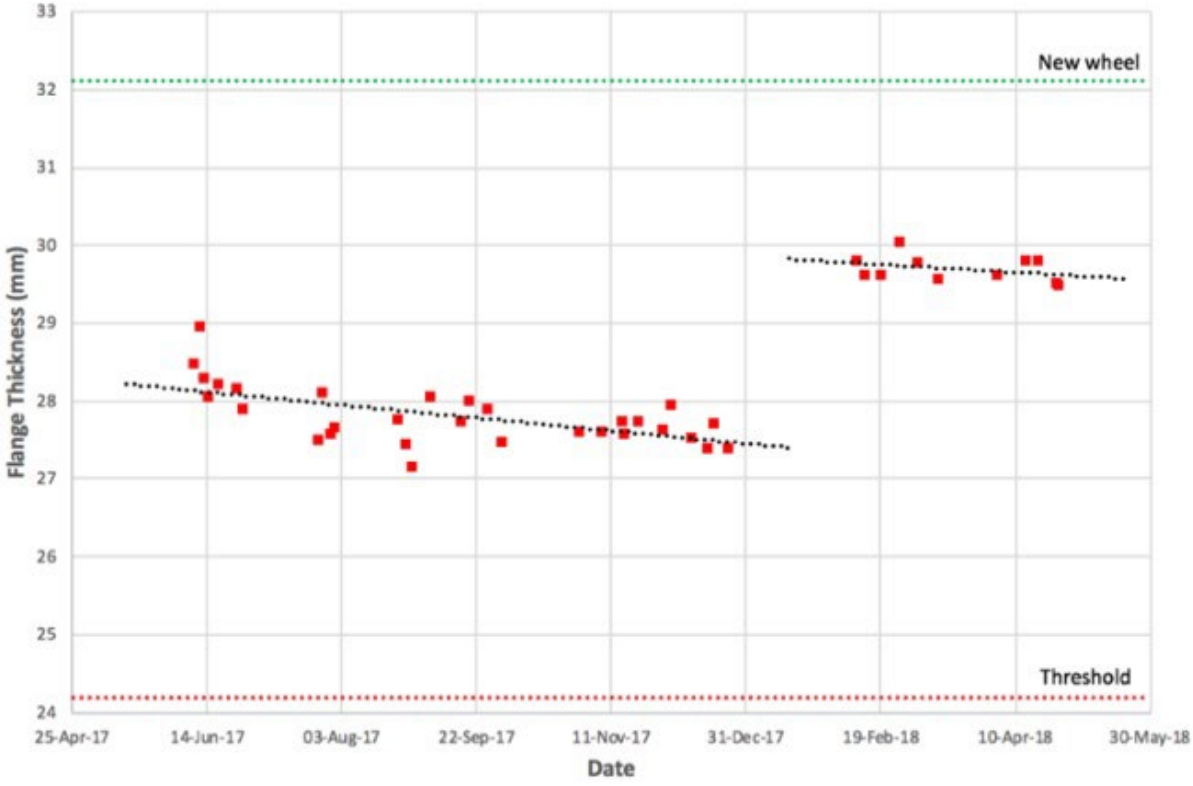

Figure 30 Exponential regression of flange thickness for Car 7502, Axle 1, right wheel.

This process was repeated for every wheel on every car and stored in the database. Upon completion of this analysis step, just over 7,000 wear rates were obtained. Any records with a positive k parameter (indicating flange thickness increasing with time) were ignored, as this would not represent the exponential decay function expected of a wheel experiencing wear. These instances were due to a lack of data points, or irregular maintenance events. A number of these were checked by hand in order to ensure the analysis was being performed correctly.

Calculation of Average Values from the L/V Measurement System and TBOGI

In addition to calculating and analyzing wear rates, the large amount of data that was made available as part of NYCTA's research efforts allowed for further relationships to be explored. For example, in theory, the data from the L/V Measurement System and TBOGI could be used to find relationships between L/V ratio, angle of attack, tracking position, and speed and wheel wear rate. However, this data needed to be first condensed into a more workable format. For instance, with the nonlinear regression completed, each wheel in the fleet has its own corresponding flange wear rate. However, the nature of the L/V Measurement System and TBOGI results in each wheel having hundreds to thousands of recorded L/V ratios and angles of attack. From a statistical perspective, it is not simple to compare one data point to thousands of data points. So, it was decided that average values of each measured parameter would be calculated for each wheel in the fleet. This was done with the thinking that when completed, there would be a population of wheels, each with their own corresponding wear rate, average L/V ratio, average angle of attack, and so on. This approach would lend itself to a more standard statistical analysis of the data. Therefore, code was written in VBA to calculate these average values for every recorded wheel in the 7 Line fleet.

Initial Analysis of the Data

With a population of wheel wear rates, as well as a population of average values from the L/V Measurement System and TBOGI for each wheel, some initial analyses of the data could be conducted. Mainly, relationships between wheel wear rate and the other measured variables would be explored. However, in order to better understand the newly obtained data, an Exploratory Data Analysis was conducted.

Exploratory Data Analysis of Wheel Wear Rates

Figure 31 below presents histograms of the A and k parameters that were obtained from the exponential regression of the wheel wear data. In addition, Table 2 presents basic descriptive statistics of the obtained A and k parameters. If Equation 2 is thought of as an exponential decay function, then it can be assumed that the A parameter is representative of the initial flange thickness of each wheel, and the k parameter is representative of the wear rate of each wheel. It is interesting to note that the mean a value of 31.855 mm is nearly equal to the new flange thickness value of 32.1 mm. In addition, it can be seen that a majority of the k values are greater than -0.001. This means that most of the wheels in the fleet are wearing at similar rates. However, there are a significant amount of k values less than -0.001. This indicates that there is a subpopulation of wheels which are wearing at a higher rate. Note that the more negative a wear rate is, the more severe the wheel is expected to wear.

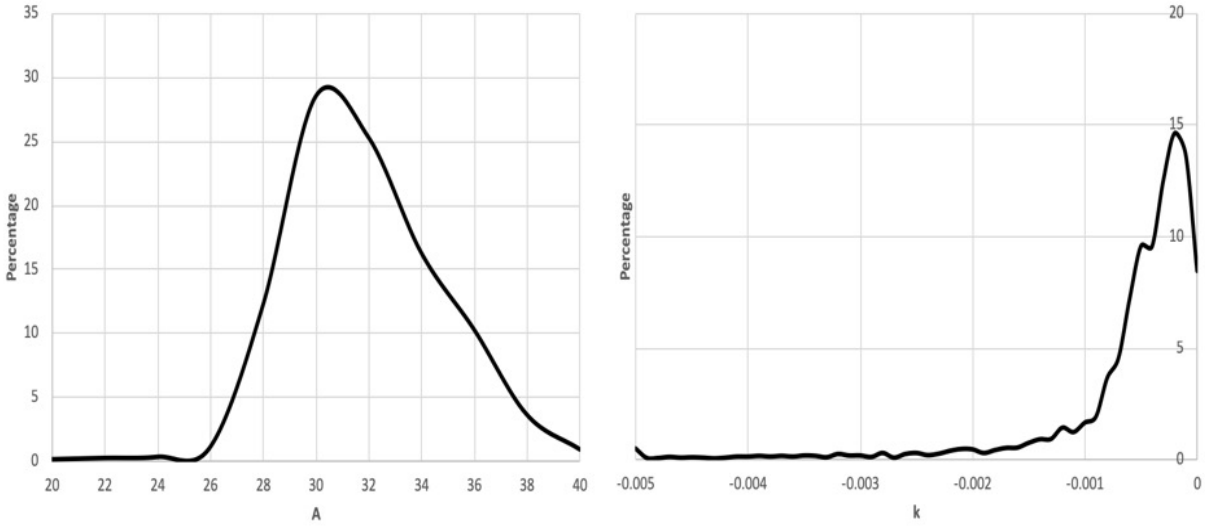

Figure 31 Histograms of A (left) and k (right) parameters derived from exponential regression.

Table 2 Descriptive Statistics for A and k Parameters

	Mean	Median	Std. Dev.	Min	1st Quartile	3rd Quartile
A	31.855	30.470	27.368	5.887	28.794	32.788
k	-0.00064	-0.00035	0.00138	-0.07607	-0.00065	-0.00016

Since the focus of this study was wheel wear rates, a histogram of k sorted by wheel position was created, and can be seen in Figure 32. In addition, Table 3 presents descriptive statistics of the k parameter by wheel position. As can be seen, the wheel wear rate is not dependent upon wheel position. The distributions of all eight wheels are nearly identical, as too are the descriptive statistics. This is because the 7 Line is nearly symmetrical. Therefore, throughout a wheel's lifetime, it will experience an equal amount of left-hand and right-hand curves, meaning each wheel should wear similarly.

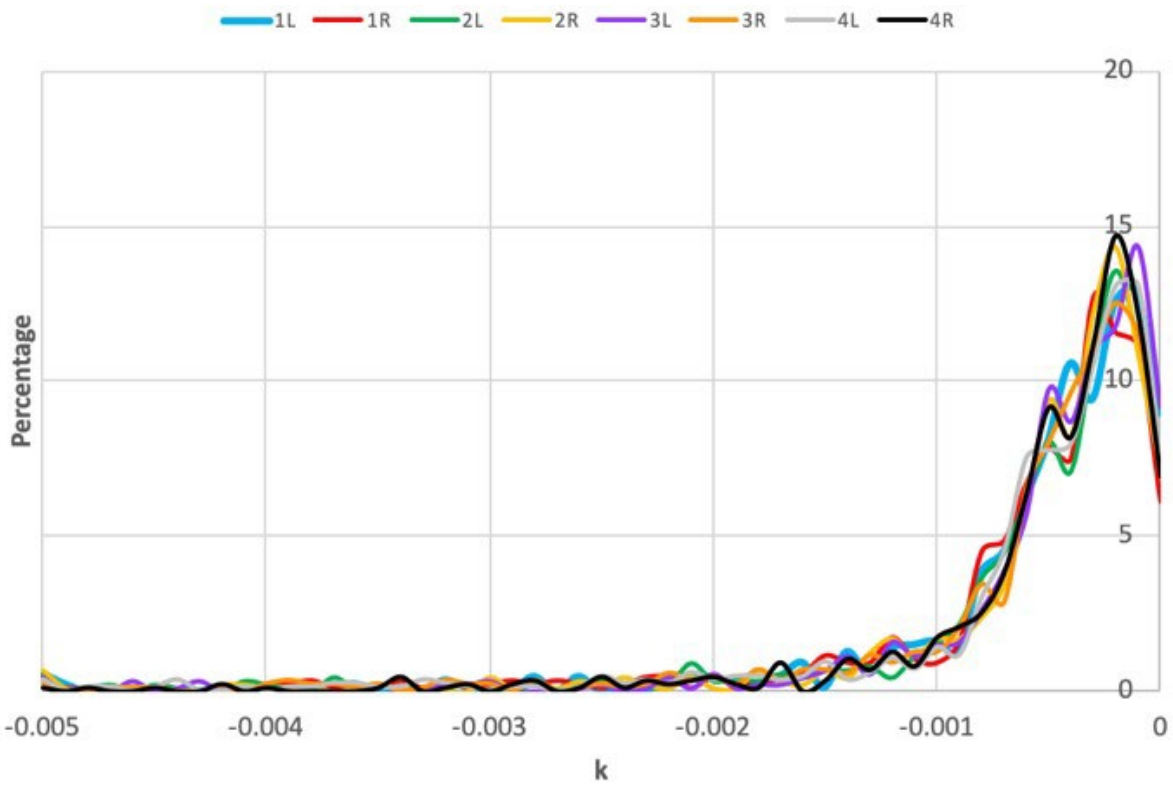

Figure 32 Histogram of k parameter by wheel position.

Table 3 Descriptive Statistics of k Parameter by Wheel Position

	Mean	Median	Std. Dev.	Min	1st Quartile	3rd Quartile
1L	-0.00050	-0.00037	0.00095	-0.00863	-0.00065	-0.00016
1R	-0.00058	-0.00037	0.00101	-0.01319	-0.00071	-0.00017
2L	-0.00050	-0.00035	0.00115	-0.00848	-0.00068	-0.00015
2R	-0.00056	-0.00035	0.00115	-0.01748	-0.00065	-0.00016
3L	-0.00056	-0.00034	0.00269	-0.07607	-0.00061	-0.00014
3R	-0.00052	-0.00036	0.00084	-0.00572	-0.00064	-0.00016
4L	-0.00044	-0.00033	0.00143	-0.00669	-0.00065	-0.00015
4R	-0.00048	-0.00034	0.00074	-0.00504	-0.00061	-0.00017

Exploratory Data Analysis of Average L/V Ratios

Once a population of average L/V ratios were obtained for each wheel in the NYCT fleet, a histogram of all average L/V ratios was created, and is shown in Figure 33. Also, to investigate the behavior of individual wheels, Figure 34 displays a histogram of average L/V ratio by wheel position. Lastly, Table 4 presents basic descriptive statistics of the obtained average L/V ratios.

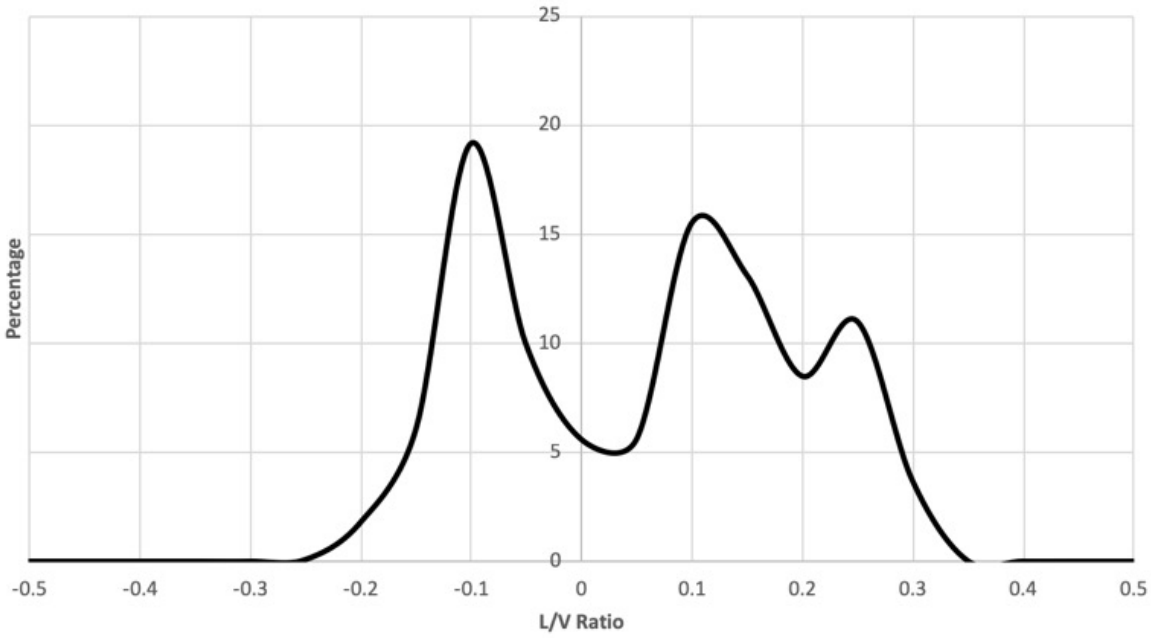

Figure 33 Histogram of average L/V ratios.

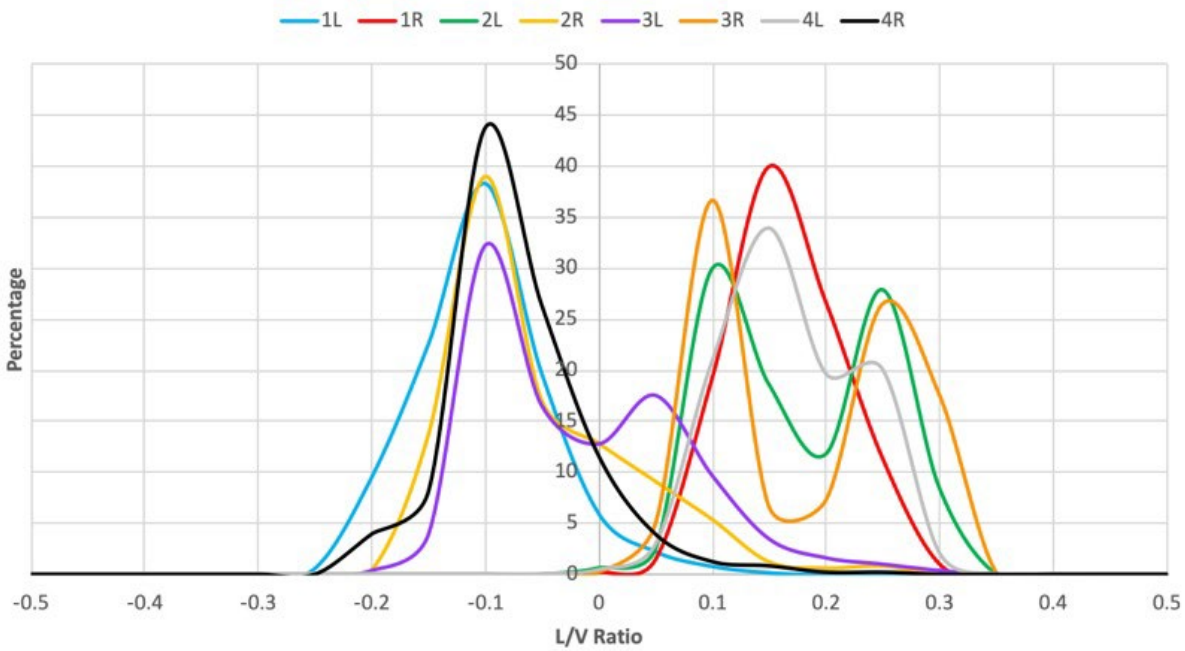

Figure 34 Histogram of average L/V ratios by wheel position.

Table 4 Descriptive Statistics of Average L/V Ratios

	Mean	Median	Std. Dev.	Min	Max	1st Quartile	3rd Quartile

ALL	0.032	0.061	0.138	-0.271	0.301	-0.106	0.138
1L	-0.127	-0.132	0.059	-0.271	0.103	-0.162	-0.095
1R	0.141	0.137	0.048	-0.002	0.286	0.107	0.175
2L	0.153	0.127	0.072	-0.031	0.295	0.092	0.224
2R	-0.079	-0.107	0.079	-0.244	0.240	-0.135	-0.035
3L	-0.040	-0.068	0.090	-0.235	0.260	-0.113	0.024
3R	0.158	0.165	0.082	-0.026	0.301	0.081	0.242
4L	0.143	0.126	0.059	-0.007	0.285	0.100	0.196
4R	-0.097	-0.106	0.061	-0.247	0.222	-0.132	-0.069

Cleary, from Figure 33 there are three distinct sub-populations within the entire population. The first one contains all negative L/V values. Then, there are two positive sub-populations, with one containing more extreme L/V values. This is different from the behavior seen earlier in Figure 16, where there only appeared to be two L/V populations. The process of averaging the data has made the more excessive L/V values more pronounced. Excessive L/V ratios can lead to accelerated wheel wear, which in turn can lead to increased likelihood of derailments. In addition, Figure 34 displays the same trends seen earlier. The population of positive L/V ratios are being seen on leading axle, right-side wheels (1R and 3R) and trailing axle, left-side wheels (2L and 4L). Conversely, the population of negative L/V ratios are being seen on leading axle, left-side wheels (1L and 3L) and trailing axle, right side wheels (2R and 4R). There are also some wheels with two different L/V populations. For example, wheel 3R shows two well-defined L/V ratio populations. Typically, this can be an indication that some cars, trucks, and axles are behaving differently than others. Ultimately, when this data is joined with and compared to the wear rate data, it will be interesting to see if the excessive average L/V ratios correlate with the excessive wear rates. If so, this would indicate that wheel wear is affected by L/V ratio.

Exploratory Data Analysis of Average TBOGI Data

Once a population of average values from the TBOGI were obtained for each axle in the NYCT fleet, histograms of these values were created, and are shown in the following figures. The following set of figures and tables present histograms of the average angles of attack and average tracking positions, as well as their descriptive statistics.

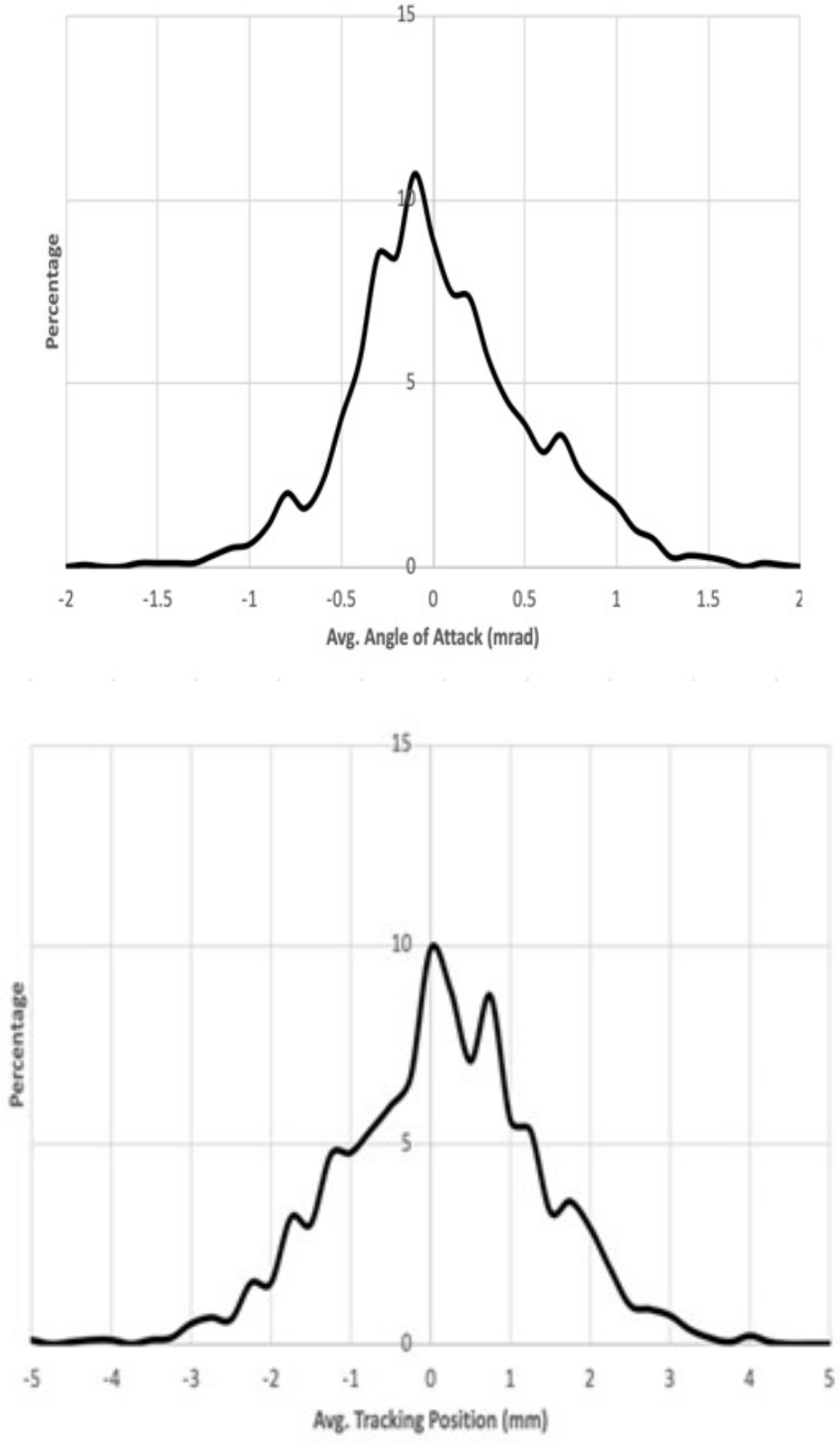

Figure 35 Histograms of average angle of attack (left) and average tracking position (right).

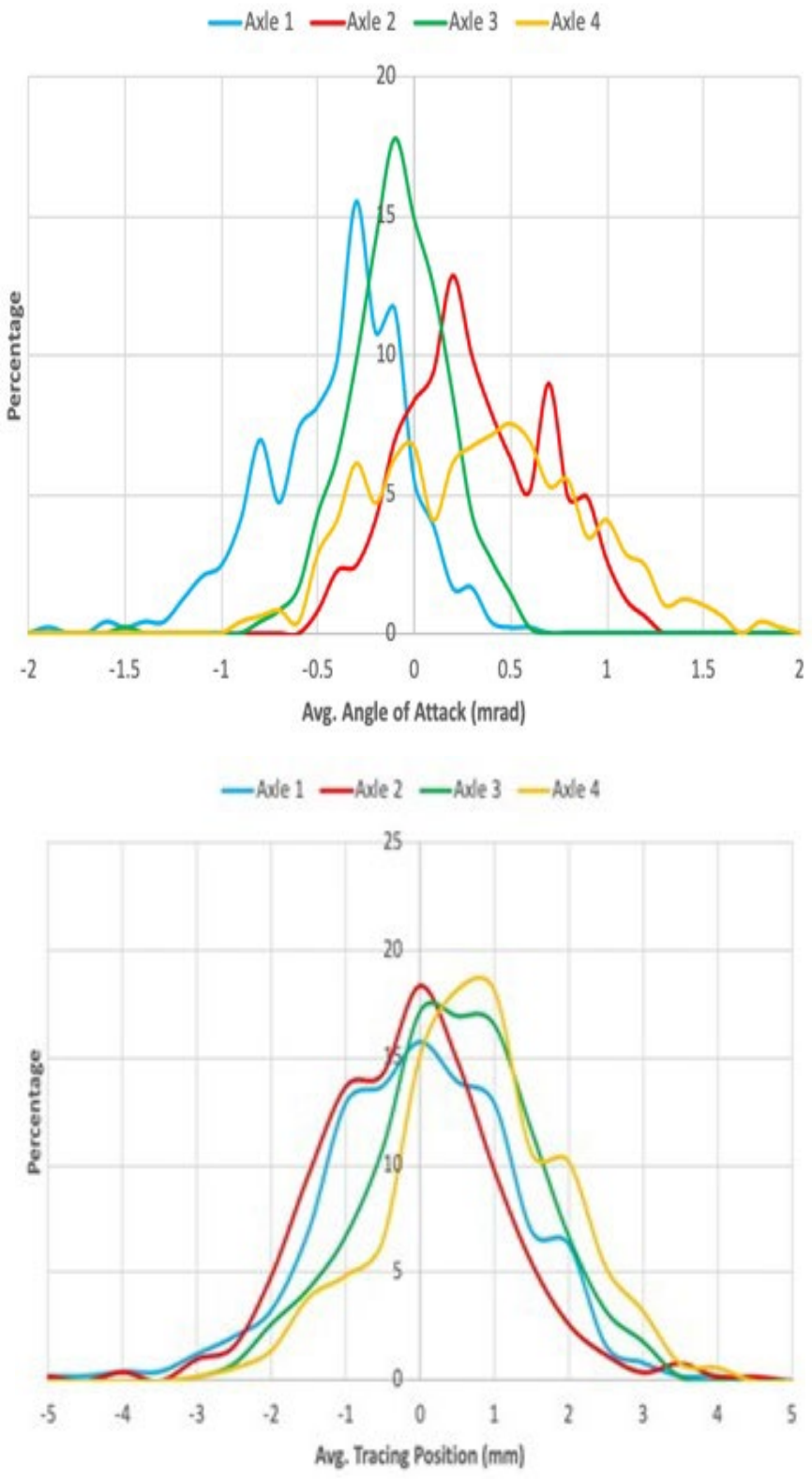

Figure 36 Histogram of average angle of attack (left) and average tracking position (right) by axle position.

Table 5 Descriptive Statistics for Average Angle of Attack (mrad)

	Mean	Median	Std. Dev.	Min	Max	1st Quartile	3rd Quartile
ALL	-0.005	-0.063	0.497	-1.998	1.816	-0.320	0.290
Axle 1	-0.449	-0.388	0.362	-1.998	0.552	-0.666	-0.199
Axle 2	0.267	0.222	0.369	-0.581	1.187	0.001	0.561
Axle 3	-0.133	-0.137	0.253	-1.526	0.589	-0.291	0.029
Axle 4	0.295	0.299	0.529	-0.977	1.816	-0.120	0.670

Table 6 Descriptive Statistics for Average Tracking Position (mm)

	Mean	Median	Std. Dev.	Min	Max	1st Quartile	3rd Quartile
ALL	0.001	0.020	1.259	-5.088	4.225	-0.818	0.783
Axle 1	-0.247	-0.205	1.288	-5.088	3.788	-1.084	0.619
Axle 2	-0.408	-0.329	1.215	-5.003	4.225	-1.186	0.291
Axle 3	0.185	0.181	1.133	-3.052	3.009	-0.518	0.928
Axle 4	0.475	0.475	1.197	-3.256	3.994	-0.201	1.229

The previous figures and tables present histograms and statistics of the average angle of attack and tracking position values for each axle in the NYCT fleet. Each distribution is generally normal about its mean. However, some other more interesting trends can be identified. First of all, the average angle of attack and tracking position when all axles are considered is nearly zero. This is due to the behavior of the other axles. It is seen that Axles 1 and 3 (the trailing axles) have a negative mean average angle of attack. On the other hand, axles 2 and 4 (the leading axles) have a positive mean average angle of attack. When referring back to the sign convention in Figure 1, it is clear that some axles may be skewed. For example, axles 1 and 2 (which are on the same truck) are contacting the rail at different directions. If all axles and trucks were behaving properly, this should not be the case. Furthermore, it is seen that Axles 1 and 2 (which are on the same truck) have a negative mean average tracking position. On the other hand, axles 3 and 4 (which are on the same truck) have a positive mean average tracking position. This suggests that as cars are traveling through the instrumented curve, the leading truck tends to shift in one direction, while the trailing truck shifts in the other direction. Again, this may be an indication of poor truck performance. Therefore, there may be a population of poor trucks that are affecting the behavior of the entire population. Ultimately, when this data is joined with and compared to the wear rate data, it will be interesting to see if high average angles of attack and tracking positions correlate with the excessive wear rates. If so, this would indicate that wheel wear is predominantly affected by truck performance.

In addition to angle of attack and tracking position, speed is also an important measured parameter. The faster an axle is traveling through a curve, the higher the generated positive forces will be on the high rail. Increased forces directly lead to increased wear. Thus, the average speed values that

were obtained were also investigated. Figure 37 and Table 7 show the distribution and descriptive statistics for the average speed of each axle measured by the TBOGI.

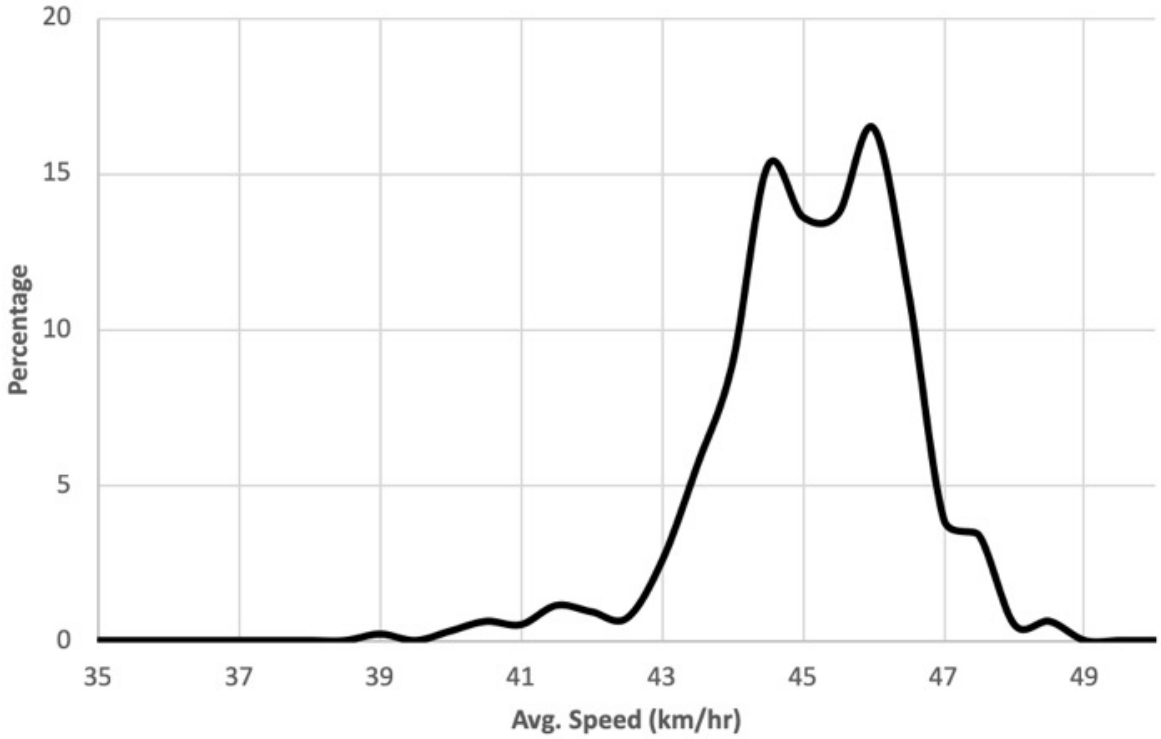

Figure 37 Histogram of average speed.

Table 7 Descriptive Statistics for Average Speed (km/hr)

	Mean	Median	Std. Dev.	Min	Max	1st Quartile	3rd Quartile
SPEED	44.899	44.995	1.371	38.690	48.163	44.157	45.832

This information reiterates what was discovered about the speed of axles through the TBOGI site earlier. It is seen that on average, nearly all axles are traveling through the TBOGI site between 43 and 47 km/hr. There are some axles outside of this range, however, the vast majority of axles are traveling at the same speed, on average. This means that the average lateral forces felt at this site should be relatively constant as well. Again, it is also seen that trains are travelling significantly under balance speed on average, possibly indicating lower high rail forces.

Figure 38 shows histograms of the averages of the other measured parameters; inter-axle misalignment, tracking error, rotation, and shift. Table 8 presents the descriptive statistics of these parameters.

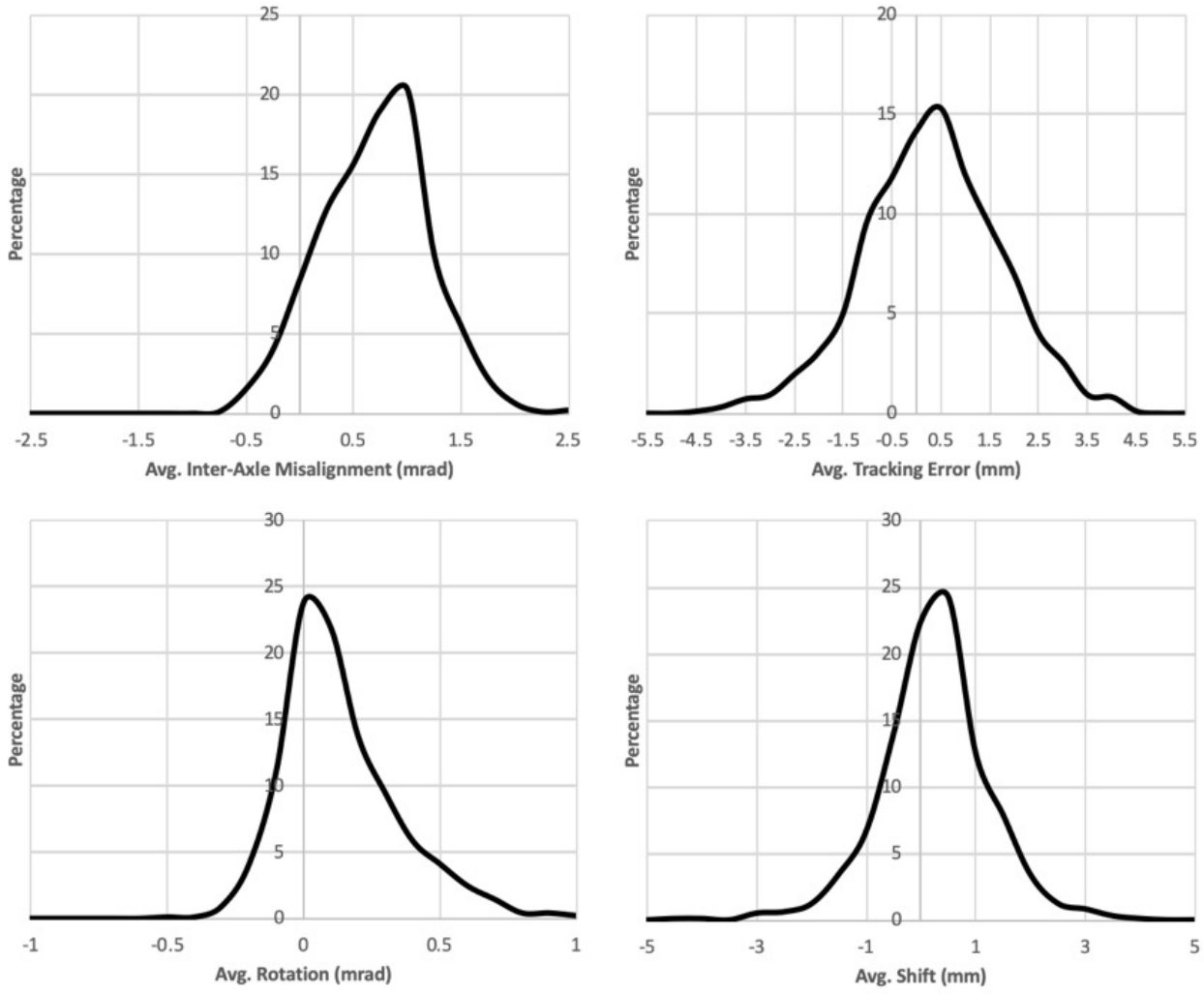

Figure 38 Histograms of average inter-axle misalignment, tracking error, rotation, and shift.

Table 8 Descriptive Statistics of Average Inter-Axle Misalignment, Tracking Error, Rotation, and Shift

	Mean	Median	Std. Dev.	Min	Max	1st Quartile	3rd Quartile
IAM (mrad)	0.572	0.607	0.506	-0.803	2.459	0.217	0.905
TE (mm)	0.065	0.085	1.419	-4.520	5.546	-0.867	0.991
ROT (mrad)	0.083	0.039	0.213	-0.520	0.909	-0.058	0.194
SHIFT (mm)	-0.001	0.009	0.987	-4.754	3.668	-0.565	0.534

The distributions for these for variables all appear to be generally normally distributed about their means. That being said, the mean average values of tracking error, rotation, and shift are all nearly zero. However, the mean average inter-axle misalignment in more significant, at 0.572 mrad. As mentioned, during NYCTA's study, it was cited that for the given speed of travel, the measured

inter-axle misalignments were alarmingly higher than expected, according to WID. Again, this indicates that there are some trucks in the 7 Line fleet exhibiting poor performance, which may ultimately be leading to accelerated wheel wear.

Initial Correlation Analysis of the Data

One of the primary objectives of this research was to find a distinct relationship between wheel wear rate and one of the other measured parameters (L/V ratio, angle of attack, tracking position, speed, etc.). There are many ways to find relationships between variables. One way is to use Pearson's correlation coefficient; a numerical value between -1 and 1 indicating the strength of the relationship between two variables. The closer the value is to -1 or 1, the stronger the relationship. Unfortunately, calculating Pearson's correlation coefficient for these variables did not yield satisfactory results, as shown in Figure 39. When looking at the relationship between wear rate (k) and the other variables, there are no strong relations. No Pearson coefficients are large enough to be significant.

	k	AvgLV	AvgLat	AvgVert	AvgAOA	AvgTP	AvgIAM	AvgTE	AvgRot	AvgShift	AvgSpeed
k	1.000000000	0.002839406	0.006371975	0.01642112	0.009850030	-0.002778877	-0.009543460	0.038154348	-0.003893673	0.005489232	-0.04281779
AvgLV	0.002839406	1.000000000	0.991829161	0.52214751	-0.008629087	-0.072563329	-0.007197121	0.001984808	0.010595511	-0.035318419	0.03135509
AvgLat	0.006371975	0.991829161	1.000000000	0.55183360	-0.013940682	-0.069275181	-0.016393104	0.001813796	0.012143800	-0.026168675	0.03436178
AvgVert	0.016421119	0.522147508	0.551833595	1.00000000	0.050144352	0.133291676	-0.276591843	0.034179518	-0.039364437	0.146915571	0.02876053
AvgAOA	0.009850030	-0.008629087	-0.013940682	0.05014435	1.000000000	0.116391919	0.167634754	0.092764972	0.572096605	0.055627724	0.03664461
AvgTP	-0.002778877	-0.072563329	-0.069275181	0.13329168	0.116391919	1.000000000	-0.005966442	0.031285374	-0.059883478	0.829284355	-0.01472817
AvgIAM	-0.009543460	-0.007197121	-0.016393104	-0.27659184	0.167634754	-0.005966442	1.000000000	0.160790416	0.386487011	-0.001742483	0.05696660
AvgTE	0.038154348	0.001984808	0.001813796	0.03417952	0.092764972	0.031285374	0.160790416	1.000000000	0.077137637	0.034663132	-0.10692175
AvgRot	-0.003893673	0.010595511	0.012143800	-0.03936444	0.572096605	-0.059883478	0.386487011	0.077137637	1.000000000	-0.068492416	0.12445583
AvgShift	0.005489232	-0.035318419	-0.026168675	0.14691557	0.055627724	0.829284355	-0.001742483	0.034663132	-0.068492416	1.000000000	-0.01330020
AvgSpeed	-0.042817789	0.031355086	0.034361784	0.02876053	0.036644606	-0.014728173	0.056966598	-0.106921752	0.124455827	-0.013300197	1.00000000

Figure 39 Correlation matrix.

Another method used to examine relationships between variables are scatter plots. Plotting the values of one variable against another can lead to assumptions being made about trends within the data. Since considering all of the data did not yield any strong results (see Figure 39), the decision was made to analyze the variables on a wheel-by-wheel basis. Organizing the data in a more focused way could lead to relationships being found that were previously hidden due to the amount of data initially considered. Furthermore, wheels 1R and 3R were chosen to be the focal points of such analyses. As seen in the previously presented L/V distributions, wheels 1R and 3R exhibited higher L/V ratios when compared to other wheels. Analyzing these wheels would highlight these high L/V values and determine whether or not they had an impact on wheel wear. Presented on the following pages are scatterplot matrices of the wheel 1R and 3R datasets. The same matrices were created for all other wheels and can be found in Appendix B. Unfortunately, once again there does not appear to be any significant relationships between wear rate and the other parameters. Again, there is a split distribution of L/V values for wheel 3R, indicating that some wheels are experiencing higher lateral forces than others. However, no clear conclusions can be drawn from these figures as to how this impacts wear rate. Therefore, further refined correlation analyses must be conducted, and will be discussed in future chapters.

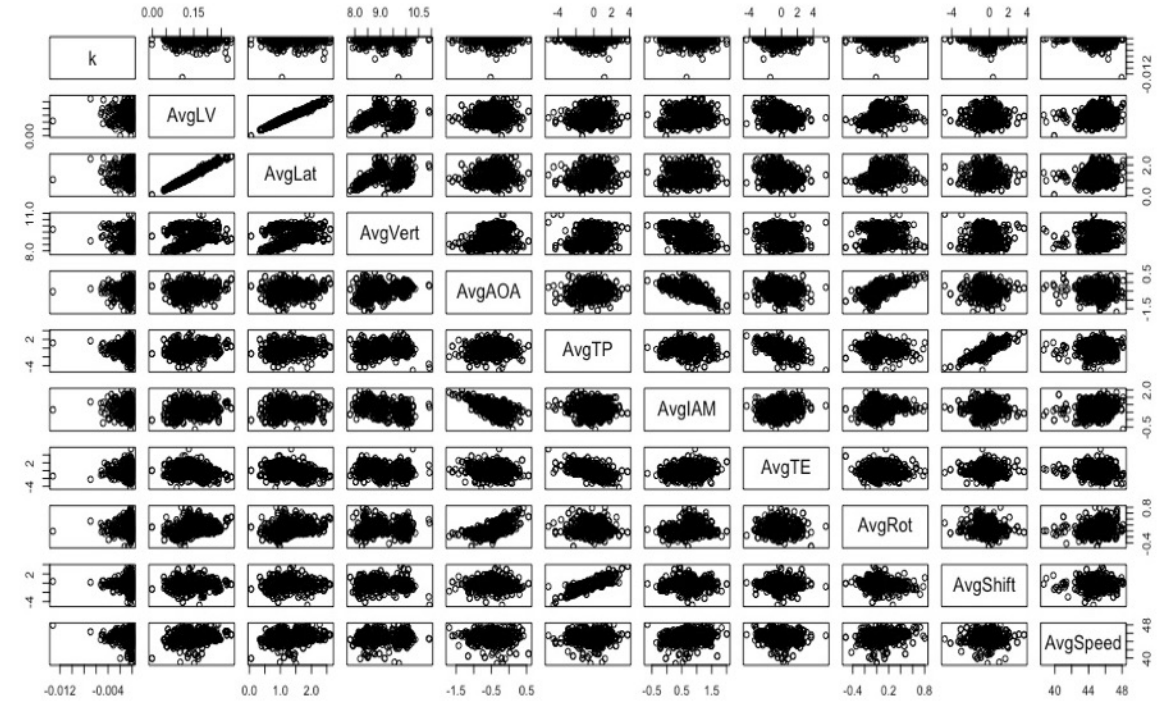

Figure 40 Scatterplot matrix for wheel 1R.

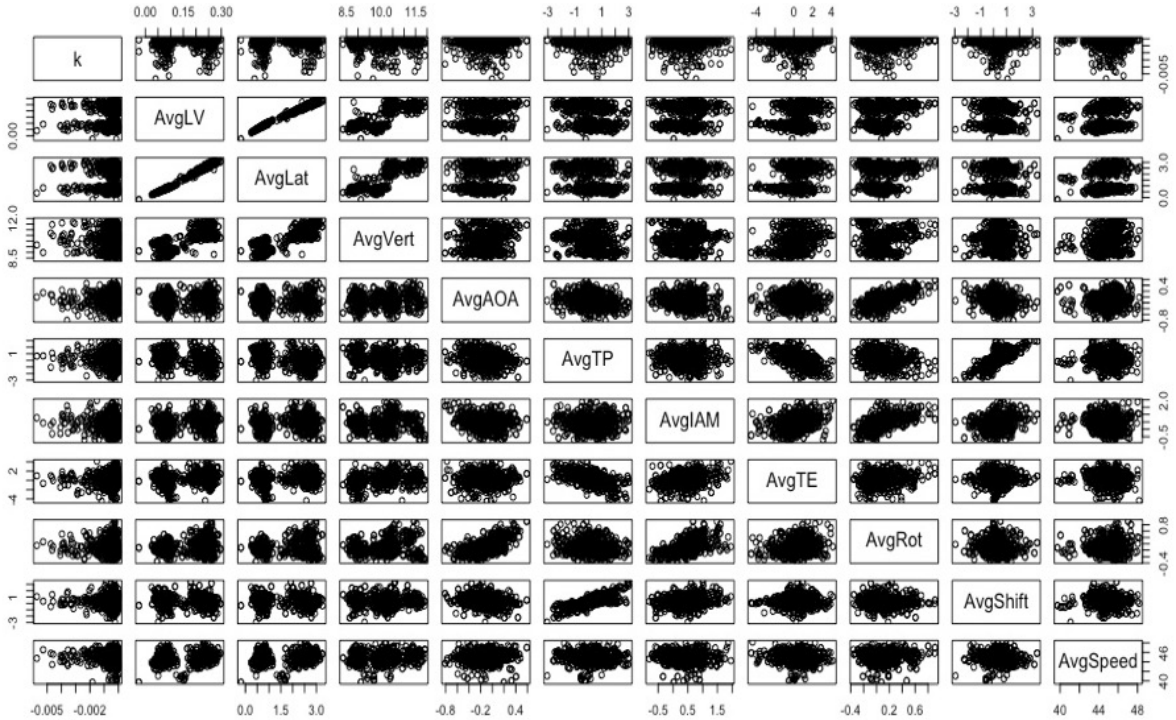

Figure 41 Scatterplot matrix for wheel 3R.

FORECASTING FUTURE MAINTENANCE EVENTS

As outlined in the prior chapters, the primary objective of this study was to calculate flange wear rates. These wear rates could then be utilized to forecast future maintenance events, according to NYCTA maintenance standards. From the wear rate data developed in the aforementioned nonlinear regression analysis, the A and k parameters for each maintenance cycle of every wheel in the 7 Line fleet are known. Thus, these values can be used to calculate the time it will take for any given wheel to reach the threshold of 24.2 mm. It is worthwhile to mention that for any given wheel, any of the life conditions shown in Figure 42 can exist. First, a wheel can have an unknown start date, meaning it is not known when it was put in service. Second, a wheel can have an unknown end date, meaning it is not known when it will be taken out of service. These are the wheels that will be used to forecast future maintenance events. Lastly, there are a small population of wheels which have a known start and end date. For these wheels, there is enough data to show two maintenance events. These wheels will be compared to the wheel forecasts in order to evaluate the forecast results. Note that Figure 42 does not correspond to any wheel in the fleet. Rather, this data was created to better visualize wheel life conditions.

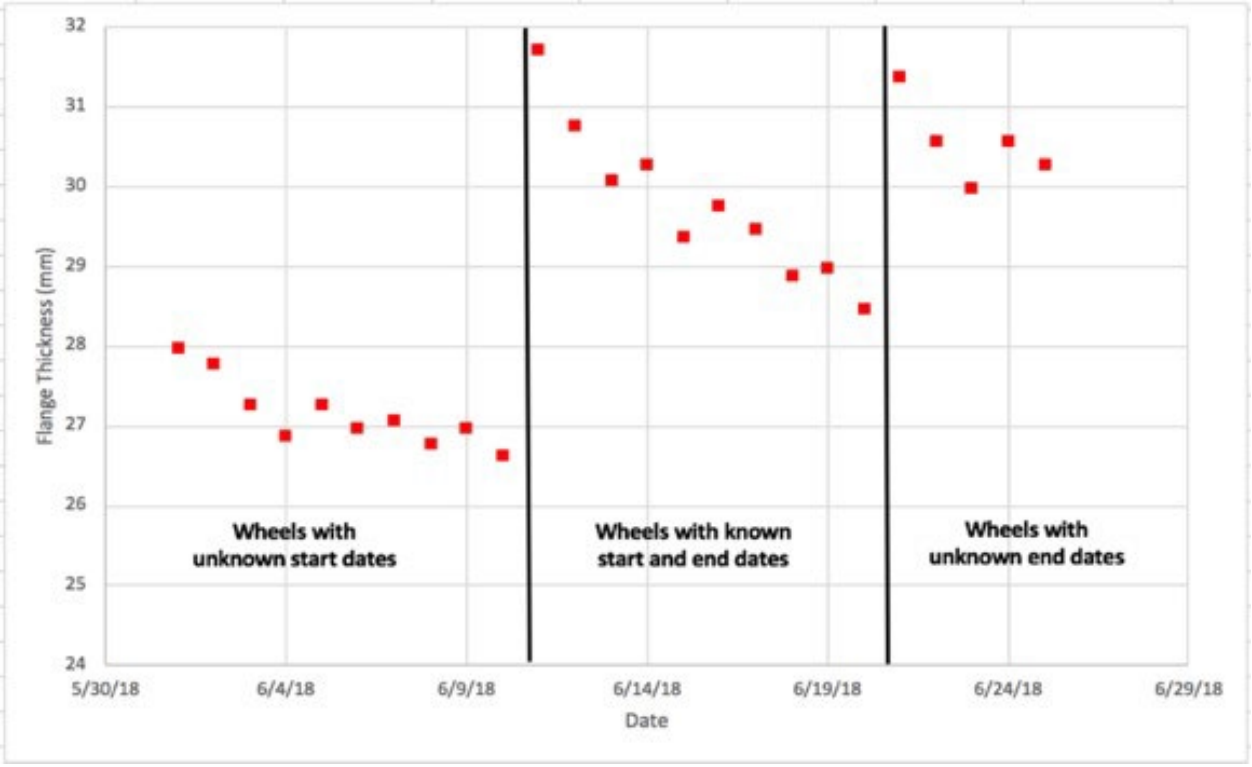

Figure 42 Examples of wheel life conditions.

Predicting Future Maintenance Events

In this analysis, any wheel that met the previously described condition of having an unknown end date was used in the forecasting of future maintenance cycles. When referring back to Equation 2, a flange thickness value can be substituted for y. From the wear rate data developed in the nonlinear regression analysis, the A and k parameters for each maintenance cycle of every wheel in the 7 Line fleet are known. With known A and k parameters, x; the time it will take to reach this flange thickness value; can be calculated. In other words, if the last recorded flange thickness measurement by the KLD Automatic Wheelscan and the NYCTA flange thickness maintenance threshold are substituted for y, wheel life can be calculated by solving for the x value. This is shown in Equation 3.

$$x = \frac{ln\left(\frac{y_{threshold}}{A}\right)}{k} - \frac{ln\left(\frac{y_{last}}{A}\right)}{k} \quad (3)$$

Where

x = time to reach the NYCTA flange thickness maintenance threshold (days)
A = constant (mm)
k = wear rate (1/days)
$y_{threshold}$ = 24.2 mm (NYCTA flange thickness maintenance threshold)
y_{last} = the last recorded flange thickness measurement mm)

By taking the results of Equation 3, and adding it to the time that the wheel was in service for prior to the measurement of y_{last} (which is known based on the nature of the data) a value for total wheel life is obtained, based on a flange thickness threshold of 24.2 mm and the wear rate parameters specific to that wheel. This calculation was performed for each wheel that met the condition of having an unknown end date. Figure 43 presents histograms of both the last recorded flange thicknesses and predicted wheel lives.

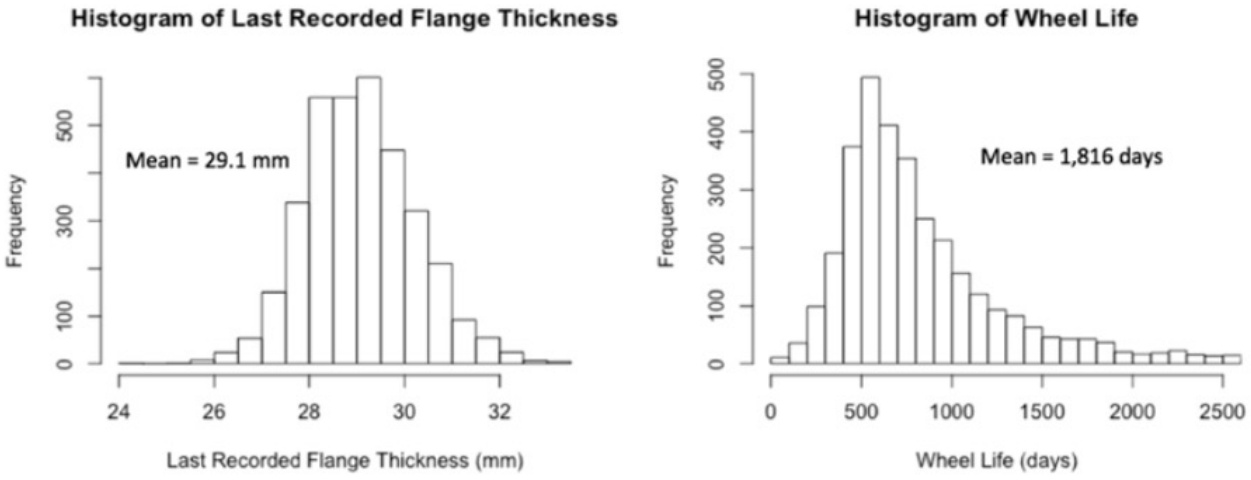

Figure 43 Histograms of last recorded flange thickness (left) and wheel life (right).

As can be seen in the histogram of the last recorded flange thickness, there is a broad range of values. Final flange thicknesses anywhere from 25 mm to just over 32 mm have been recorded. While new wheels are expected to have a flange thickness no greater than 32.1mm, it is understood that there is a system tolerance which can introduce variability. This range of values indicates that there are wheels at different points in their life cycle. Some wheels have very low measurements, meaning they are approaching the time when maintenance must occur. Other wheels have higher flange measurements, meaning that they have recently been installed or trued. In addition, there is a large group of wheels with a last flange thickness value between 28 mm and 30 mm. This would suggest that on average, most wheels in this fleet should have a significant amount of life remaining before maintenance would become necessary.

The results shown in the histogram of predicted wheel life are not as clear. At first glance, a mean maintenance cycle of 1,816 days is clearly excessive. This high mean is a result of a few extremely high maintenance intervals that are not displayed in the figure. Since the wear rate is exponential, the data may appear to behave asymptotically, with results approaching infinity. This is not realistic. To account for this issue, wheels with extremely low k values were removed, so that the overall population would not be skewed by these few wheels. Another issue that was found is that some wheels have very few data points. This too can cause abnormally long lives to be calculated. In addition, this can also result in abnormally short lives. As discussed earlier, there is a sharp initial wear-in period that a majority of these wheels experience. If too few data points exist, the regression fit will be entirely within this wear-in period and will not account for the overall behavior of the wheel across its whole life. Thus, any wheels with less than ten data points were removed. After investigating numerous wheels with the sharp wear-in period, a value of ten was determined to be the minimum number of points needed to encompass a wheel's full behavior. Lastly, any wheel with a R2 value less than 0.50 was removed. This ensured that only the wheels fit well by the exponential function were included in the analyses. Applying such filters resulted in 2,460 total wheels to be included in further analyses. Figure 44 shows revised histograms of those shown in Figure 43, with the aforementioned data filtering criteria applied.

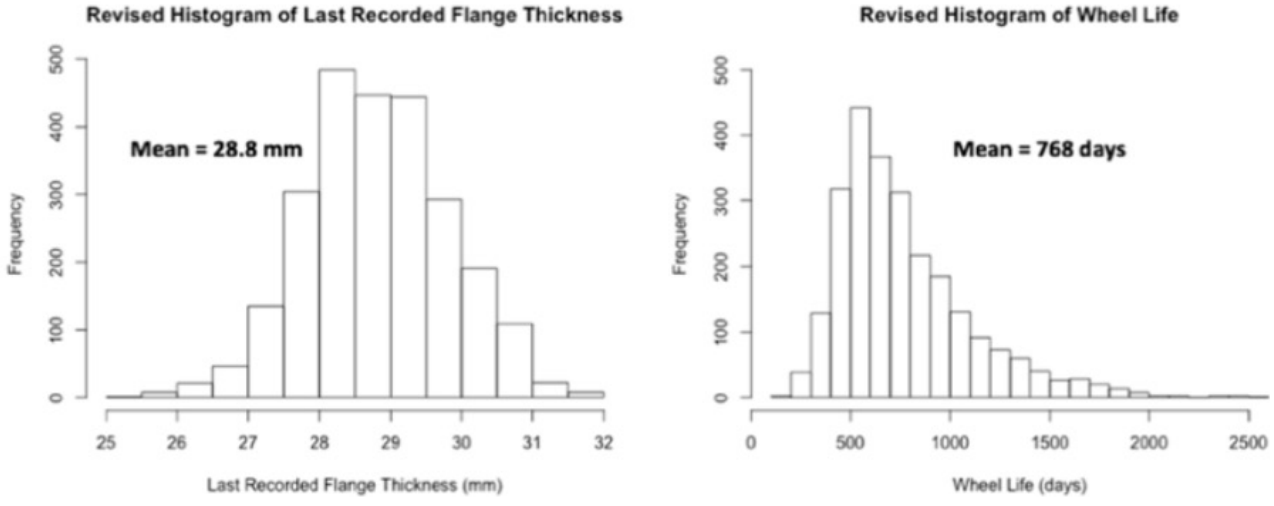

Figure 44 Revised histograms of last recorded flange thickness (left) and wheel life (right).

While the shapes of the histograms presented in Figure 44 remained relatively unchanged, the unrealistic and outlier data points have been removed from the analysis. This allows for more accurate results that are representative of the fleet's behavior, namely a mean maintenance cycle of 768 days. This value is still quite excessive, and suggests that on average, a wheel in the NYCT 7 Line fleet can last for about two years without maintenance. Although a majority of the outlier data points have been removed, this value is still likely overestimated. As mentioned, exponential regression treats the data asymptotically. This assumes that the wheels will continue to wear at a very slow rate once the initial sharp wear in period ends. In practice, this is most likely not the case. Defects can form in the wheel or the rail that can lead to accelerated wear. The exponential regression model cannot account for such factors. In addition, it is important to keep in mind that the calculated wear rates are based solely on time. In the rail industry, time is seldom used as a benchmark due to differences in tonnage and mileage. However, this data was not made available for this study, and thus could not be incorporated. Had this data been available, key information such as vehicle out of service time and total mileage could have been utilized to produce more accurate wear rates.

Yet, with a more focused data set and improved data accuracy, a plot of flange thickness against maintenance interval could be created. Figure 45 shows how maintenance interval is affected by the last flange measurement and wear rate. Each point on this plot represents one wheel. As can be seen, there is a widespread distribution of wheels with varying behaviors. Some wheels have very high last flange measurements, but short maintenance intervals. This indicates that these wheels have a high wear rate, and may be associated with cars that have poor steering characteristics, misaligned trucks, or high generated forces. If so, it could be inferred that these wheels are behaving poorly and can be deemed "bad actors". This idea will be expounded upon in future sections. In addition, there are some wheels that are projected to last many years until the next maintenance cycle. As noted previously, this is not realistic and is simply a result of the asymptotic behavior of the exponential fit, as well as the lack of mileage information. Yet, this plot still shows that there are some wheels that are performing better than other wheels. From a practical perspective, this means that some wheels in the 7 Line fleet may not need to be maintained or inspected as frequently. On the other hand, those wheels displaying poor performance need to be more regularly maintained and inspected, as to preserve appropriate levels of safety. Thus, it is of great importance to be able to classify wheels based upon their performance, in order to better understand the inherent characteristics that govern their behavior.

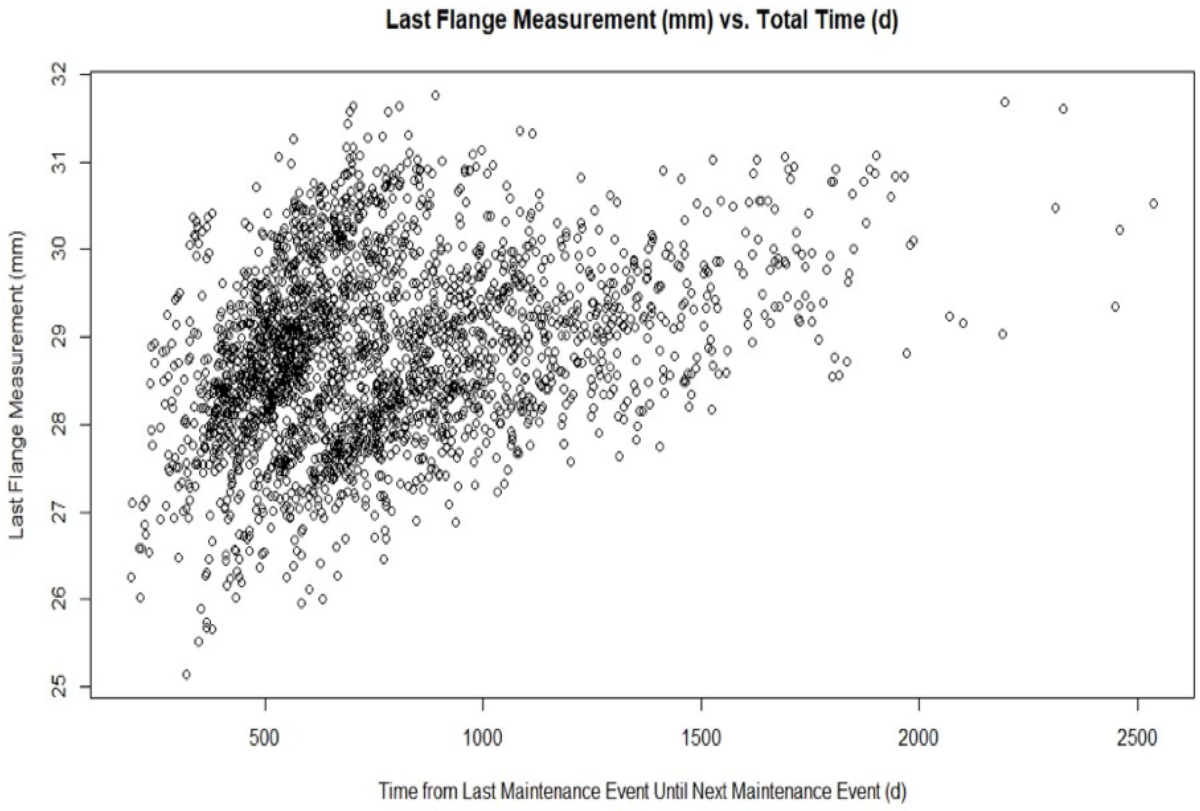

Figure 45 Plot of last recorded flange thickness (mm) vs. predicted wheel life (days).

Comparison to Wheels with Known Lives

The prediction of wheel life presented in the previous section revealed a great deal about wheel behavior. However, in order to better interpret these results, it is important to analyze the small population of wheels which have known start and end dates. As presented in Figure 42, there is a small population of wheels which have a known start and end date. For these wheels, there is enough data to show two maintenance events. Therefore, it is easily possible calculate the lives of these wheels by simply taking the difference between the start and end dates. Essentially, this is the life of that specific wheel. By comparing these known lives to those lives which have been predicted, more sense can be made of the obtained results. While there are not many of these wheels in the database (555 total wheels), there are enough to form a few conclusions. Figure 46 presents a histogram of wheel life for those wheels whose start and end dates are known. As can be seen here, a majority of the wheels in this population have lives less than 100 days, or about 3 months. However, there are some wheels that are lasting close to 300 days, or almost 10 months. Again, the split between good and poor wheel performance is seen. Note however that the term "life" refers to the time from the last maintenance event until the next maintenance event.

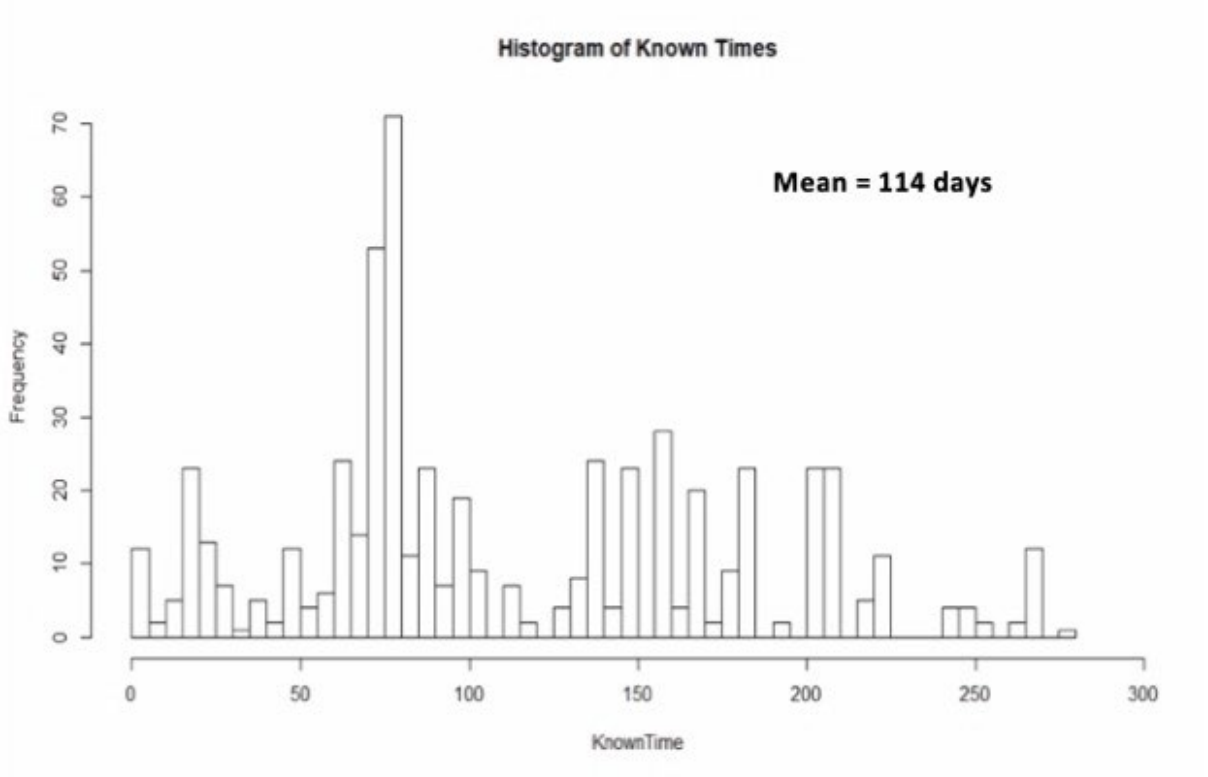

Figure 46 Histogram of known wheel lives.

Figure 46 becomes particularly interesting when it is compared to the histogram of predicted wheel life shown in Figure 44. Figure 47 compares the predicted wheel lives and the known wheel lives. Although the population sizes greatly differ, it is clear that substantially longer lives are being predicted than the lives that are actually known. Again, this could be an indication of some of the shortcomings discussed earlier. As discussed, the asymptotic nature of exponential regression may tend to overestimate wheel life. Also, missing information such as mileage, rail defects, and wheel defects did not allow for the model to be as robust as possible. This may also be an indication that using exponential regression is not the best way to fit and project the data at hand. However, by applying the aforementioned R^2 threshold of 0.50, this issue should be somewhat addressed, since that is indicative of a good fit with the data. Using such a threshold ensures only those wheels with accurately fitted regression lines are used in the analysis. While it may be true that the lives that have been predicted are slightly overestimated, there is another explanation for the difference between the red and blue histograms. Figure 47 could be a sign that wheels are being trued too early. This theory will be investigated in the following section.

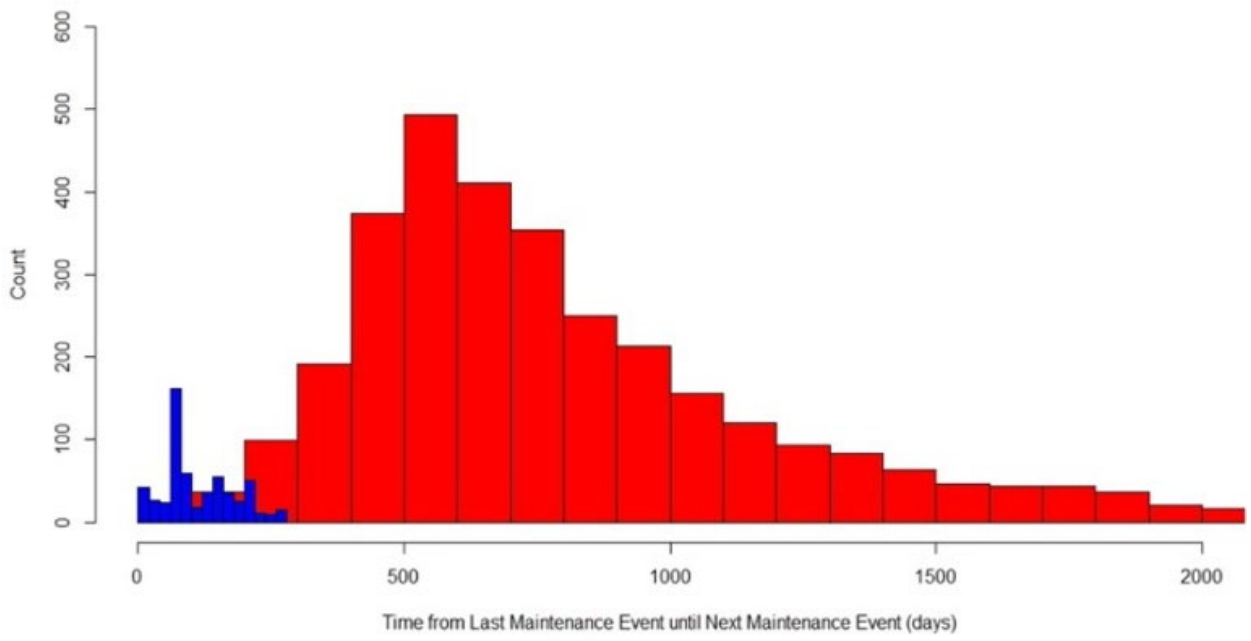

Figure 47 Histogram of wheel life for predicted (red) and known (blue) wheel lives.

Examination of Current Maintenance Practices

As previously noted, Figure 47 suggests that wheels are being trued or replaced too early. According to the current NYCTA standards, truing occurs when the flange thickness approaches an "8" on the AAR finger gauge, or 24.2 mm. In addition, a new or recently trued wheel will read "0" on the AAR finger gauge, or 32.1 mm. However, Figure 47 shows that wheels are not reaching their full potential "lifespan". In Figure 47, the red histogram shows that when wheel life is forecasted to a flange thickness limit of 24.2 mm (the NYCTA standard), significantly longer maintenance intervals are predicted than what have been seen in the field thus far.

In order to examine whether or not wheels were being trued too early, two histograms of the last recorded flange thickness measurement were created. Figure 48 and Figure 49 present histograms of the last known flange thickness measurements, normalized to give a percentage. Moreover, the data shown here represent a specific wheel's flange thickness measurement just before a maintenance event is known to occur. Referring back to Figure 42, the flange thickness measurement just before a maintenance event can be determined for two of the three wheel life conditions. Figure 48 displays the last flange thickness measurements for any wheel that meets the known start and end date condition. These are those 555 wheels used for comparisons in the previous section. In addition, Figure 49 combines these data with those of any wheel with an unknown start date. Although the exact lifespan of these wheels is unknown, the last flange thickness measurement just before maintenance can be utilized to further investigate whether or not wheels are being trued too early. This results in a total of 4,144 wheels. In Figure 48 and Figure 49, it can be observed that the mean last flange thickness measurements before maintenance were 28.5 mm and 27.9 mm, respectively. This confirms that maintenance is occurring too early. On average, the last flange thickness measurement just before a maintenance event is nearly 4 mm

greater than the 24.2 mm NYCTA standard for wheel replacement or truing. Essentially, this means that an average of 4 mm of life is being wasted, as wheels are not being allowed to wear to the limit. This type of practice restricts wheels from reaching their full potential in terms of life, and in turn, can greatly increase maintenance costs and out of service time. Ultimately, this fact appears to be the reason why the forecasted lives are significantly greater than known lives.

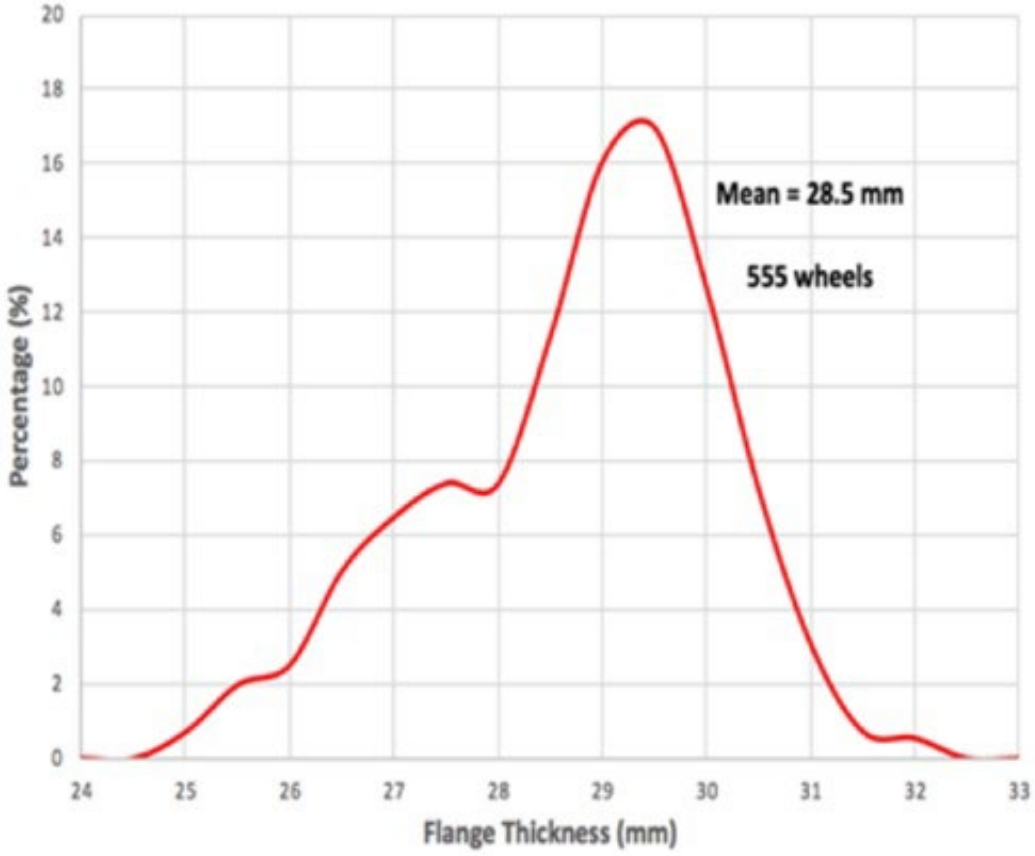

Figure 48 Histogram of last recorded flange thickness measurements before maintenance for wheels with known lives.

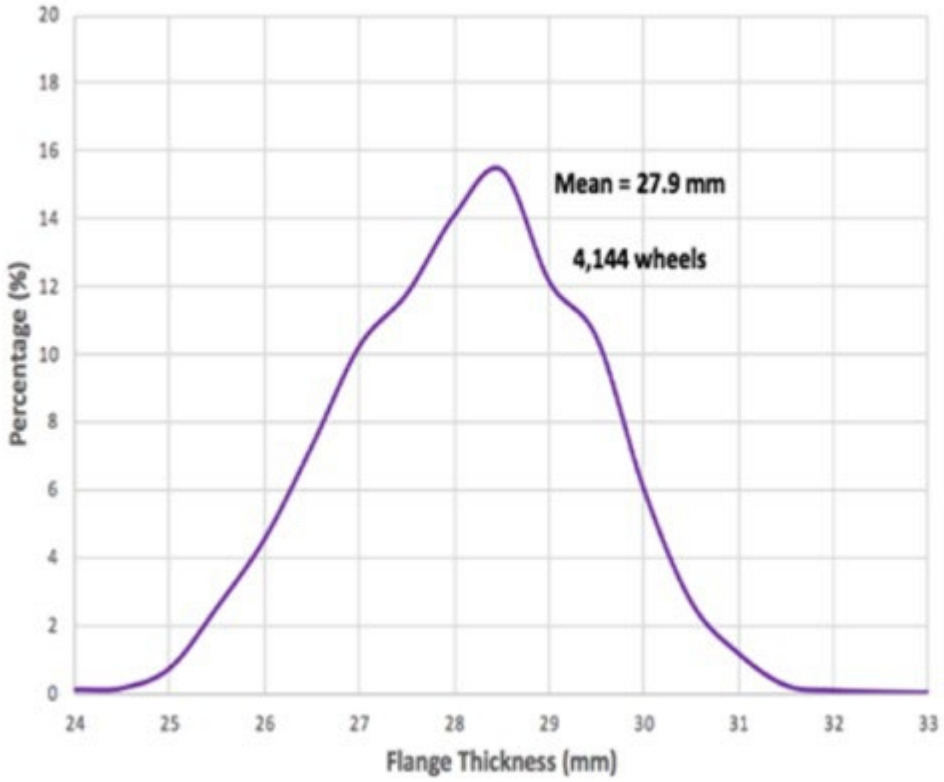

Figure 49 Histogram of all known last recorded flange thickness measurements before maintenance.

Adjusting current practices to allow wheels to wear to the flange limit may prove beneficial to NYCTA. In order to better visualize and understand the implications of such adjustments, new forecasts were made. As before, the 2,460 total wheels with unknown end dates were used. By substituting new values for $y_{threshold}$ into Equation 3, new predictions could be made as to when wheels will reach various flange thickness values. Here, it was decided that forecasts would be made to 27.9 mm; the mean last flange thickness measurement before maintenance in Figure 49. It should be noted that any wheel whose last flange measurement was already below the mean value of 27.9 mm would have a life equal to the time that had already elapsed since the last maintenance event. Thus, based on this new threshold of 27.9 mm, this wheel should have been trued or replaced already. These forecasts were then converted into histograms normalized to give a percentage. In addition, they were compared to the predicted lives when a threshold of 24.2 mm is used, as well as those lives which are known. These results are presented in Figure 50. Table 9 shows the average wheel life for each of these distributions.

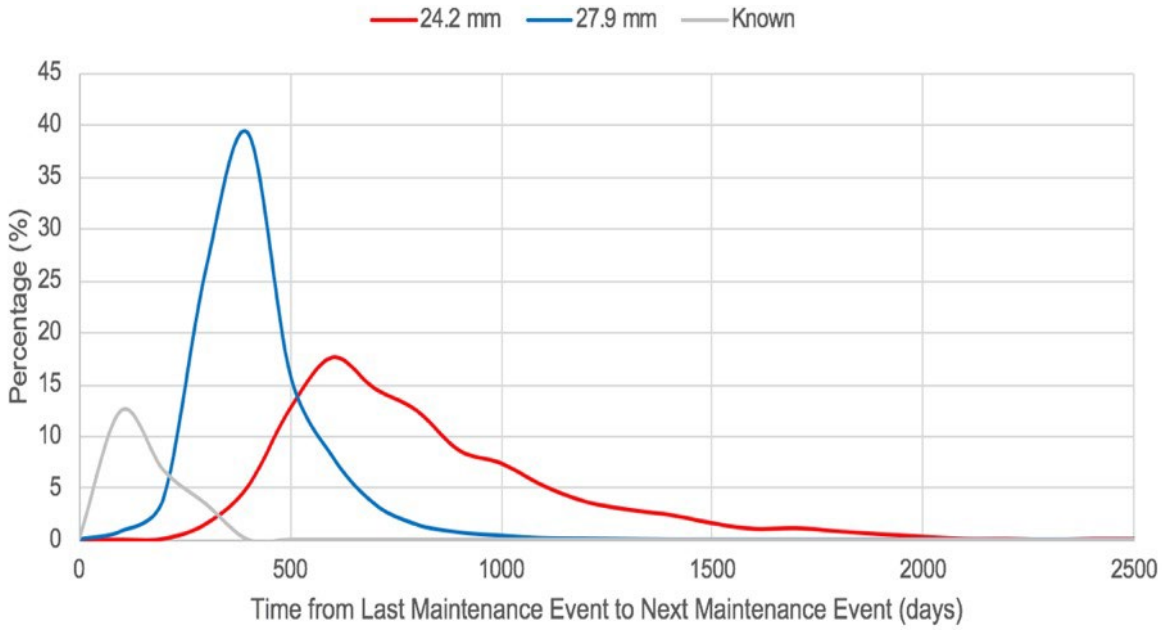

Figure 50 Comparison of predicted wheel lives.

Table 9 Comparison of Average Wheel Lives

Distribution	Average Wheel Life (days)
24.2 mm limit (red)	768
27.9 mm limit (blue)	368
Known lives (gray)	114

Figure 50 compares predicted wheel maintenance intervals for varying flange thickness thresholds. Wheel maintenance based on a threshold of 24.2 mm is shown in red and based on a threshold of 27.9 mm is shown in blue. In addition, the known intervals for wheels with known cycles is shown in gray. Again, this is a much smaller population, however, it falls much more in line with the new projections. The slight shift to the right could once again be due to the asymptotic nature of the exponential fit, as well as the other shortcomings associated with the manner in which wear rates were calculated. However, although the predictions are still overestimated, the manner in which they were calculated is sound. Therefore, it can still be confidently stated that maintenance is occurring too early, and adjustments should be made to maximize the service time of these particular wheels.

Based on the results of Figure 50, it appears that NYCTA is currently being quite conservative in its maintenance efforts. By consistently performing maintenance at higher flange thickness limits, wheels may be trued or removed prematurely. It can be seen that on average, 300 days of life is being wasted. While truing at higher thresholds allows for a greater factor of safety against accidents and derailments, it can decrease the overall life of the wheel. From a cost perspective, truing at higher thresholds may lead to increased maintenance, labor, and out of service time. For

all operating railroads, one of the highest annual costs is consistently maintenance cost. By allowing wheels to continue to wear, great savings could be experienced. In addition, out of service time hinders a passenger system such as NYCTA. The greater the out of service time is, the less trains there are in service. This greatly impacts passenger experience and overall customer service.

However, it should be noted that NYCTA currently trues an entire truck during a maintenance cycle. In other words, if one wheel on a truck reaches the NYCTA flange thickness maintenance limit of 24.2 mm, all four wheels are trued regardless. This is done in order to reduce maintenance costs and out of service time. It is a more efficient maintenance approach than just truing one wheel at a time. Truing an entire truck also allows for the lateral stability and effective conicity of the wheelsets to be preserved; which is crucial in derailment prevention. This approach could be the underlying reason as to why an average last flange thickness measurement before maintenance of 27.9 mm was identified. One excessively worn wheel is forcing the other three to be trued. Nonetheless, there are still some wheels on a truck that are being trued or replaced before it is necessary. Again, in order to maximize wheel life, adjustments to current practice could be made. Perhaps NYCTA could investigate truing on an "axle-basis" rather than a "truck basis". This would result in only two wheels being trued at a time rather than four, effectively reducing the number of prematurely maintained wheels. However, the safety implications and risks of such changes need to be examined prior to a decision being made.

INVESTIGATION OF WHEELS WITH POOR PERFORMANCE

As previously discussed, Figure 45 displays the results of the forecasting study. For those wheels whose maintenance cycle is unknown, the last flange thickness measurement is plotted against total maintenance interval. As shown, it is clear that there are some wheels that have a higher rate of wear than other wheels. Thus, there are wheels with relatively short lives even though their final recorded flange thickness was quite high. For example, refer to the population of wheels whose final recorded flange thickness was greater than 30 mm. When forecasting to the threshold of 24.2 mm, these wheels should last the longest. However, it is seen that a small population of these wheels have some of the shortest predicted lives. Conversely, there are some wheels with lower final flange thickness values, yet longer predicted lives. The data suggest that within the NYCTA fleet of cars, there are some wheels that have extremely high rates of wear and some wheels with very low rates of wear. These wheels could be exhibiting high wear rates for a variety of reasons, including poorly steering trucks and associated high lateral forces, softer wheels, or other causes associated with either the wheel itself or with the car or truck.

Clearly, it is of great practical significance to be able to identify these "bad actor" wheels, so that they may be more regularly inspected and maintained before their poor behavior compromises overall safety. In addition, determining the causal factors related to poor wheel performance would promote better and maintenance of the truck and vehicle to reduce the rate of wear. Furthermore, if it could be predicted which wheels would exhibit poor performance, then more preventive maintenance measures could be taken to reduce the likelihood of such behavior occurring. The following sections present a method for both classifying and predicting these bad actor wheels.

Classification of Wheels with Poor Performance

In order to accurately and appropriately classify the population of wheels, two unique methods were implemented. The first method involves the use of k-means cluster analysis. Unfortunately, its results were not ideal. Therefore, a second method which created statistical performance bands was explored. The results of this approach were much more in line with the behavior of the fleet and engineering judgment. The findings of the k-means cluster analysis and statistical performance band approaches are outlined in the following sections.

Cluster Analysis

First, a method for classifying wheels based on their performance needed to be established. This would be done by using the data shown in Figure 45. In data analytics, one technique that is commonly used to classify data is cluster analysis. Cluster analysis is usually performed in order to combine observations into unknown groups. Unlike other classification methods, the number and characteristics of the groups must be derived from tendencies within the dataset, and are unknown prior to the work being done (Afifi et. al., 2012). Here, it was thought that the wheels in the upper-left corner would be the bad actors. However, a more concrete analysis method was desired. There are many different types of cluster analysis that can be used, but for this work, k-means clustering was used. K-means clustering is one of the most common forms of cluster analysis, as it groups observations based on their distance from the means of predetermined clusters (Afifi et. al., 2012). It was decided that three clusters would be ideal for this analysis; one cluster of bad actors, one of good actors, and one of wheels that lie in between. The results of a k-means cluster analysis can be seen in Figure 51, where the three clusters are shown in different colors.

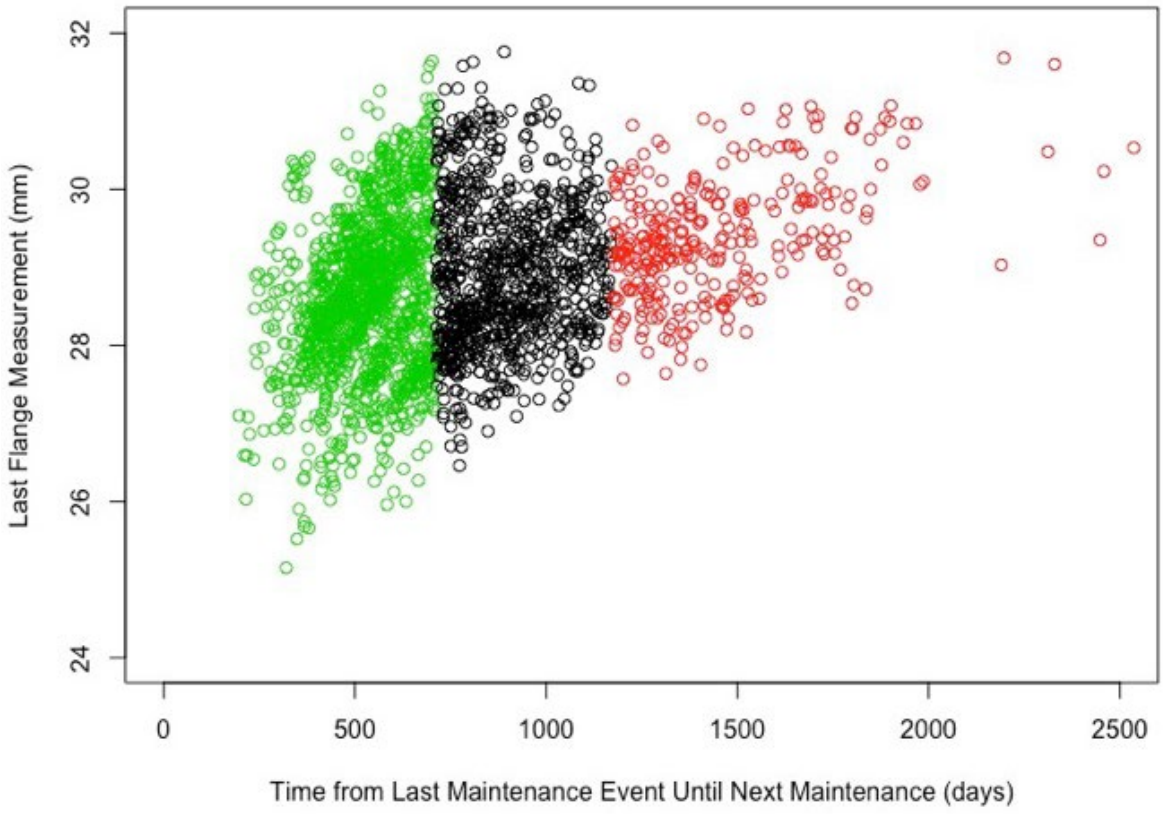

Figure 51 Results of K-means cluster analysis.

The results of the k-means cluster analysis show that wheels have been sorted into three performance-based clusters. The green cluster contains all of the wheels classified as bad actors. The red cluster contains all of the wheels classified as good actors. The black cluster contains all of the wheels that are somewhere between the two. While the k-means cluster analysis did create three distinct groups, it does not appear to appropriately take the last flange measurement into consideration when doing so. Rather, the wheels are sorted based solely on their predicted life. For example, all wheels with a life less than approximately 700 days were placed in the bad actor group. However, within this group, there are wheels are different points in their life cycle. For example, there are some wheels in this group with a last flange thickness measurement of less than 26 mm, while there are others with a last flange thickness measurement of more than 30 mm. Those wheels above 30 mm are likely bad actors, as they are expected to wear rapidly. However, those wheels less than 26 mm are most likely not bad actors. The expected life they have remaining is low due to the fact that they are so further along in their life cycle. It is important to account for where a wheel is in its life cycle when evaluating their performance. Thus, it is not acceptable to classify wheels based on a k-means cluster analysis.

Statistical Performance Bands

As the k-means cluster analysis did not yield ideal results, a secondary approach was undertaken. The approach used was to define performance bands to separate the good wheels from the bad wheels. This was done through an analysis of the data's standard deviation. The mean and standard

deviation was calculated for both variables (last flange thickness measurement and predicted wheel life). Each mean was adjusted by adding or subtracting one standard deviation. These boundaries were then set by passing lines through these points and the origin: a last flange thickness measurement of 24.2 mm (NYTA maintenance limit) and a wheel life of zero days. Based on this analysis approach, adding and subtracting a value of 1.5 times the standard deviation appeared to create the best results at first. Figure 52 presents these wheel performance bands.

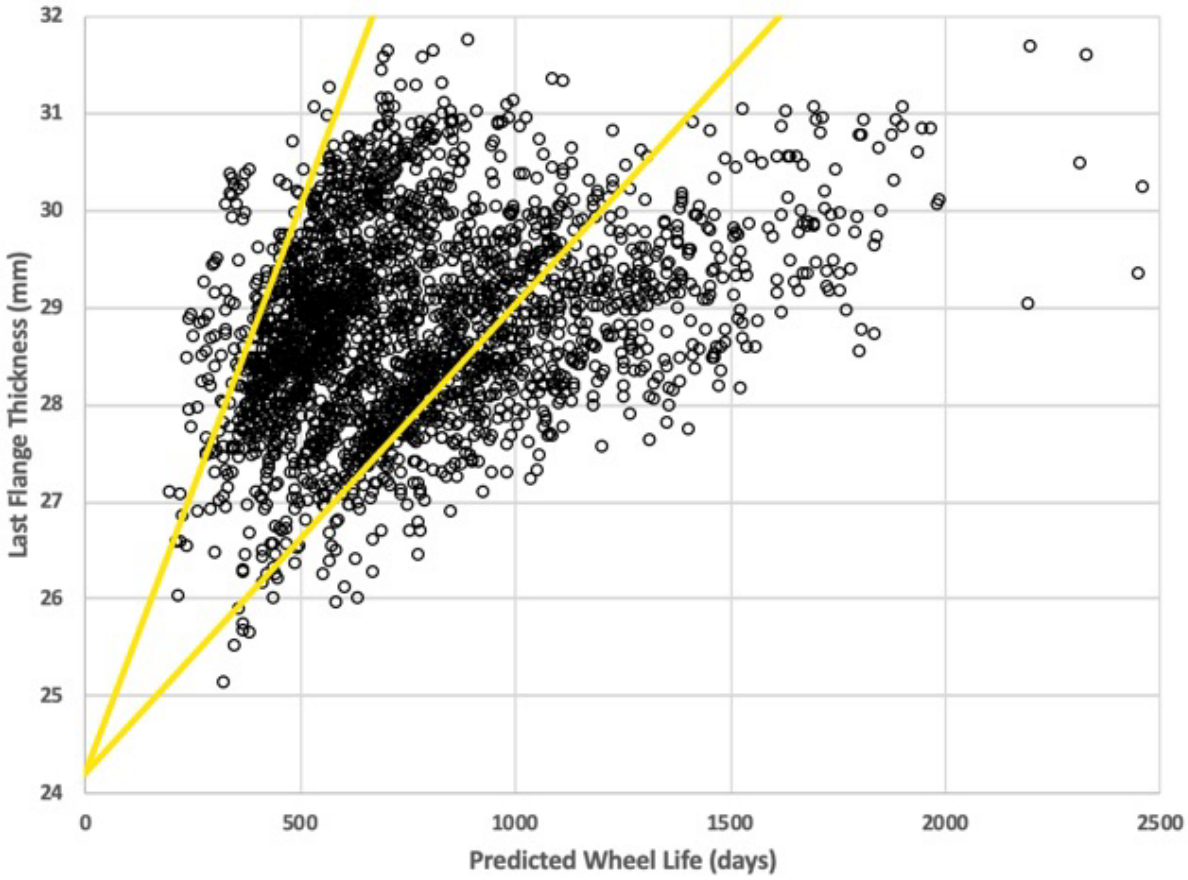

Figure 52 Plot of last flange thickness measurement vs. wheel life with performance bands.

As seen in, three distinct performance bands have been developed. The first set, consisting of a large population of wheels on the right side of the figure, are exhibiting relatively low wear rates. The second set, consisting of a small population of wheels on the left side, are exhibiting high wear rates. These are the "bad actor" wheels with high wear rates and relatively short lives, even though their final recorded flange thickness may have been relatively high. Finally, there is a large population of wheels that are somewhat in the middle exhibiting "average" wear rates. Also, this approach seems to better account for the last recorded flange thickness measurement; unlike k-means clustering. Using the performance bands better encompasses the full behavior of these wheels and creates more representative groupings. However, in Figure 52, only 89 of the 2,460 wheels were classified as bad actors. This means that in the entire NYCTA 7 line fleet, only 3.5% of the wheels are behaving poorly. Such a small sample size does not allow for one to form accurate conclusions. Therefore, the bands in Figure 52 were adjusted by adding and subtracting a value of 1 standard deviation, rather than 1.5. This is shown in Figure 53.

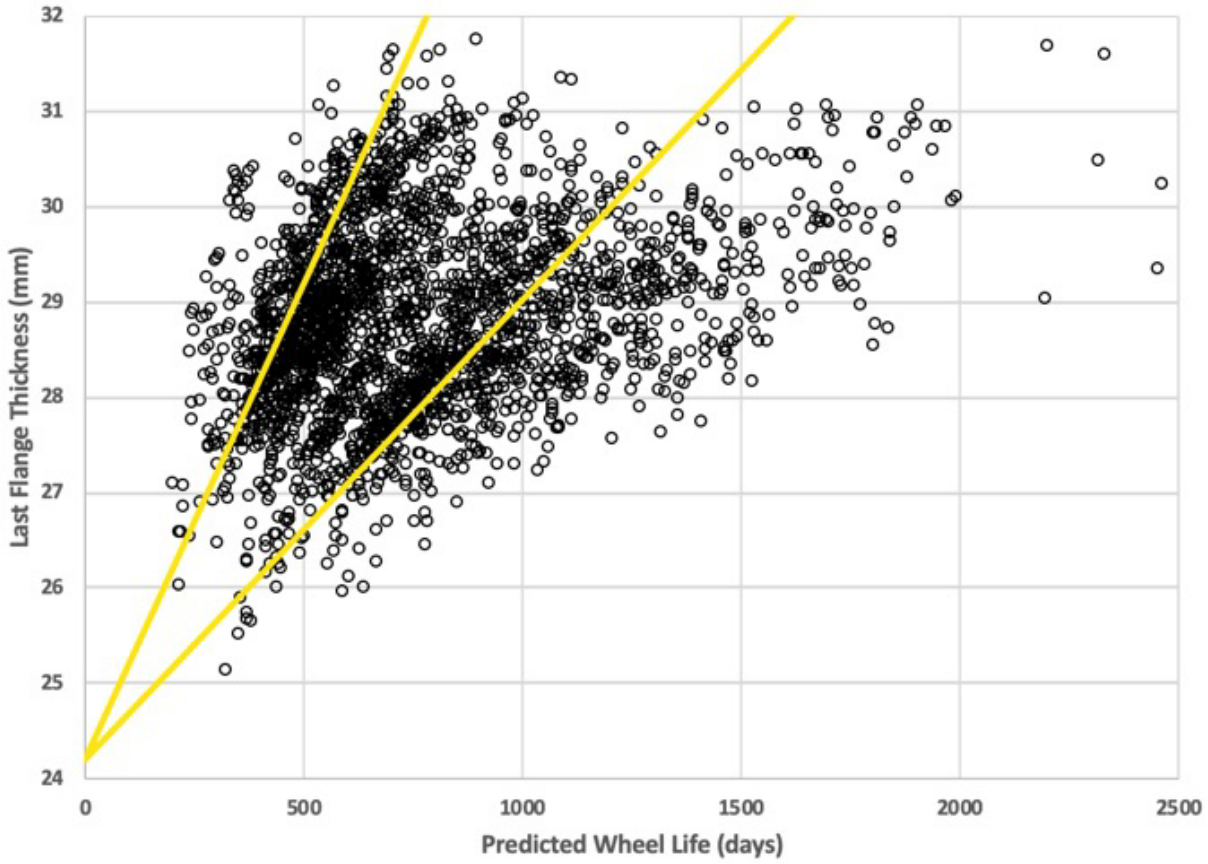

Figure 53 Revised plot of last flange thickness measurement vs. wheel life with performance bands.

Figure 53 shows the same tendencies as Figure 52. Three groups of wheels have been created, based upon their performance. However, by adjusting the bands to 1 standard deviation rather than 1.5, a larger population of bad actor wheels was obtained. The performance bands shown in Figure 53 results in a total of 295 bad actor wheels. This means that in the entire NYCTA 7 Line fleet, 11.8% of the wheels are behaving poorly. This is a much more substantial population of bad actors, and would allow for a more valid prediction model to be generated. Thus, it was decided that bad actor wheels would be classified based upon the statistical performance bands shown in Figure 53. A list of those 295 bad actor wheels can be found in Appendix C.

Wheel Performance Prediction Model

Once the wheels were classified as discussed in the prior section, the next step of the analysis was to create a model to predict a wheel's performance. The creation of an accurate model would allow for poor wheel performance to be identified earlier in its life cycle, allowing for more preventive maintenance measures to be enacted. For this work, a logistic regression model was created to calculate the probability of any given wheel being a bad actor wheel.

Introduction to Logistic Regression

Logistic regression is a common technique used in the realms of statistics, data science, and engineering. It is often used in order to classify observations into one of two populations, and applies to both discrete and continuous variables. A discrete variable is thought of as a binary classification variable. Examples include male or female, even or odd, and yes or no. Continuous variables on the other hand have an infinite number of possible measured values, and in logistic regression, are used in order to predict the value of a discrete variable. Therefore, an initial logistic regression analysis requires knowledge of both the dependent and independent variables, and its results can be later applied to cases where only the independent variables are known (Afifi et. al., 2012).

The basic form of the logistic regression function is:

$$P_Z = \frac{e^{\alpha+\beta_1 X_1+\beta_2 X_2+\cdots+\beta_n X_n}}{1+e^{\alpha+\beta_1 X_1+\beta_2 X_2+\cdots+\beta_n X_n}} \quad (4)$$

Where

P_Z = probability of occurrence
e = 2.71828 (mathematical constant)
α = logistic regression constant
β_n = logistic regression coefficients
X_n = independent variables

One of the fundamental assumptions of logistic regression is that the probability of occurrence is linearly related to each of the independent variables. Additionally, no assumptions need to be made about the distributions of the various independent variables. Unlike other methods which requires variables to be continuous and normal, logistic regression can account for all distributions and handle both discrete and continuous variables. This is one of the major advantages of using logistic regression: that it can be essentially applied to all data types. Furthermore, logistic regression uses the method of maximum likelihood. The method of maximum likelihood is an iterative estimation process that can be used to determine model parameters. These parameters are found in such a way that maximizes the likelihood that the observed data will be accurately produced by the generated model. The theories behind it are complex and beyond the scope of this work. However, the use of this method allows for the logistic regression parameters to be more robust than other linear classification methods (Afifi et. al. 2012).

Logistic Regression Model

The overarching goal of this portion of the research was to create a model that would predict the likelihood that a given wheel will exhibit poor performance and behavior. Based on the nature of the data that would be used to create a wheel performance prediction model, logistic regression was deemed the most appropriate method. As discussed, logistic regression is used to classify observations into one of two populations, and applies to both discrete and continuous variables. For the purposes of this work, the two populations that observations would be grouped into would be a bad and good actor wheel. Although the performance bands shown in Figure 53 create three

populations, applying logistic regression requires only two. Therefore, those 295 wheels originally classified as bad actors would remain bad actors. However, all of the remaining wheels would be thought of as the good actors, rather than splitting their population.

In turn, this would allow for the creation of a discrete variable; whether or not a wheel is a bad actor. Using the performance bands allowed for a simple binary variable to be generated. All of the bad actor wheels would be given a value of 1, while all of the good actor wheels would be given a value of 0. In addition, other discrete variables were created in order to classify the wheels in varying ways. These discrete variables were based solely on the predicted life of each wheel, with different values being used as thresholds for a bad actor. By creating multiple discrete variables, multiple logistic regression models were created. Each model was then analyzed and investigated, allowing for the most robust and realistic model possible to be selected. A summary of the different discrete variables used is presented in Table 10.

Table 10 Description of Discrete Variables

Name	Description	No. of Bad Actors
Bands	Classification of bad actors based upon the results shown in Figure 53.	295
Year	Any wheel with a life less than 1 year (365 days) would be classified as a bad actor.	98
Mean	Any wheel with a life less than the overall mean life (768 days) would be classified as a bad actor.	1230
MeanSD	Any wheel with a life less than the overall mean life minus 1 standard deviation (437 days) would be classified as a bad actor.	268
Quartile	Any wheel with a life less than the 25% quartile (533 days) would be classified as a bad actor.	615

However, in order to create a complete logistic regression model, continuous variables need to be incorporated. These continuous variables would come from the suite of instrumentation systems made available as part of NYCTA's research project, and would be used to develop a model that would predict the probability of a wheel being a bad actor. Values that were derived from the exponential regression of the KLD Automatic WheelScan data, as well as values directly measured by the L/V System and TBOGI would be included. Similar to the manner in which there were multiple discrete variables, different combinations of continuous variables were tested to obtain a final model. The variables that were used in order to develop a wheel performance prediction model can be seen in Table 11.

Table 11 Description of Continuous Variables

Variable	Abbreviation	Units	Instrumentation System
Wear Rate	k	$days^{-1}$	KLD Automatic WheelScan
Last Flange Thickness	Y_{last}	mm	KLD Automatic WheelScan
L/V Ratio	LV	N/A	L/V Measurement System

Angle of Attack	AOA	mrad	TBOGI
Tracking Position	TP	Mm	TBOGI
Speed	S	km/hr	TBOGI

With the various discrete and continuous variables outlined, a logistic regression model was created using R software. Different discrete variables and varying combinations of continuous variables were repeatedly tested. Yet, the best results were obtained when all six continuous variables were used to predict the discrete variable defined by the performance bands. If all six continuous variables were not used, the accuracy of the model was greatly compromised. This was especially true if the wear rate was excluded from the model. Similarly, using discrete variables other than that defined by the performance bands decreased accuracy. In addition, when referring back to Table 10, applying each discrete variable results in a different bad actor sample size. Using the Year variable only results in 98 bad actors, which is likely an underestimation. Conversely, using the Mean and Quartile variables likely overestimates the number of bad actors in the fleet. The MeanSD variable yields a similar bad actor population, but in the end, was not as accurate as the performance band approach. The resulting logistic regression function that was developed to predict the likelihood that a given wheel will exhibit poor performance and behavior is shown in Equation 5. From the R software, the various statistical parameters that are associated with the logistic regression function in Equation 5 can be seen in Figure 54.

$$P_{bad\ actor} = \frac{e^{(-53.860-18{,}960*k+2.202*Y_{last}-0.212*LV+0.147*AOA-0.053*TP-0.522*S)}}{1+e^{(-53.860-18{,}960*k+2.202*Y_{last}-0.212*LV+0.147*AOA-0.053*TP-0.522*S)}} \quad (5)$$

Where

$P_{bad\ actor}$ = probability of a wheel being a bad actor
e = 2.71828 (mathematical constant)
k = wear rate (1/days)
Y_{last} = last flange thickness measurement (mm)
LV = average L/V ratio
AOA = average angle of attack (mrad)
TP = average tracking position (mm)
S = speed (km/hr)

```
Deviance Residuals:
    Min       1Q   Median       3Q      Max
-2.5623  -0.2062  -0.0340  -0.0083   3.8231

Coefficients:
             Estimate Std. Error z value Pr(>|z|)
(Intercept) -5.386e+01  6.060e+00  -8.887  < 2e-16 ***
k           -1.896e+04  1.144e+03 -16.571  < 2e-16 ***
YLast        2.202e+00  1.616e-01  13.624  < 2e-16 ***
AvgLV       -2.122e-01  7.034e-01  -0.302    0.763
AvgAOA       1.465e-01  1.905e-01   0.769    0.442
AvgTP       -5.342e-02  8.581e-02  -0.623    0.534
AvgSpeed    -5.220e-01  9.742e-02  -5.358 8.43e-08 ***
---
Signif. codes:
0 ‘***’ 0.001 ‘**’ 0.01 ‘*’ 0.05 ‘.’ 0.1 ‘ ’ 1

(Dispersion parameter for binomial family taken to be 1)

    Null deviance: 1804.47  on 2459  degrees of freedom
Residual deviance:  748.24  on 2453  degrees of freedom
AIC: 762.24

Number of Fisher Scoring iterations: 8
```

Figure 54 Logistic regression function statistical parameters.

Based on the results of the logistic regression analysis, it can be concluded that wear rate has the greatest impact on determining a bad actor wheel. This can be seen by the values presented in Figure 54. Additionally, performing a basic parametric study reveals similar results. A parametric study is commonly done in the realm of statistics in order to evaluate the importance and influence of different independent variables. By changing the values of one independent variable while keeping all others constant, conclusions can be made regarding the impact of the altered variable. Essentially, this approach shows how one variable affects the outcome compared to other variables. Such an analysis was performed for this work, and the results can be seen in Figure 55.

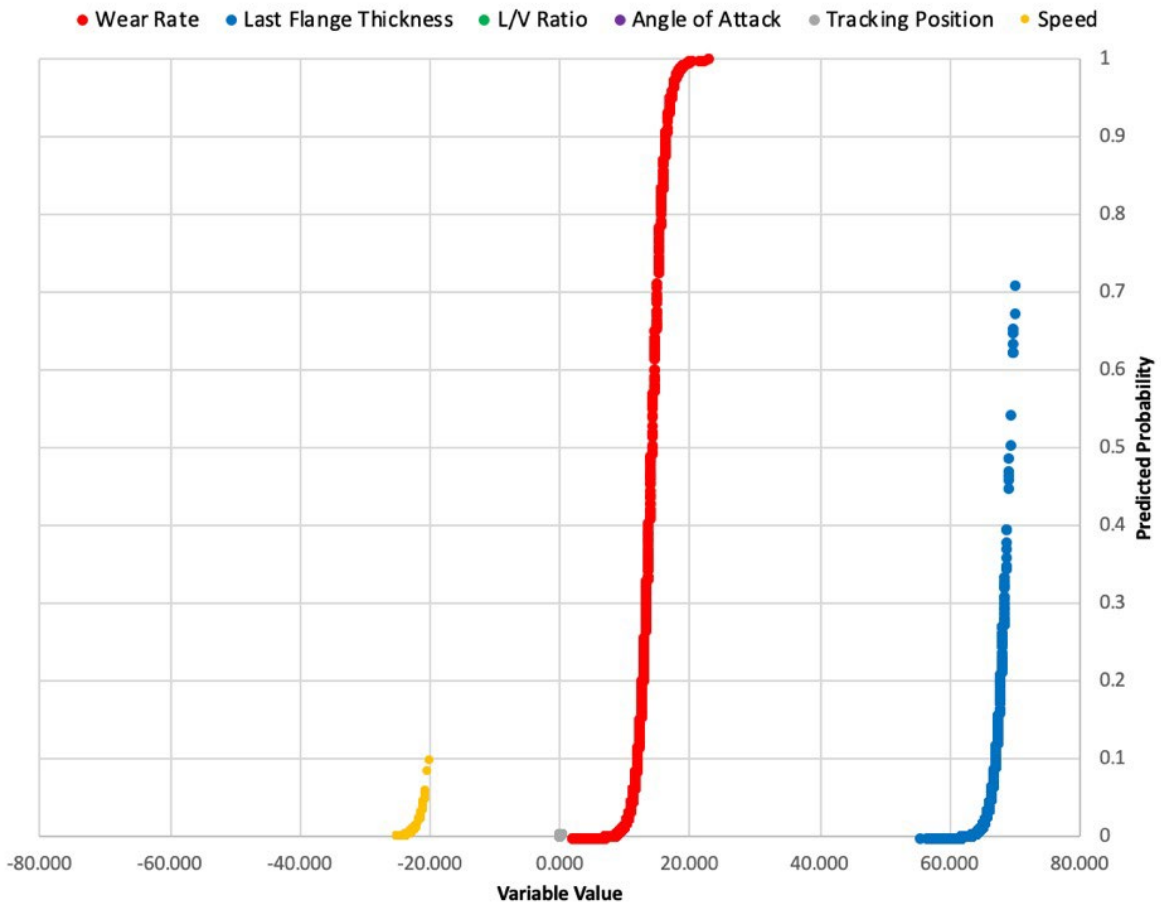

Figure 55 Parametric study of the variables included in the Logistic regression equation.

Figure 55 shows how altering wear rate, last flange thickness, L/V ratio, angle of attack, tracking position, and speed impact the probability of a bad actor wheel. Note that the x-axis displays the value of the variable when multiplied by its coefficient. This allows for all values to be on a similar scale, making comparisons easier. Again, it is clear that wear rate has the greatest impact on the probability of a bad actor. The variation in the wear rate value primarily governs whether or not the result of Equation 5 will be 0 or 1. Furthermore, last flange thickness also plays a large role. Intuitively, this makes reasonable sense, as the classification of bad actors relied heavily on wear rate, last flange thickness, and life. It is also a representation of where a wheel is in its life cycle, which is incorporated into the classification. Speed also appears to have some impact on the outcome, but not as significant as wear rate and last flange thickness. Lastly, L/V ratio, angle of attack, and tracking position are seemingly invisible on this plot. They all overlap one another near the point (0,0) and have no real impact on the outcome of Equation 5. This suggests that L/V ratio, angle of attack, and tracking position have no impact on a wheel's behavior. From an engineering perspective, this does not seem reasonable. It is expected that the greater these values are, the greater the lateral forces and subsequent wear will be. This should have some correlation with wheel performance. However, it is not apparent through logistic regression. This may be due to the fact that these variables are only measured at one location on the 7 line. The behavior at the instrumented site north of 103rd Street station may not be fully representative of the entire line.

Had data been available for more points along the entire line, perhaps the results of the parametric study would have been different. Nevertheless, the relationships between these variables (specifically L/V ratio) and wear rate will be further explored in the next chapter.

With the model created and the variables examined, the next step was to assess the accuracy of the results. As previously discussed, values for wear rate and last flange thickness were calculated from the KLD WheelScan data and average values for L/V ratio, angle of attack, tracking position, and speed were derived from the L/V Measurement System and TBOGI for every wheel in the fleet. These values were then substituted into Equation 5, calculating a value for $P_{bad\ actor}$ for every wheel in the fleet. A range of probability values were obtained, and it was determined from engineering judgement, as well as through trial and error, that a $P_{bad\ actor}$ value greater than 0.25 would identify a wheel as a bad actor. These results were then compared to the original classifications from the performance bands in order to assess the accuracy of the generated logistic regression model. All in all, the model that was created and shown in Equation 5 is quite accurate. This can be seen in the following figures and tables. Figure 56 shows the receiver operating characteristic (ROC) curve for the model. Table 12 shows the confusion matrix generated when the predicted results are compared to the actual results.

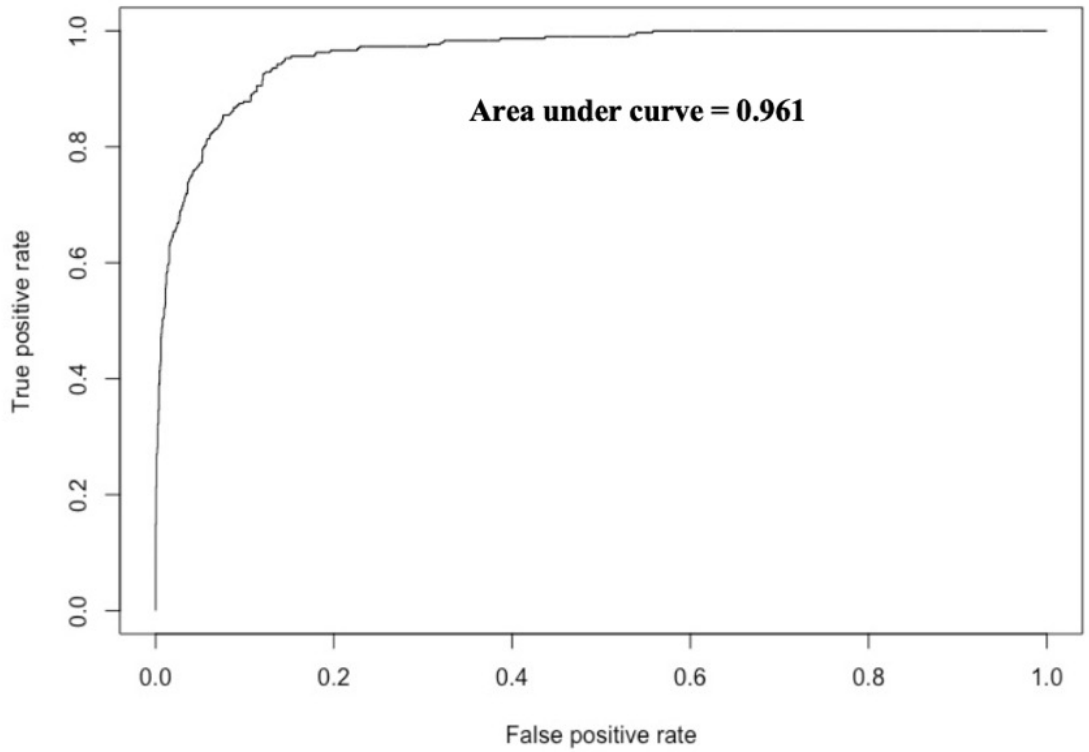

Figure 56 ROC curve for Logistic regression model.

Table 12 Confusion Matrix for Logistic Regression Model

	Actual Good Actor (0)	Actual Bad Actor (1)

Predicted Good Actor (0)	2,019 (93.3 %)	50 (16.9 %)
Predicted Bad Actor (1)	146 (6.7 %)	245 (83.1 %)

From the ROC curve, an area under the curve of 0.961 was calculated. The area under a ROC curve essentially represents how good a model is at differentiating between classes. It can range from 0 to 1, with 1 meaning the model perfectly classifies all observations (Afifi et. al., 2012). Therefore, an area under curve value of 0.961 means that the logistic regression model created performs very well, and is capable of distinguishing between good and bad actor wheels. The accuracy of the model is further validated by the confusion matrix. Out of the 2,165 total good actor wheels, 2,019 of them were correctly identified (93.3 %). Moreover, out of the 295 bad actor wheels, 245 of them were correctly identified (83.1 %). Although there are some observations that were falsely identified, the model is still quite accurate overall. Of the 2,460 total wheels used in the analysis, 2,264 were correctly classified. This means that the logistic regression model is operating at an overall accuracy of 92.1 % and can be deemed successful. To further validate the successfulness of the model, those wheels that were falsely identified were examined. The following figures show those wheels that are actually good actors but predicted as bad actors, and vice versa.

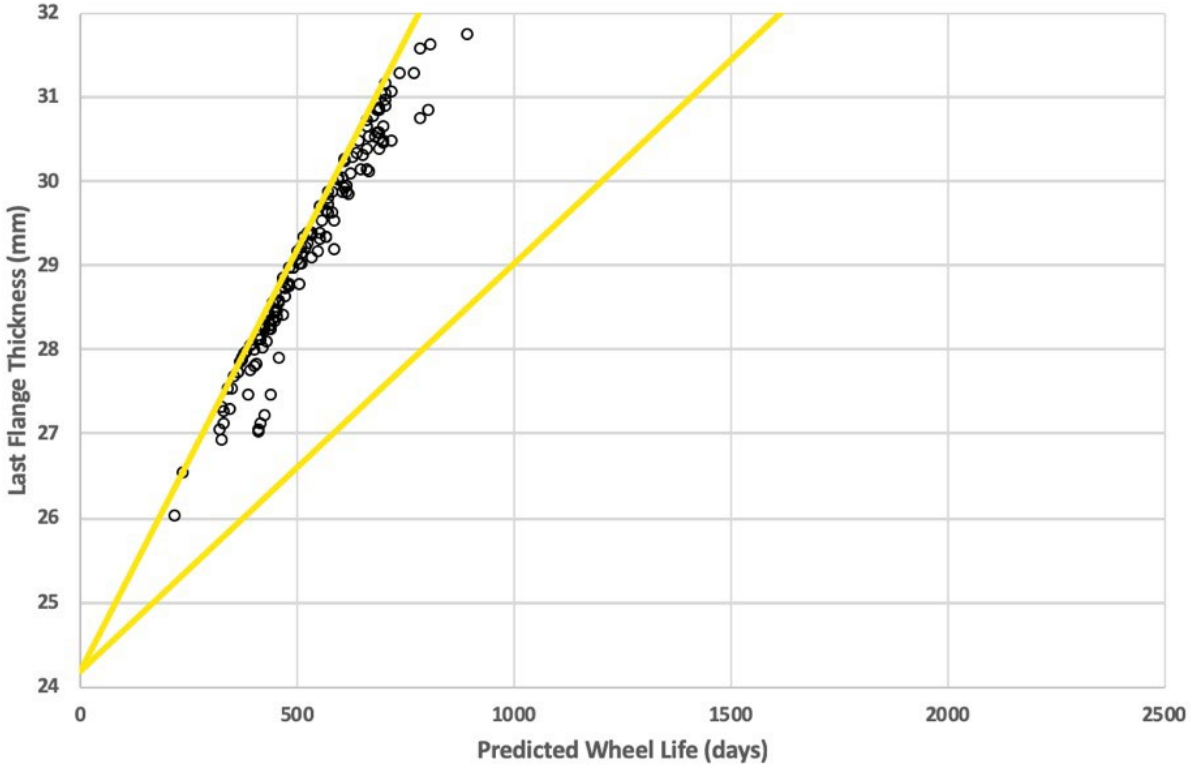

Figure 57 Good actors wheels predicted as bad actors (false positives).

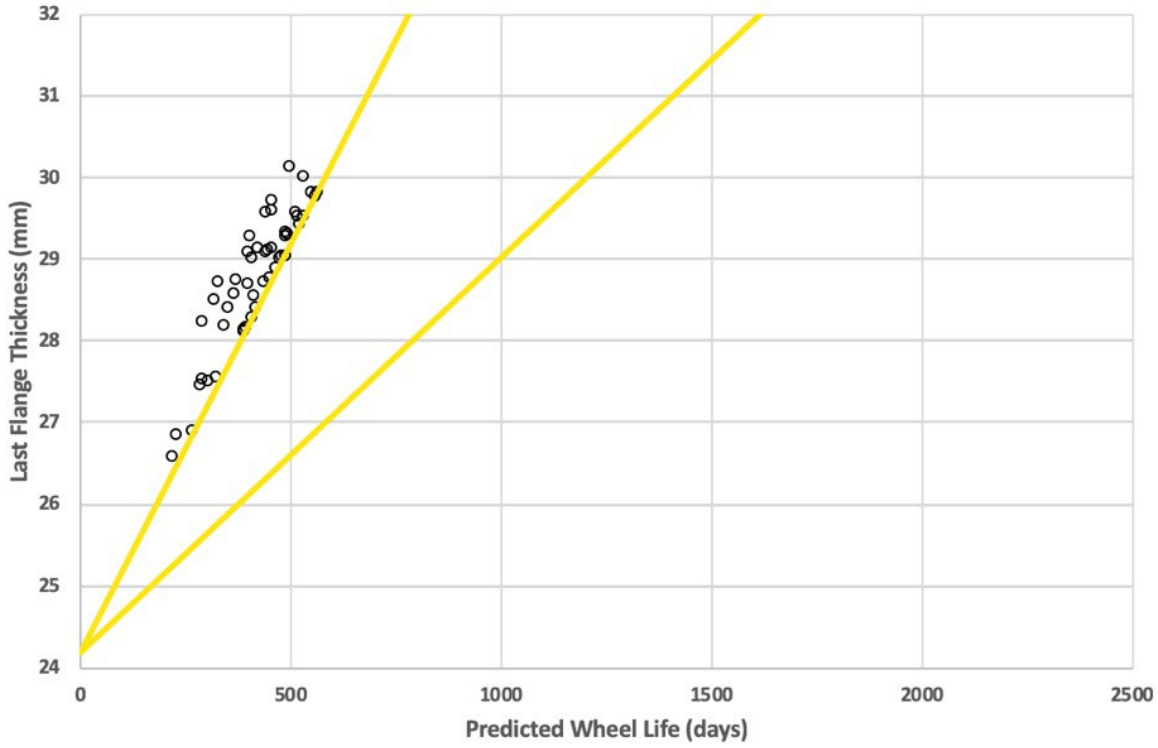

Figure 58 Bad actors wheels predicted as good actors (false negatives).

As can be seen in the two previous plots, those wheels that were incorrectly classified by the logistic regression model all hover on or near the performance band that was created to separate good and bad actors. This would suggest that the model is successful in classifying those wheels more towards the extremes; i.e. it can correctly identify the very bad actors and the very good actors. However, the model has some trouble correctly identifying those wheels which are near the performance band threshold. Yet, overall the model is still quite successful. Only 6.7 % of wheels were false positives, which is not necessarily a drawback. This would just mean that more preventive maintenance would take place. In fact, these wheels could be thought of as "at risk" of becoming a bad actor, and thus, maintenance would be beneficial in the long run. The 16.9 % of false negative wheels is a bit more alarming. When a wheel is not classified as a bad actor, preventive maintenance action cannot take place, and thus, safety may be compromised by allowing such wheels to continue to be in service. An ideal model would correctly identify all of the 295 bad actor wheels. However, for the scope of this work, 83.1 % was deemed to be an acceptable level of accuracy.

CORRELATING WHEEL WEAR RATE AND L/V RATIO

As shown in Figures 40 and 41, no apparent relationships can be determined between wear rate and the other measured variables. As discussed, split distributions of L/V values are seen for wheel 3R, indicating that some wheels are experiencing higher lateral forces than others. However, no clear conclusions can be drawn from these figures as to how this impacts wear rate. In addition, from the logistic regression model presented in the previous chapter, it was discovered that L/V ratio, angle of attack, and tracking position had little to no impact on the probability of a wheel behaving as a bad actor. This could lead to the assumption that these variables do not impact the wear rate of a rail wheel. From an engineering point of view, this is generally not the case. For the case of L/V ratio and even more likely L (Lateral load), there should be a strong positive correlation between with wear rate. An increase L/V ratio usually corresponds to an increase in the lateral forces between the wheel and the rail. This should generally increase the wheel's wear rate and decrease its expected life. However, this trend is not clear from the results presented thus far. Therefore, further refined correlation analyses were conducted in order to find a better relationship between wear rate and L/V ratio.

First, it was believed that the nature in which L/V ratio data was collected was contributing to the lack of a relationship with wheel wear. As explained earlier, the L/V ratios for all wheels were only measured at one location on the 7 line. The behavior at the instrumented site north of 103rd Street station may not be fully representative of the entire line. L/V data along the entire line is available thanks to the instrumented wheelsets, however, this is only for four wheels in the fleet. Had data been available for more wheels along the entire line, perhaps better relationships would have been found. Regardless though, the data from the L/V measurement system still should have some relation to the wheel wear data. A high L/V ratio should correlate with a high wear rate, and vice versa. Therefore, the decision was made to trim down the data shown in Figures 40 and 41 to only include those wheels with excessive wear rates. This would allow for a better understanding and visualization of how high wear rates are impacted by high L/V values.

When the exploratory data analysis of the L/V Measurement System data was conducted, it was found that wheels 1R and 3R exhibited higher L/V ratios when compared to other wheels. Continuing to analyze these wheels in particular would highlight the higher L/V values and determine whether or not they had an impact on increased wheel wear. The following figures present plots of L/V ratio against wheel wear rate. Only those wheels with high flange wear rates of less than -0.007 $days^{-1}$ are shown. In earlier scatterplots, all wheels were included. While including all wheels does have its advantages; such as the ability to draw conclusions regarding the entire population; it did tend to clutter the plots and make it more difficult to identify trends. Removing the wheels with less severe wear rates allows for a clearer and more concise dataset from which more effective conclusions can be drawn. Figures 59 and 60 present these plots for wheels 1R and 3R, respectively.

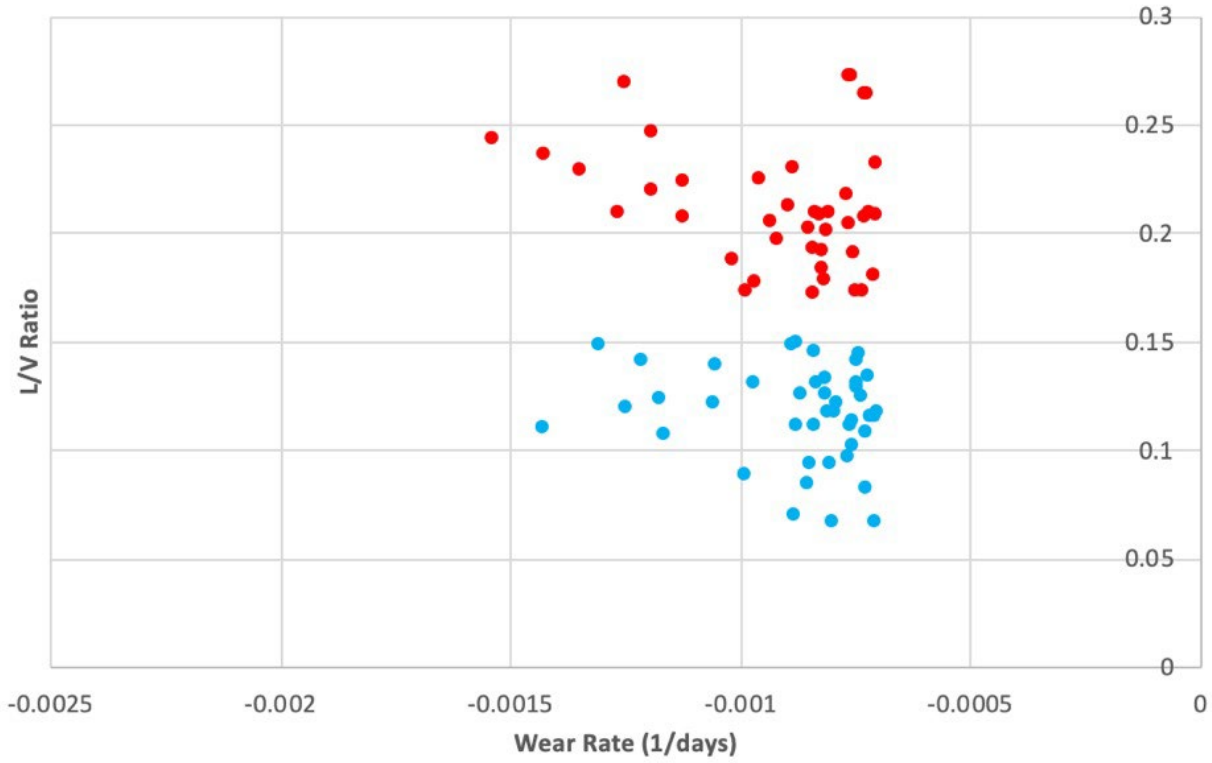

Figure 59 Scatterplot of L/V ratio vs. wear rates < -0.007 days^{-1} for 1R wheels.

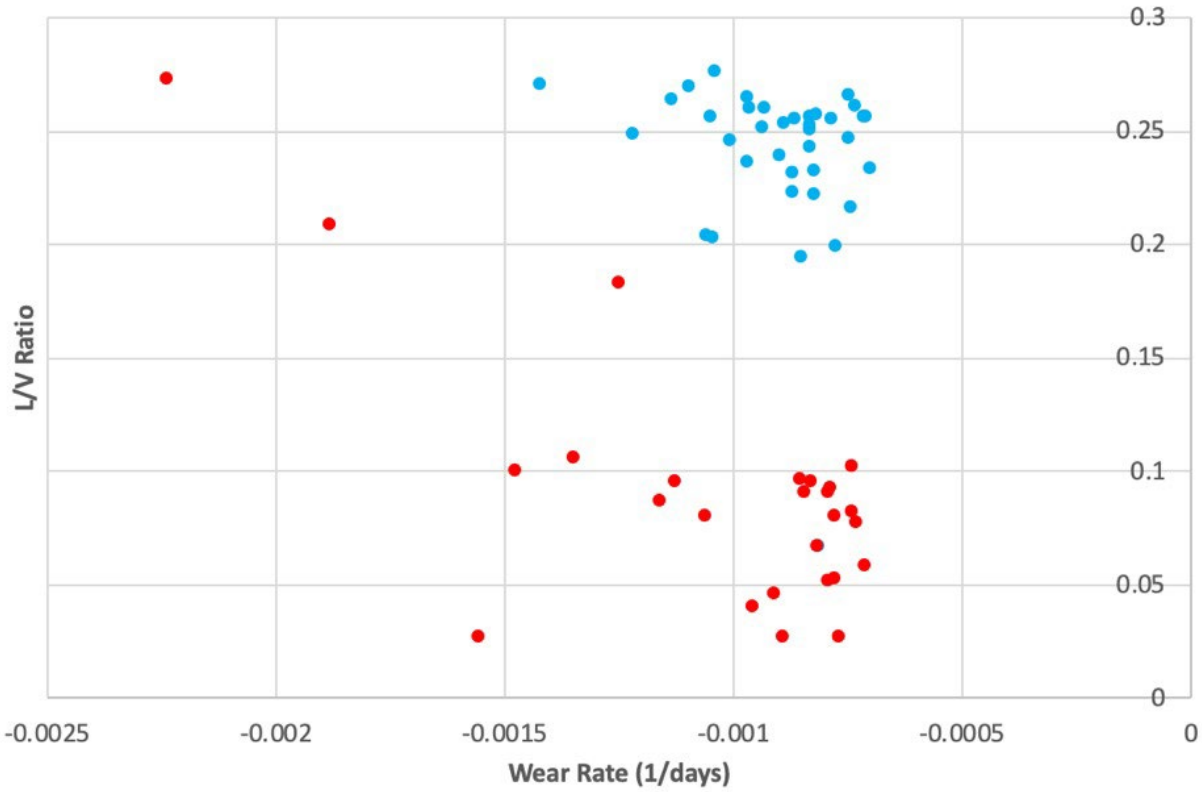

Figure 60 Scatterplot of L/V ratio vs. wear rates < -0.007 days^{-1} for 3R wheels.

These scatterplots prove that there is some relationship between L/V ratio and wheels with excessive wear rates. More specifically, for those wheels indicated by a red marker, there is a strong positive relationship between the two variables. As a wheel's L/V ratio increases, so too does its flange wear rate. This is the type of behavior that was anticipated. However, this relationship does not hold true for all wheels. The flange wear rates of those wheels indicated by a blue marker appear to be independent of L/V ratio. For these wheels, even though L/V ratio is varying, the flange wear rate stays within a very narrow range. Of particular interest are those blue markers in Figure 60. The measured L/V ratios are towards the upper end of the spectrum, but the flange wear rates are not as severe as some of the other wheels. This leads to the belief that another variable is controlling the wear rate for these wheels. However, when these plots are produced for angle of attack, tracking position, and speed, the relationships are still unclear. Yet, it can be stated that within the fleet of cars on the 7 line, there are differences in performance. Some cars may have proper steering capability and lateral stability, thus leading to a lower flange wear rate. Other cars however may have steering issues or truck issues that are leading to increased lateral forces and wear rate. Note that this idea stems from the behavior of those wheels in the 1R and 3R positions. At the site of the L/V Measurement System, these wheels are in the leading axle position and are traveling on the high rail. This means that they will experience the greatest lateral forces through the curve. Wheels in other positions exhibit different lateral force tendencies, and thus, their relationships with wear rate at the L/V Measurement System location may vary. Nonetheless, Figures 59 and 60 still lead to the conclusion that within this particular population of wheels, some

wheel wear rates have a strong dependence upon L/V ratio, while others appear to be more independent.

This idea of L/V ratio dependence was further explored by further investigating those bad actor wheels as identified by the statistical performance bands. For all of the bad actor wheels in the 1R and 3R positions, plots of L/V ratio against wear rate were created and are shown in Figures 61 and 62.

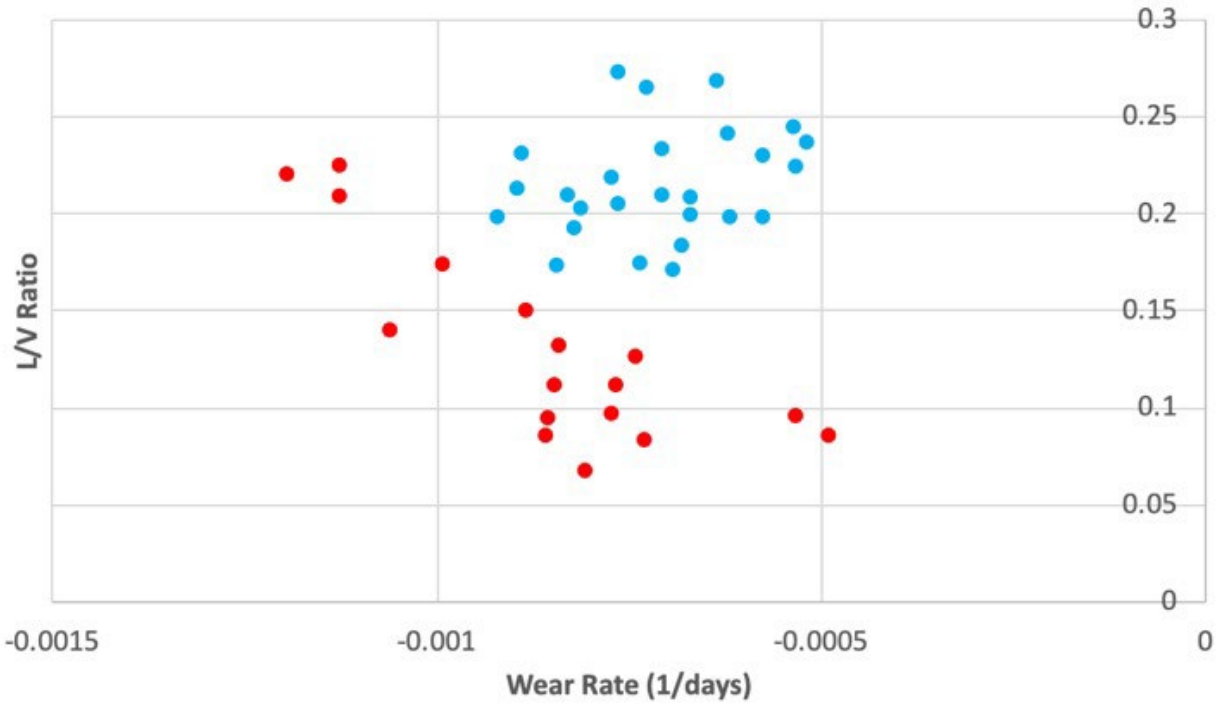

Figure 61 Scatterplot of L/V ratio vs. wear rate for bad actor 1R wheels.

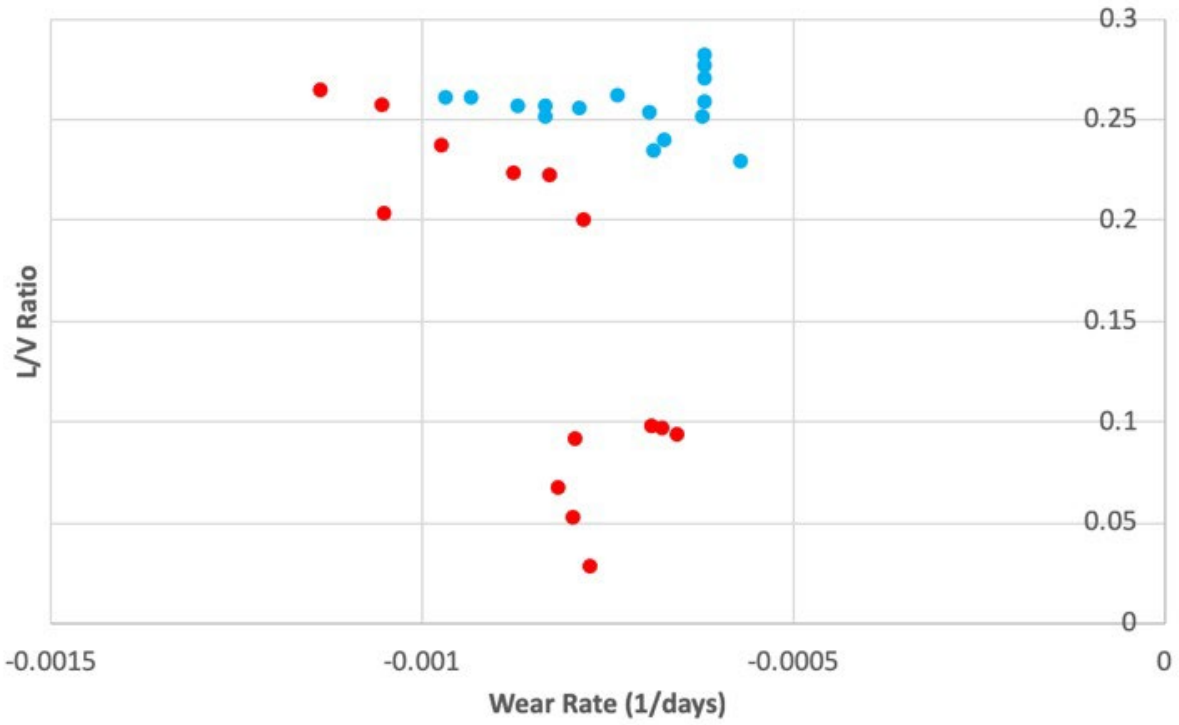

Figure 62 Scatterplot of L/V ratio vs. wear rate for bad actor 3R wheels.

Again, it can be seen that some wheel wear rates have a strong dependence upon L/V ratio, while others appear to be more independent. Those bad actor wheels denoted by red markers have a strong dependence on L/V ratio, while those denoted by blue markers appear to be more independent. For those blue wheels, another variable is most likely leading to their higher rates of wear. At the moment, there is not enough available data to determine the cause of the excessive rates of wear in these wheels. Examinations of angle of attack, tracking position, and speed do not yield clear results. Future work shall include continuing to examine these wheels in order to determine what is attributing to their high rates of wear and poor performance.

CONCLUSIONS

The purpose of this research was to the analyze the wear patterns of transit vehicle wheels in order to better understand their behavior and life cycle. Thanks to the vast network of instrumentation services installed as a part of NYCTA's work; specifically, the KLD Automatic WheelScan; automated and frequent wheel inspection data was made available for every wheel in the study fleet. Initial exploratory data analysis proved that wheels were being trued on a regular basis. In order to maintain an acceptable flange thickness, wheels were trued back to their original unworn profile. Thus, exponential regression was utilized to calculate the wear rate of each wheel on every vehicle in the fleet, based upon the WheelScan data.

The calculation of these wear rates allowed for a projection to when the next maintenance event will occur. In other words, it became possible to forecast the time until a given wheel will have a flange thickness of 24.2 mm, the NYCTA maintenance limit. Ultimately, these forecasts allow for an assessment of the performance of NYCTA's vehicle fleet from a wheel wear perspective, and can be used to optimize current maintenance practices. It was found that on average, wheels in this particular fleet are being trued too early.

In addition, advanced statistical techniques such as logistic regression were used in order to identify and predict which wheels in the fleet will perform poorly in terms of projected life. Such wheels can be classified as "bad actors", and are important to identify so that they may be more regularly inspected, maintained, and replaced. Data that was made available from the L/V Measurement System and TBOGI was also used in order to better understand the behavior of these "bad acting" wheels. Based on the analyses that were conducted and presented, the following conclusions can be made as a result of this research:

1. Based on the behavior of the wheel wear data and the results of the analysis, an exponential fit appears to be an appropriate method for calculating the wear rate of these particular wheels. Initially, linear regression was thought to provide an adequate representation of the fleet's wheel wear. However, upon further investigation of the data, it was realized that linear regression would not be acceptable. The flange thickness of a new or recently trued wheel exhibited a sharp and rapid wearing in period, whereby the flange would wear at a higher rate early on and eventually settle into a steady wear rate. Typically, this type of behavior is thought of as an exponential decay. Thus, simple linear regression would not accurately portray the wheel's behavior. Instead, a nonlinear regression analysis technique would be needed. This allowed for a more accurate prediction of wheel wear. However, there were some shortcomings associated with using exponential regression. By nature, exponential regression treats data asymptotically. This assumes that the wheels will continue to wear at a very slow rate once the initial sharp wear in period ends. In practice, this is most likely not the case. Defects can form in the wheel or the rail that can lead to accelerated wear. The exponential regression model cannot account for such factors. In addition, it is important to keep in mind that the calculated wear rates are based solely on time. In the rail industry, time is seldom used as a benchmark due to differences in tonnage and mileage. However, this data was not made available for this study, and thus could not be incorporated. Had this data been available, key information such

as vehicle out of service time and total mileage could have been used to produce more accurate wear rates.

2. The wear rates that were calculated allowed for forecasting of when the next maintenance event is likely to occur. In other words, it became possible to forecast the time until a given wheel will have a flange thickness of 24.2 mm, the current NYCTA maintenance limit. Then, based on the rim thickness value, a decision must be made as to whether the wheel should be trued or replaced. From these forecasts, it was discovered that NYCTA may be truing their wheels too early. Rather than allowing the wheels to wear until the threshold, they are being trued before reaching their actual maintenance limit. This is a more conservative and safety-oriented approach. It is important to note that NYCTA trues on a truck basis; if one wheel on the truck reaches the maintenance limit, all four wheels are trued. This reduces the out-of-service time, and also maintains the lateral stability and effective conicity of the axle sets. The operational and economic effects of altering these practices should be examined.

3. Within the overall population of wheels, there appears to be three different sub-populations based on their actual wear performance. There is a large group of wheels that are behaving as expected. Next, there is a slightly smaller group of wheels that are behaving better than expected. These subpopulations of wheels are exhibiting a very low rate of flange wear, and as such, can be classified as "good actors". Lastly, there is a small group of wheels that are behaving worse than expected. This subpopulation of wheels is exhibiting a very high rate of flange wear, and as such, can be classified as "bad actors". It is of practical significance to be able to identify and understand these bad actor wheels, so that they may be more regularly inspected and maintained.

4. A logistic regression model was built in order to predict the likelihood of a given wheel behaving as a "bad actor". The wheel's wear rate, last flange thickness measurement, average L/V ratio, average angle of attack, average tracking position, and average speed were used to build such a model. Upon construction, it was found that wear rate has the greatest impact on the probability of a wheel being a bad actor. Last flange thickness measurement and speed also played minor roles. The remaining variables on the other hand; L/V ratio, angle of attack, and tracking position; did not appear to have any impact whatsoever. This may be due to the fact that these variables were only measured at one point along the track. The model correctly identified 83.1 % of the "bad acting" wheels and 93.3 % of the "good acting" wheels. Overall, the logistic regression model operated at an accuracy of 92.1 %. Those wheels that were misclassified were just on the cusp of being a "bad actor", as defined by the performance bands that were created. Thus, the model that was built was able to successfully identify those wheels at the extreme ends of the spectrum, but had difficulty differentiating between those wheels that are near the performance threshold.

5. By correlating those wheels with excessive rates of flange wear with L/V ratio, it was found that wheels are behaving in two distinct ways. There are some wheels in the fleet whose high rate of flange wear is largely dependent on a high L/V ratio. On the other hand, there are other wheels in the fleet whose high rate of flange wear is largely independent of a high L/V ratio. Another unknown variable is likely controlling these excessive rates of wear.

RECOMMENDATIONS FOR FUTURE RESEARCH

Based on the results of this thesis, there is a clear opportunity for further, more aggressive analysis using higher order data analytics. In general, there are two overall approaches that can be taken in a next phase analysis. The first would be a standard engineering-based approach, in which the available data is combined with existing railway engineering knowledge to draw conclusions. The second would be a higher-order big data analytics approach. The results of this research prove that certain big data techniques can be successfully applied to the available data. Performing such an analysis may yield to be more insightful than standard approaches. Specific tasks that can be explored in the future include:

1. Gain a better understanding of the underlying causes for a wheel exhibiting a high rate of flange wear. The wide range of data streams that are available, in addition to higher order data analytics methods, can be used to find the root of poor wheel behavior.

2. Continue to develop a logistic regression model that accurately predicts whether or not a given wheel will exhibit a high rate of flange wear, and thus be deemed a “bad actor”. By creating as accurate a model as possible, better maintenance decisions can be made for those wheels exhibiting poor behavior.

3. Investigate additional regression methods that could be used to better calculate a flange wear rate for each wheel in the fleet. Other techniques, such as bilinear regression, could be more effective and should be considered.

ACKNOWLEDGEMENTS

Special thanks to the following parties for the continuous support throughout this research effort:

- University of Delaware, Department of Civil Engineering
- RailTEAM, USDOT Tier 1 University Transportation Center on Railroad Infrastructure Durability and Sustainability
- New York City Transit Authority
- Federal Transit Administration
- United States Department of Transportation
- KLD Labs
- NRC Canada
- Dayton T. Brown
- Plasser American
- Wayside Inspection Devices
- Instrumentation Services Inc.

REFERENCES

1. Railway Education Bureau (2015). The Basics of Railroad Wheels and Wheel Inspection, 5th ed. Railway Education Bureau.
2. Braghin, F., et. al. (2009). Wheel - Rail Interface Handbook, Chapter 6: Railway Wheel Wear, 172 - 210. Woodhead Publishing.
3. International Heavy Haul Association (2001). Guidelines to Best Practices for Heavy Haul Railway Operations: Wheel and Rail Interface Issues, 1st ed. IHHA.
4. Braghin, F., et. al. (2006). "A mathematical model to predict railway wheel profile evolution due to wear". WEAR, 261, pp. 1253 - 1264.
5. Pradhan, S., et. al. (2018). "Prediction of railway wheel wear and its influence on the vehicle dynamics in a specific operating sector of Indian railways network." Wear, 406 - 407, pp. 92 - 104.
6. Ayasse, J. and Chollet, H. (2006). Handbook of Railway Vehicle Dynamics, Chapter 4: Wheel - Rail Contact, 85 - 121. Taylor & Francis.
7. Oldknow, K. (2017). "Wheel-Rail Interaction Fundamentals." WRI 2017.
8. Attoh-Okine, N. (2017). Big Data and Differential Privacy: Analysis Strategies for Railway Track. Wiley.
9. New York City Transit Authority (2019). Integrated Wheel/Rail Characterization Through Advanced Monitoring and Analytics.
10. Afifi, A., et. al. (2012). Practical Multivariate Analysis, 5th ed. CRC Press.

APPENDIX

Appendix A - VBA Code to Perform Exponential Regression

```
Option Compare Database
Option Explicit
Type typRegData
    nNumPts As Integer
    nNumEvents As Integer
    nEvents(1 To 5, 1 To 2) As Integer
    fDiff(1 To 5) As Single
    fX(1 To 100) As Single
    fY(1 To 100) As Single
    fZ(1 To 100) As Single
End Type
Type typCarData
    nRim_Thickness As Single
    nFlange_Angle As Single
    nFlange_Height As Single
    nFlange_Thickness As Single
    nData_Quality As Single
    nData_Quality_Binary As Single
End Type
Type typCarInfo
    dDate As Date
    tCarData(1 To 4, 1 To 2) As typCarData
End Type
Type typKLDData
    nCarNum As Long
    nNoDates As Long
    tCarInfo(1 To 100) As typCarInfo
End Type
Type typDefRegResults
    fInt As Single
    fSlope As Single
    fR2 As Single
    fCycle As Integer
    fXFirst As Single
    fYFirst As Single
    fXLast As Single
    fYLast As Single
    fDeltaFirstLast As Single
    fYMin As Single
    fXMin As Single
    fYMax As Single
    fXMax As Single
    fDeltaMinMax As Single
    fA As Double
    fK As Double
    fExpR2 As Double
    fBiSlopeA As Single
    fBiIntA As Single
    fBiR2A As Single
    fBiSlopeB As Single
    fBiIntB As Single
    fBiR2B As Single
```

```
End Type

Private Sub subAddCars()
Dim rsCarDataTemp As ADODB.Recordset
Dim rsCars As ADODB.Recordset
Dim rsCarData As ADODB.Recordset
Dim nCarNum As Long
Dim strSQL As String
Dim nCtr As Integer, nCtr2 As Integer, nCtr3 As Integer
Dim tKLDData As typKLDData
Dim dTempDate As Date
Dim nCarCtr As Integer, nAxleIndex As Integer, nSideIndex As Integer
nCarCtr = 0

    Set rsCarDataTemp = New ADODB.Recordset
    rsCarDataTemp.ActiveConnection = CurrentProject.Connection
    rsCarDataTemp.CursorType = adOpenKeyset
    rsCarDataTemp.CursorLocation = adUseClient
    rsCarDataTemp.LockType = adLockOptimistic
    rsCarDataTemp.Open "DELETE * FROM [Temp Truing_Table]"
    rsCarDataTemp.Open "SELECT * FROM [Temp Truing_Table]"

    Set rsCars = New ADODB.Recordset
    rsCars.ActiveConnection = CurrentProject.Connection
    rsCars.CursorType = adOpenKeyset
    rsCars.CursorLocation = adUseClient
    rsCars.LockType = adLockOptimistic
    rsCars.Open "SELECT DISTINCT [Vehicle_SN] FROM [ALL_KLD]"
        If rsCars.EOF = False And rsCars.BOF = False Then
            rsCars.MoveFirst
            nCarCtr = 1
            Do While Not rsCars.EOF
                If Not IsNull(rsCars("Vehicle_SN")) Then
                   If rsCars("Vehicle_SN") > 0 Then
                        tKLDData.nCarNum = rsCars("Vehicle_SN")
                        strSQL = "SELECT*FROM [ALL_KLD] WHERE [Vehicle_SN] =
" & rsCars("Vehicle_SN") & " ORDER BY [Date], [Car_Axle], [Car_side]"
'Selecting car #s (Vehicle_SN) from the table

                        Set rsCarData = New ADODB.Recordset
                        rsCarData.ActiveConnection =
CurrentProject.Connection
                        rsCarData.CursorType = adOpenKeyset
                        rsCarData.CursorLocation = adUseClient
                        rsCarData.LockType = adLockOptimistic
                        rsCarData.Open strSQL

                        If rsCarData.EOF = False And rsCarData.BOF = False
Then
                            rsCarData.MoveFirst
                            dTempDate = rsCarData("Date")
                            tKLDData.tCarInfo(nCarCtr).dDate = dTempDate
                            Do While Not rsCarData.EOF
                                If rsCarData("Date") = dTempDate Then
                                    nAxleIndex = rsCarData("Car_Axle")
                                    If (rsCarData("Car_Side") = "L") Then
                                        nSideIndex = 1
```

```
                                    Else
                                        nSideIndex = 2
                                    End If
                                    If Not IsNull(rsCarData("Rim_Thickness"))
Then

tKLDData.tCarInfo(nCarCtr).tCarData(nAxleIndex, nSideIndex).nRim_Thickness =
rsCarData("Rim_Thickness")
                                    Else

tKLDData.tCarInfo(nCarCtr).tCarData(nAxleIndex, nSideIndex).nRim_Thickness =
-9
                                    End If
                                    If Not IsNull(rsCarData("Flange_Angle"))
Then

tKLDData.tCarInfo(nCarCtr).tCarData(nAxleIndex, nSideIndex).nFlange_Angle =
rsCarData("Flange_Angle")
                                    Else

tKLDData.tCarInfo(nCarCtr).tCarData(nAxleIndex, nSideIndex).nFlange_Angle = -
9
                                    End If
                                    If Not IsNull(rsCarData("Flange_Height"))
Then

tKLDData.tCarInfo(nCarCtr).tCarData(nAxleIndex, nSideIndex).nFlange_Height =
rsCarData("Flange_Height")
                                    Else

tKLDData.tCarInfo(nCarCtr).tCarData(nAxleIndex, nSideIndex).nFlange_Height =
-9
                                    End If
                                    If Not
IsNull(rsCarData("Flange_Thickness")) Then

tKLDData.tCarInfo(nCarCtr).tCarData(nAxleIndex, nSideIndex).nFlange_Thickness
= rsCarData("Flange_Thickness")
                                    Else

tKLDData.tCarInfo(nCarCtr).tCarData(nAxleIndex, nSideIndex).nFlange_Thickness
= -9
                                    End If
                                    If Not IsNull(rsCarData("Data_Quality"))
Then

tKLDData.tCarInfo(nCarCtr).tCarData(nAxleIndex, nSideIndex).nData_Quality =
rsCarData("Data_Quality")
                                    Else

tKLDData.tCarInfo(nCarCtr).tCarData(nAxleIndex, nSideIndex).nData_Quality = -
9
                                    End If
                                    If Not
IsNull(rsCarData("Data_Quality_Binary")) Then
```

```
tKLDData.tCarInfo(nCarCtr).tCarData(nAxleIndex,
nSideIndex).nData_Quality_Binary = rsCarData("Data_Quality_Binary")
                                    Else

tKLDData.tCarInfo(nCarCtr).tCarData(nAxleIndex,
nSideIndex).nData_Quality_Binary = -9
                                    End If
                                   rsCarData.MoveNext
                                Else
                                    nCarCtr = nCarCtr + 1
                                    dTempDate = rsCarData("Date")
                                    tKLDData.tCarInfo(nCarCtr).dDate =
dTempDate
                                End If
                            Loop
                            tKLDData.nNoDates = nCarCtr

                            For nCtr = 1 To nCarCtr
                                For nCtr2 = 1 To 4 '1
                                     For nCtr3 = 1 To 2 '1
                                        rsCarDataTemp.AddNew
                                        rsCarDataTemp("Vehicle_SN") =
tKLDData.nCarNum
                                        rsCarDataTemp("Date") =
tKLDData.tCarInfo(nCtr).dDate
                                        rsCarDataTemp("Car_Axle") = nCtr2
                                        rsCarDataTemp("Car_Side") = nCtr3
                                        rsCarDataTemp("Rim_Thickness") =
tKLDData.tCarInfo(nCtr).tCarData(nCtr2, nCtr3).nRim_Thickness
                                        rsCarDataTemp("Flange_Angle") =
tKLDData.tCarInfo(nCtr).tCarData(nCtr2, nCtr3).nFlange_Angle
                                        rsCarDataTemp("Flange_Height") =
tKLDData.tCarInfo(nCtr).tCarData(nCtr2, nCtr3).nFlange_Height
                                        rsCarDataTemp("Flange_Thickness") =
tKLDData.tCarInfo(nCtr).tCarData(nCtr2, nCtr3).nFlange_Thickness
                                        rsCarDataTemp("Data_Quality") =
tKLDData.tCarInfo(nCtr).tCarData(nCtr2, nCtr3).nData_Quality
                                        rsCarDataTemp("Data_Quality_Binary")
= tKLDData.tCarInfo(nCtr).tCarData(nCtr2, nCtr3).nData_Quality_Binary

                                       rsCarDataTemp.Update
                                    Next nCtr3
                                Next nCtr2
                            Next nCtr

                            Call subAnalyzeCar(tKLDData)

                            nCarCtr = 1
                        End If
                    rsCarData.Close
                    End If
                End If
                 rsCars.MoveNext
            Loop
            Else
                MsgBox "No Data Found"
```

```
        End If
        rsCars.Close
        MsgBox "DONE!"
End Sub

Sub subAnalyzeCar(tData As typKLDData)
Dim nCtr As Integer, nCtr2 As Integer, nCtr3 As Integer
Dim tRegData As typRegData, tRegData2 As typRegData, tRegData3 As typRegData
Dim tresults As typDefRegResults
Dim rsRegression As ADODB.Recordset, rsClean As ADODB.Recordset
Dim t As Integer, t2 As Integer, t3 As Integer
Dim nStart As Integer, nStop As Integer
Dim Truing As String
Dim Replacement As String
Dim Wheel As String
Dim DiffBefore As Single
Dim DiffAfter As Single


Set rsRegression = New ADODB.Recordset
    rsRegression.ActiveConnection = CurrentProject.Connection
    rsRegression.CursorType = adOpenKeyset
    rsRegression.CursorLocation = adUseClient
    rsRegression.LockType = adLockOptimistic
    rsRegression.Open "SELECT * FROM [RegTableNEW]"

 Set rsClean = New ADODB.Recordset
    rsClean.ActiveConnection = CurrentProject.Connection
    rsClean.CursorType = adOpenKeyset
    rsClean.CursorLocation = adUseClient
    rsClean.LockType = adLockOptimistic
    rsClean.Open "SELECT * FROM [Cleaned Truing Table]"

    For nCtr2 = 1 To 4
        For nCtr3 = 1 To 2
            For nCtr = 1 To tData.nNoDates
                If tData.tCarInfo(nCtr).tCarData(nCtr2,
nCtr3).nData_Quality_Binary = 1 Then
                    tRegData.nNumPts = tRegData.nNumPts + 1
                    tRegData.fX(tRegData.nNumPts) =
tData.tCarInfo(nCtr).dDate
                    tRegData.fY(tRegData.nNumPts) =
tData.tCarInfo(nCtr).tCarData(nCtr2, nCtr3).nFlange_Thickness
                    tRegData.fZ(tRegData.nNumPts) =
tData.tCarInfo(nCtr).tCarData(nCtr2, nCtr3).nRim_Thickness

                    rsClean.AddNew
                    rsClean("Date") = tData.tCarInfo(nCtr).dDate
                    rsClean("Flange_Thickness") =
tData.tCarInfo(nCtr).tCarData(nCtr2, nCtr3).nFlange_Thickness
                    rsClean("Rim_Thickness") =
tData.tCarInfo(nCtr).tCarData(nCtr2, nCtr3).nRim_Thickness
                    rsClean("Vehicle_SN") = tData.nCarNum
                    rsClean("Car_Axle") = nCtr2
                    rsClean("Car_Side") = nCtr3
                    rsClean.Update
                End If
```

```
            Next nCtr
            tRegData2.nNumPts = 1
            tRegData2.fX(1) = tRegData.fX(1)
            tRegData2.fY(1) = tRegData.fY(1)
            tRegData2.fZ(1) = tRegData.fZ(1)
            For t = 2 To tRegData.nNumPts - 1
                If Not ((Abs(tRegData.fZ(t - 1) - tRegData.fZ(t)) > 8#) And
(Abs(tRegData.fZ(t + 1) - tRegData.fZ(t)) > 8#)) Then
                    tRegData2.nNumPts = tRegData2.nNumPts + 1
                    tRegData2.fX(tRegData2.nNumPts) = tRegData.fX(t)
                    tRegData2.fY(tRegData2.nNumPts) = tRegData.fY(t)
                    tRegData2.fZ(tRegData2.nNumPts) = tRegData.fZ(t)
                End If
            Next t
            tRegData2.nNumPts = tRegData2.nNumPts + 1
            tRegData2.fX(tRegData2.nNumPts) = tRegData.fX(t)
            tRegData2.fY(tRegData2.nNumPts) = tRegData.fY(t)
            tRegData2.fZ(tRegData2.nNumPts) = tRegData.fZ(t)

            tRegData2.nNumEvents = 0
            For t = 1 To tRegData2.nNumPts - 1
                If ((tRegData2.fZ(t + 1) - tRegData2.fZ(t)) < -6#) Then
                    tRegData2.nNumEvents = tRegData2.nNumEvents + 1
                    tRegData2.nEvents(tRegData2.nNumEvents, 1) = t
                    tRegData2.nEvents(tRegData2.nNumEvents, 2) = 1
                    tRegData2.fDiff(tRegData2.nNumEvents) = (tRegData2.fZ(t +
1) - tRegData2.fZ(t))
                ElseIf ((tRegData2.fZ(t + 1) - tRegData2.fZ(t)) > 6#) Then
                    tRegData2.nNumEvents = tRegData2.nNumEvents + 1
                    tRegData2.nEvents(tRegData2.nNumEvents, 1) = t
                    tRegData2.nEvents(tRegData2.nNumEvents, 2) = 2
                    tRegData2.fDiff(tRegData2.nNumEvents) = (tRegData2.fZ(t +
1) - tRegData2.fZ(t))
                Else
                End If
            Next t

            If tRegData2.nNumEvents = 0 Then
                tresults = fncLinearRegression(tRegData2)
                rsRegression.AddNew
                rsRegression("Vehicle_SN") = tData.nCarNum
                rsRegression("Car_Axle") = nCtr2
                rsRegression("Car_Side") = nCtr3
                rsRegression("FT_Slope") = tresults.fSlope
                rsRegression("Intercept") = tresults.fInt
                rsRegression("R2") = tresults.fR2
                rsRegression("NumPts") = tRegData2.nNumPts
                rsRegression("Cycle Time") = tresults.fCycle
                rsRegression("XFirst") = tresults.fXFirst
                rsRegression("YFirst") = tresults.fYFirst
                rsRegression("XLast") = tresults.fXLast
                rsRegression("YLast") = tresults.fYLast
                rsRegression("DeltaFirstLast") = tresults.fDeltaFirstLast
                rsRegression("YMin") = tresults.fYMin
                rsRegression("XMin") = tresults.fXMin
                rsRegression("YMax") = tresults.fYMax
                rsRegression("XMax") = tresults.fXMax
```

```
        rsRegression("DeltaMinMax") = tresults.fDeltaMinMax
        rsRegression("A") = tresults.fA
        rsRegression("k") = tresults.fK
        rsRegression("ExpR2") = tresults.fExpR2
        rsRegression("BiSlopeA") = tresults.fBiSlopeA
        rsRegression("BiIntA") = tresults.fBiIntA
        rsRegression("BiR2A") = tresults.fBiR2A
        rsRegression("BiSlopeB") = tresults.fBiSlopeB
        rsRegression("BiIntB") = tresults.fBiIntB
        rsRegression("BiR2B") = tresults.fBiR2B
        rsRegression("Rim Change Before") = 0#
        rsRegression("Rim Change After") = 0#
        rsRegression.Update
    Else
        For t = 1 To (tRegData2.nNumEvents + 1)
            If t = 1 Then
                nStart = 1
                nStop = tRegData2.nEvents(t, 1)
                DiffBefore = 0#
                DiffAfter = tRegData2.fDiff(t)
            ElseIf t = (tRegData2.nNumEvents + 1) Then
                nStart = tRegData2.nEvents(t - 1, 1) + 1
                nStop = tRegData2.nNumPts
                DiffBefore = tRegData2.fDiff(t - 1)
                DiffAfter = 0#
            Else
                nStart = tRegData2.nEvents(t - 1, 1) + 1
                nStop = tRegData2.nEvents(t, 1)
                DiffBefore = tRegData2.fDiff(t - 1)
                DiffAfter = tRegData2.fDiff(t)
            End If
            tRegData3.nNumPts = (nStop - nStart) + 1
            For t3 = nStart To nStop
                tRegData3.fX(t3 - nStart + 1) = tRegData2.fX(t3)
                tRegData3.fY(t3 - nStart + 1) = tRegData2.fY(t3)
                tRegData3.fZ(t3 - nStart + 1) = tRegData2.fZ(t3)
            Next t3

            If DiffBefore = 0 And DiffAfter = 0 Then
                Wheel = "No maintenance"
            Else
                Wheel = "Maintenance"
            End If

            If tRegData3.nNumPts > 1 Then
                tresults = fncLinearRegression(tRegData3)
                rsRegression.AddNew
                rsRegression("Vehicle_SN") = tData.nCarNum
                rsRegression("Car_Axle") = nCtr2
                rsRegression("Car_Side") = nCtr3
                rsRegression("FT_Slope") = tresults.fSlope
                rsRegression("Intercept") = tresults.fInt
                rsRegression("R2") = tresults.fR2
                rsRegression("NumPts") = tRegData3.nNumPts
                rsRegression("Cycle Time") = tresults.fCycle
                rsRegression("XFirst") = tresults.fXFirst
                rsRegression("YFirst") = tresults.fYFirst
```

```
                        rsRegression("XLast") = tresults.fXLast
                        rsRegression("YLast") = tresults.fYLast
                        rsRegression("DeltaFirstLast") =
tresults.fDeltaFirstLast
                        rsRegression("YMin") = tresults.fYMin
                        rsRegression("XMin") = tresults.fXMin
                        rsRegression("YMax") = tresults.fYMax
                        rsRegression("XMax") = tresults.fXMax
                        rsRegression("DeltaMinMax") = tresults.fDeltaMinMax
                        rsRegression("A") = tresults.fA
                        rsRegression("k") = tresults.fK
                        rsRegression("ExpR2") = tresults.fExpR2
                        rsRegression("BiSlopeA") = tresults.fBiSlopeA
                        rsRegression("BiIntA") = tresults.fBiIntA
                        rsRegression("BiR2A") = tresults.fBiR2A
                        rsRegression("BiSlopeB") = tresults.fBiSlopeB
                        rsRegression("BiIntB") = tresults.fBiIntB
                        rsRegression("BiR2B") = tresults.fBiR2B
                        rsRegression("Rim Change Before") = DiffBefore
                        rsRegression("Rim Change After") = DiffAfter
                        rsRegression("Wheel") = Wheel
                        rsRegression.Update
                    End If
                Next t
            End If

            tRegData.nNumPts = 0

        Next nCtr3
    Next nCtr2

End Sub

Private Function fncLinearRegression(ByRef tData As typRegData) As
typDefRegResults
Dim nCtr As Integer
Dim N As Double
Dim Xsum As Double
Dim Ysum As Double
Dim XY As Double
Dim XYsum As Double
Dim X2sum As Double
Dim Y2sum As Double
Dim fSlope As Double, fInt As Double, fR2 As Double
Dim fCycle As Integer

Dim fXFirst As Single
Dim fYFirst As Single
Dim fXLast As Single
Dim fYLast As Single
Dim fDeltaFirstLast As Single
Dim i As Double
Dim iCtr As Integer
Dim fYMin As Single
Dim fXMin As Single
Dim j As Double
Dim jCtr As Integer
```

```
Dim fYMax As Single
Dim fXMax As Single
Dim fDeltaMinMax As Single

Dim fA As Double
Dim fK As Double
Dim fExpR2 As Double
Dim expM As Single
Dim expB As Single
Dim nexpCtr As Integer
Dim expN As Double
Dim expXsum As Double
Dim expYsum As Double
Dim expXY As Double
Dim expXYsum As Double
Dim expX2sum As Double
Dim expY2sum As Double
Dim StartDate As Single, EndDate As Single
Dim Numerator As Double, Denominator As Double

Dim fBiSlopeA As Single
Dim fBiIntA As Single
Dim fBiR2A As Single
Dim fBiSlopeB As Single
Dim fBiIntB As Single
Dim fBiR2B As Single
Dim nBiCtrA As Integer
Dim BiNA As Integer
Dim BiXsumA As Single
Dim BiYsumA As Single
Dim BiXYA As Single
Dim BiXYsumA As Single
Dim BiX2sumA As Single
Dim BiY2sumA As Single
Dim nBiCtrB As Integer
Dim BiNB As Integer
Dim BiXsumB As Single
Dim BiYsumB As Single
Dim BiXYB As Single
Dim BiXYsumB As Single
Dim BiX2sumB As Single
Dim BiY2sumB As Single

Dim sStrX As String, sStrY As String, expsStrX As String, expsStrY As String
sStrX = ""
sStrY = ""
expsStrX = ""
expsStrY = ""

Dim tRegData As typRegData

    Xsum = 0#
    Ysum = 0#
    XY = 0#
    XYsum = 0#
    X2sum = 0#
    Y2sum = 0#
```

```
    N = CSng(tData.nNumPts)
    For nCtr = 1 To tData.nNumPts
        Xsum = Xsum + tData.fX(nCtr)
        Ysum = Ysum + tData.fY(nCtr)
        XY = tData.fX(nCtr) * tData.fY(nCtr)
        XYsum = XYsum + XY
        X2sum = X2sum + (tData.fX(nCtr) ^ 2)
        Y2sum = Y2sum + (tData.fY(nCtr) ^ 2)

        sStrX = sStrX & tData.fX(nCtr) & ", "
        sStrY = sStrY & tData.fY(nCtr) & ", "

    Next nCtr

    StartDate = tData.fX(1)
    EndDate = tData.fX(tData.nNumPts)

    fInt = (Ysum * X2sum - Xsum * XYsum) / (N * X2sum - (Xsum) ^ 2)
    fSlope = (N * XYsum - Xsum * Ysum) / (N * X2sum - (Xsum) ^ 2)
    If fSlope <> 0 Then
        fR2 = (N * XYsum - Xsum * Ysum) ^ 2 / ((N * X2sum - (Xsum) ^ 2) * (N
* Y2sum - (Ysum) ^ 2))
    End If
    fCycle = EndDate - StartDate

    expXsum = 0#
    expYsum = 0#
    expXY = 0#
    expXYsum = 0#
    expX2sum = 0#
    expY2sum = 0#

    expN = CSng(tData.nNumPts)
    For nexpCtr = 1 To tData.nNumPts
        expXsum = expXsum + (tData.fX(nexpCtr) - 42886)
        expYsum = expYsum + Log(tData.fY(nexpCtr))
        expXY = (tData.fX(nexpCtr) - 42886) * Log(tData.fY(nexpCtr))
        expXYsum = expXYsum + expXY
        expX2sum = expX2sum + ((tData.fX(nexpCtr) - 42886) ^ 2)
        expY2sum = expY2sum + Log(tData.fY(nexpCtr)) ^ 2

        expsStrX = expsStrX & tData.fX(nexpCtr) & ", "
        expsStrY = expsStrY & tData.fY(nexpCtr) & ", "
    Next nexpCtr

    expB = (expYsum * expX2sum - expXsum * expXYsum) / (expN * expX2sum -
(expXsum) ^ 2)
    expM = (expN * expXYsum - expXsum * expYsum) / (expN * expX2sum -
(expXsum) ^ 2)
    If expM <> 0 Then
        Numerator = (expN * expXYsum - expXsum * expYsum) ^ 2
        Denominator = ((expN * expX2sum - (expXsum) ^ 2) * (expN * expY2sum -
(expYsum) ^ 2))
        If Denominator <> 0 Then
            fExpR2 = Numerator / Denominator
        End If
```

```
End If

If expB < 500 Then
    fA = ((2.71828) ^ expB)
    fK = (expM)
Else
    fA = 0#
    fK = 0#
End If

fXFirst = tData.fX(1)
fYFirst = tData.fY(1)
fXLast = tData.fX(tData.nNumPts)
fYLast = tData.fY(tData.nNumPts)

If tData.nNumPts = 2 Then
    fDeltaFirstLast = 0#
Else
    fDeltaFirstLast = Abs((fYLast - fYFirst) / (fXLast - fXFirst))
End If

i = CSng(tData.nNumPts)
fYMin = tData.fY(1)
fXMin = tData.fX(1)
For iCtr = 1 To tData.nNumPts
    If tData.fY(iCtr) <= fYMin Then
        fYMin = tData.fY(iCtr)
        fXMin = tData.fX(iCtr)
    Else
        fYMin = fYMin
        fXMin = fXMin
    End If
Next iCtr

j = CSng(tData.nNumPts)
fYMax = tData.fY(1)
fXMax = tData.fX(1)
For jCtr = 1 To tData.nNumPts
    If tData.fY(jCtr) >= fYMax Then
        fYMax = tData.fY(jCtr)
        fXMax = tData.fX(jCtr)
    Else
        fYMax = fYMax
        fXMax = fXMax
    End If
Next jCtr

If tData.nNumPts = 2 Then
    fDeltaMinMax = 0#
Else
    fDeltaMinMax = Abs((fYMax - fYMin) / (fXMax - fXMin))
End If

fncLinearRegression.fInt = fInt
fncLinearRegression.fSlope = fSlope
fncLinearRegression.fR2 = fR2
fncLinearRegression.fCycle = fCycle
```

```
    fncLinearRegression.fXFirst = fXFirst
    fncLinearRegression.fYFirst = fYFirst
    fncLinearRegression.fXLast = fXLast
    fncLinearRegression.fYLast = fYLast
    fncLinearRegression.fDeltaFirstLast = fDeltaFirstLast
    fncLinearRegression.fYMin = fYMin
    fncLinearRegression.fXMin = fXMin
    fncLinearRegression.fYMax = fYMax
    fncLinearRegression.fXMax = fXMax
    fncLinearRegression.fDeltaMinMax = fDeltaMinMax
    fncLinearRegression.fA = fA
    fncLinearRegression.fK = fK
    fncLinearRegression.fExpR2 = fExpR2
    fncLinearRegression.fBiSlopeA = fBiSlopeA
    fncLinearRegression.fBiIntA = fBiIntA
    fncLinearRegression.fBiR2A = fBiR2A
    fncLinearRegression.fBiSlopeB = fBiSlopeB
    fncLinearRegression.fBiIntB = fBiIntB
    fncLinearRegression.fBiR2B = fBiR2B

    StartDate = 0
    EndDate = 0

End Function
```

Appendix B - Scatterplot Matrices for All Wheels

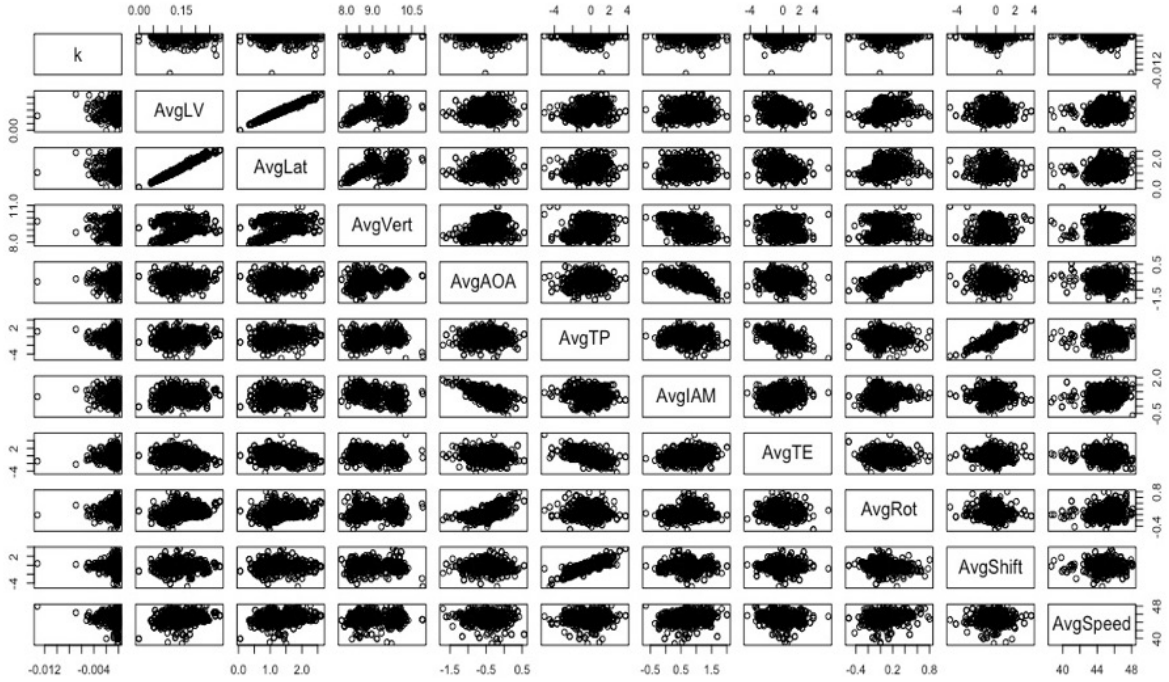

Figure B1 Wheel 1L scatterplot matrix.

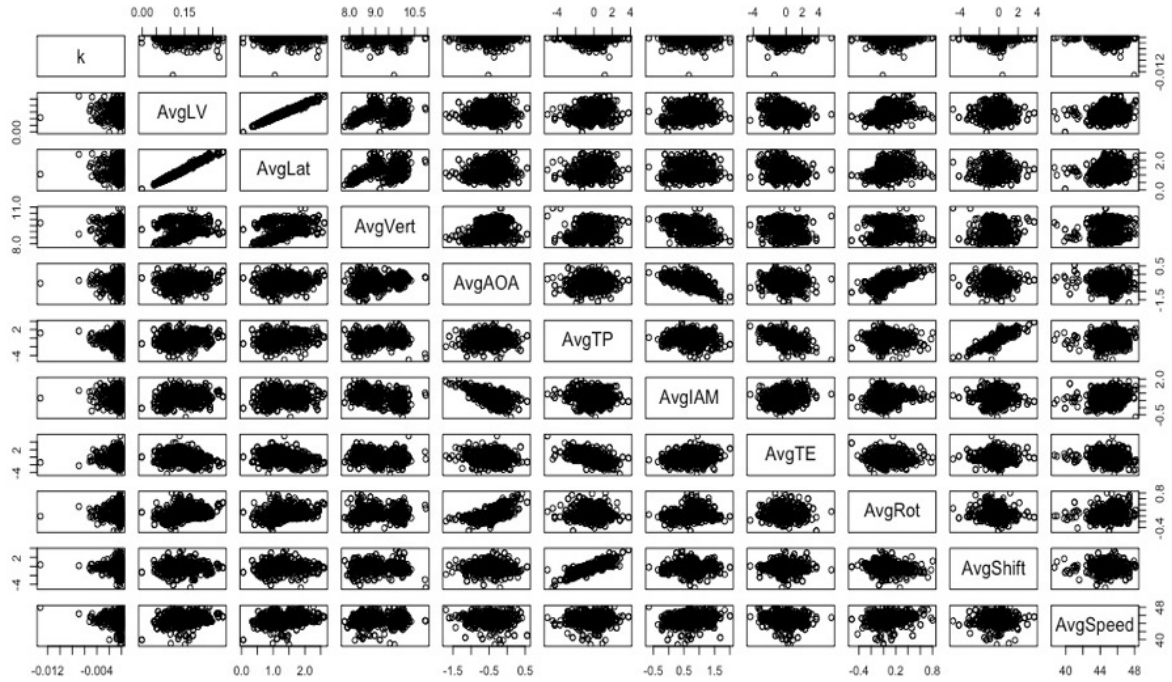

Figure B2 Wheel 1R scatterplot matrix.

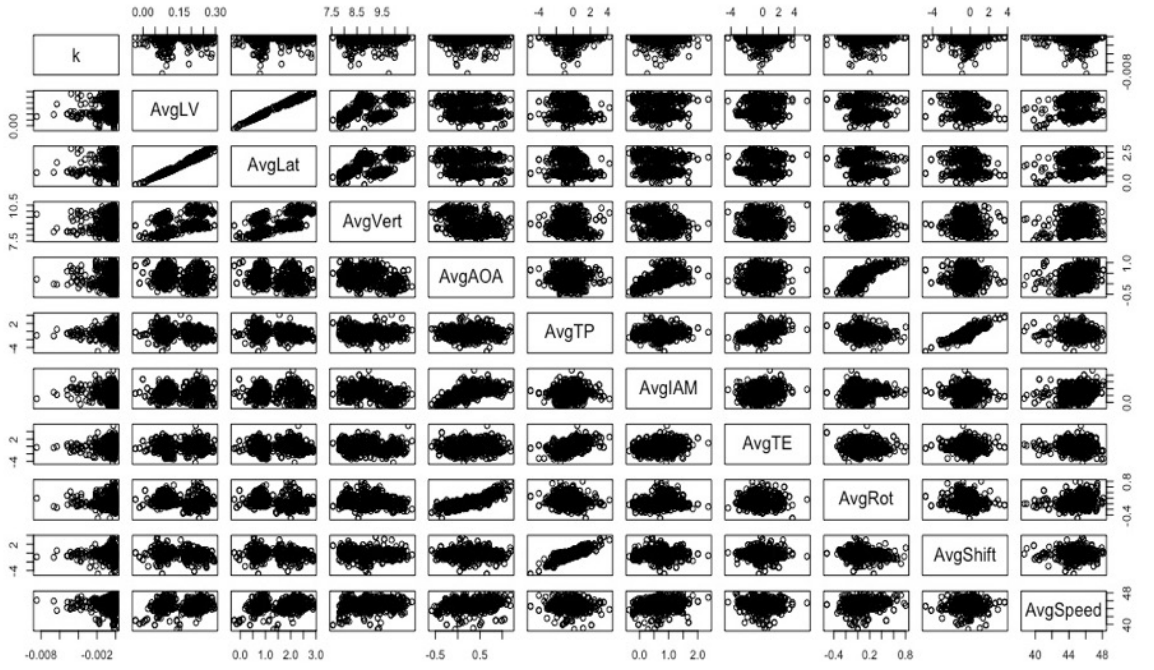

Figure B3 Wheel 2L scatterplot matrix.

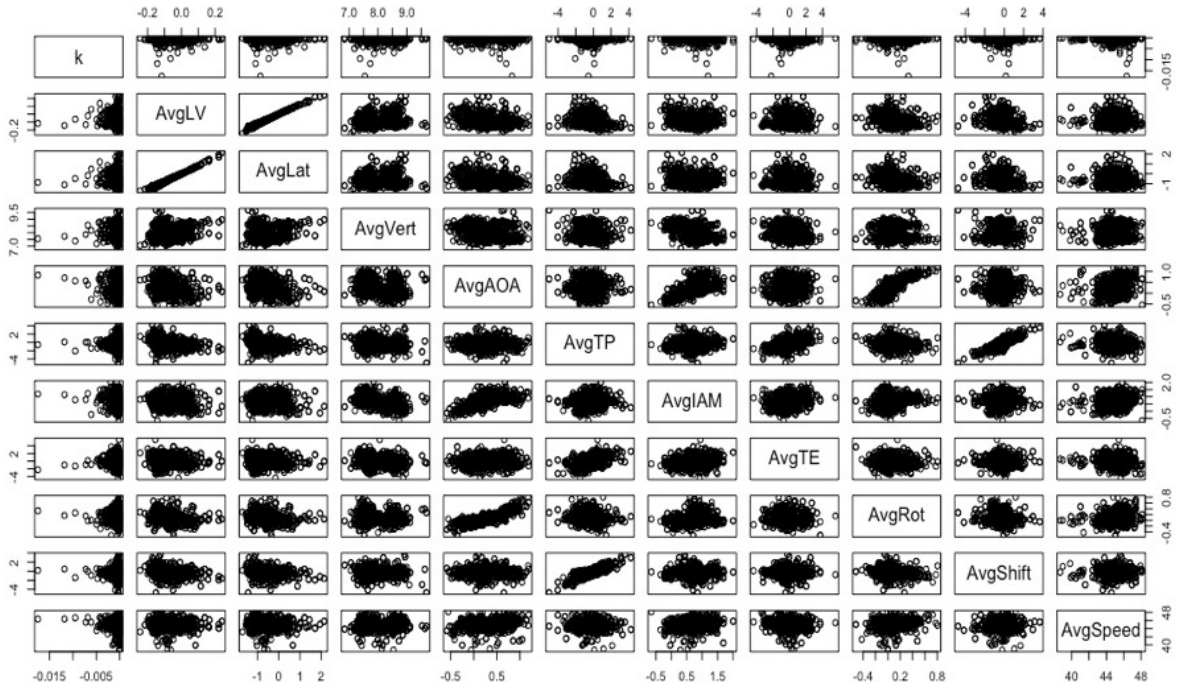

Figure B4 Wheel 2R scatterplot matrix.

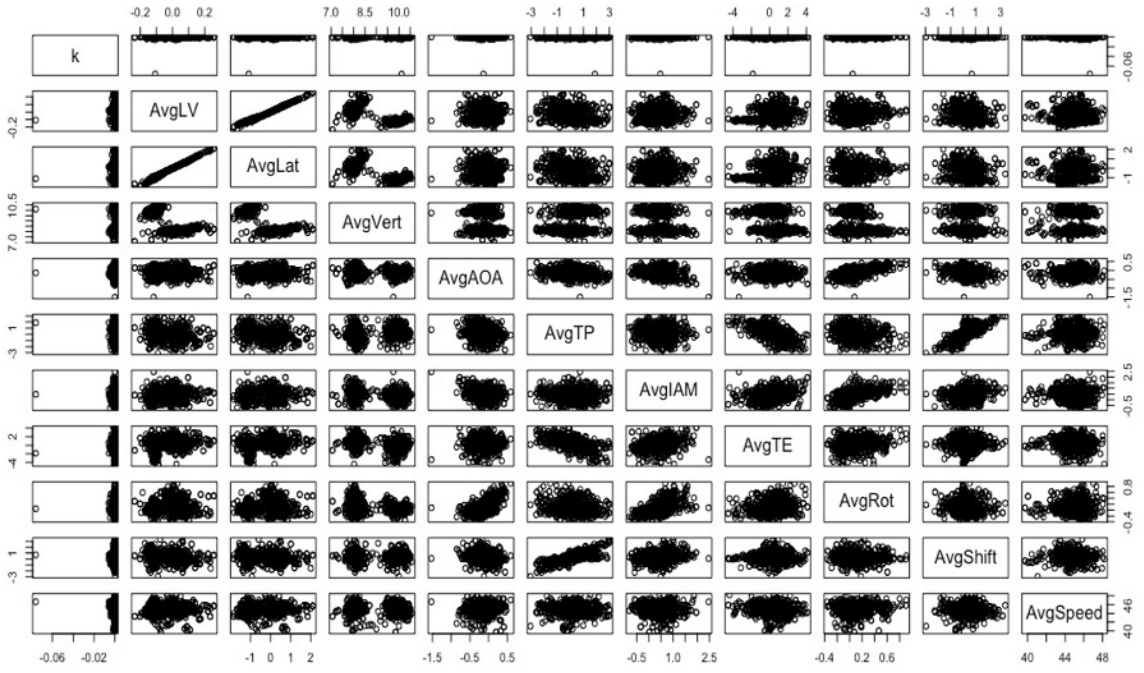

Figure B5 Wheel 3L scatterplot matrix.

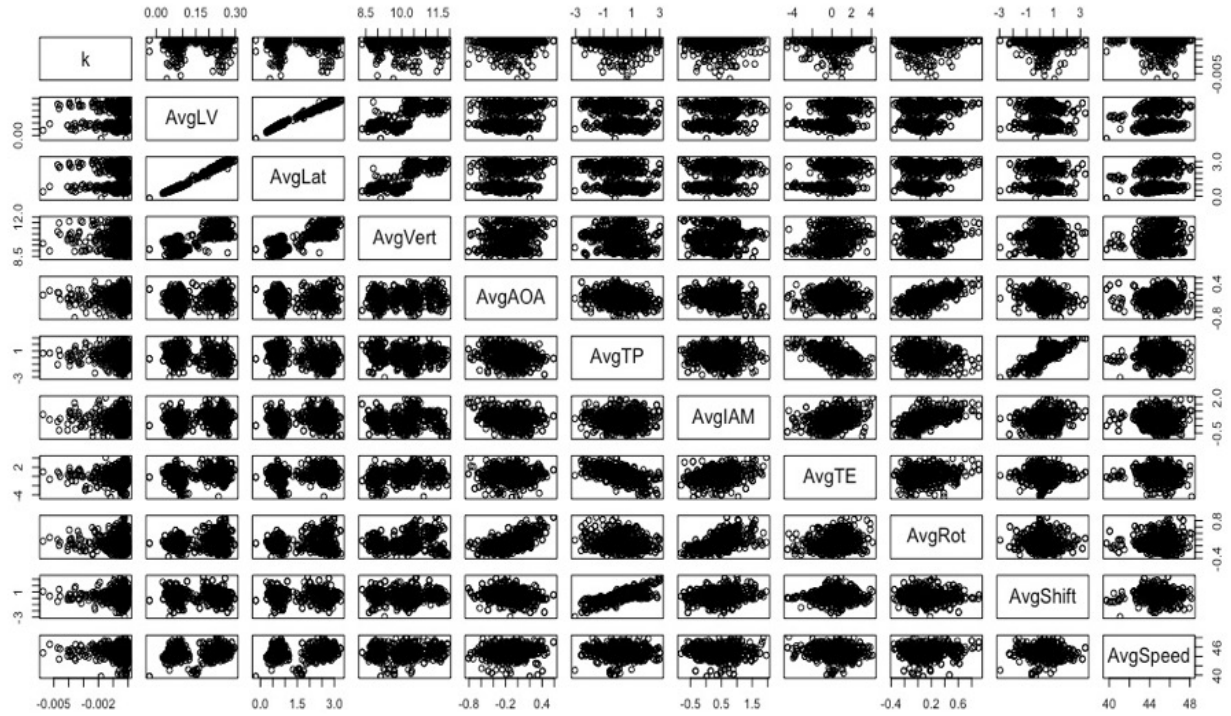

Figure B6 Wheel 3R scatterplot matrix.

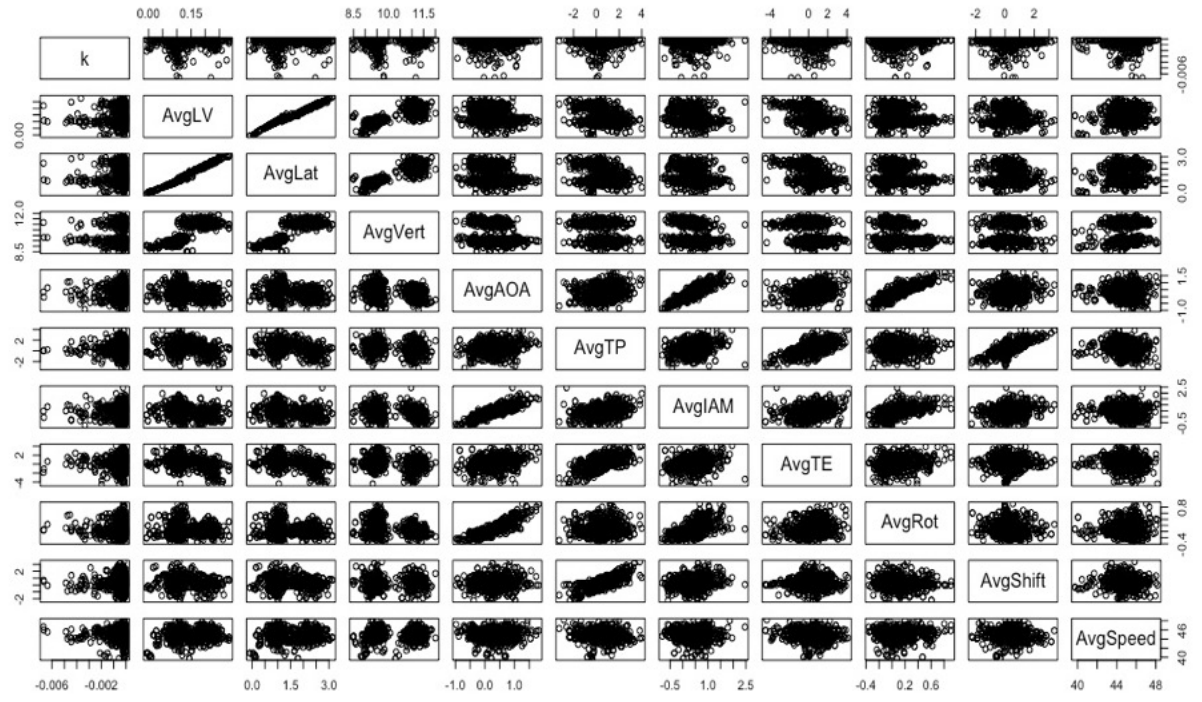

Figure B7 Wheel 4L scatterplot matrix.

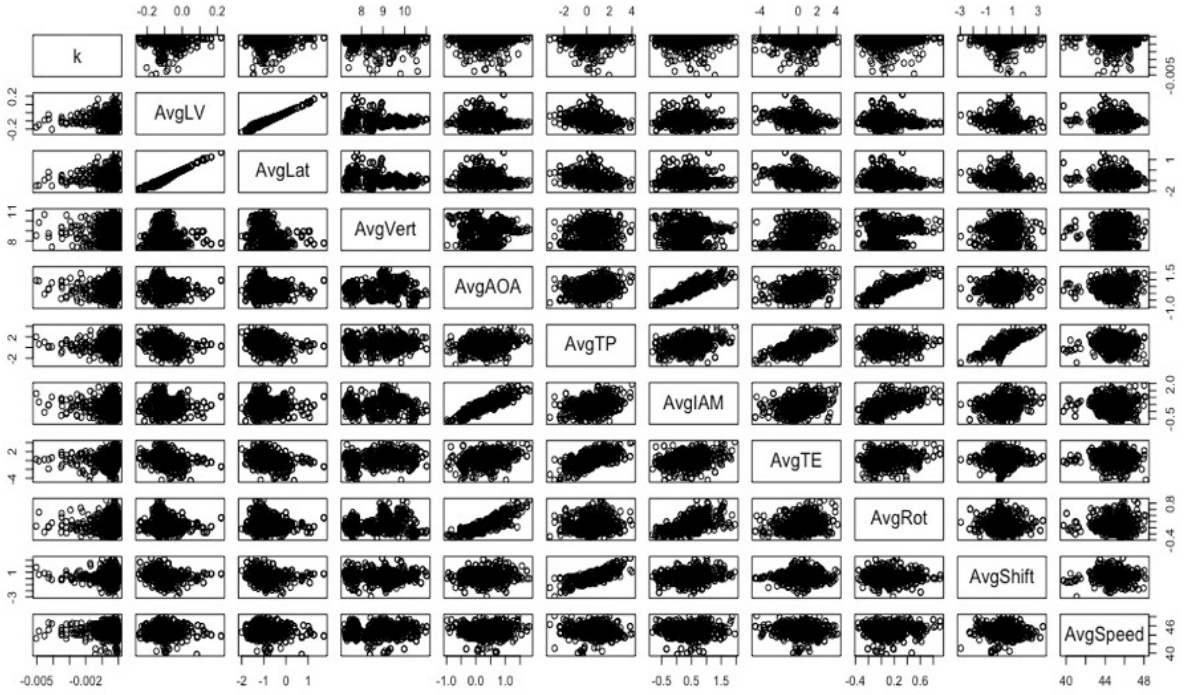

Figure B8 Wheel 4R scatterplot matrix.

Appendix C - List of Bad Actor Wheels

Table C1 List of Bad Actor Wheels Identified by Performance Bands

Vehicle No.	Car Axle	Car Side	k (1/days)	Ylast (mm)	Life (days)
7212	1	Right	-0.00086	28.180	363
7212	2	Right	-0.00102	27.820	322
7212	3	Right	-0.00081	28.410	382
7212	4	Right	-0.00103	27.290	302
7213	1	Left	-0.00053	30.030	530
7213	1	Right	-0.00077	27.540	289
7213	2	Left	-0.00113	27.080	221
7213	2	Right	-0.00105	26.590	211
7213	3	Left	-0.00052	29.600	509
7213	3	Right	-0.00079	27.470	280
7213	4	Left	-0.00069	29.240	396
7213	4	Right	-0.00068	28.590	364
7231	1	Right	-0.00052	29.790	555
7231	2	Left	-0.00058	29.620	501
7231	2	Right	-0.00067	29.260	435
7231	4	Right	-0.00061	29.540	481
7232	2	Left	-0.00051	30.260	592
7232	2	Right	-0.00058	29.650	505
7232	4	Left	-0.00054	30.320	570
7232	4	Right	-0.00054	30.020	549
7233	1	Right	-0.00054	29.450	520
7233	2	Right	-0.00055	30.030	542
7233	4	Right	-0.00057	29.860	520
7234	1	Right	-0.00057	29.330	488
7234	2	Right	-0.00051	29.830	562
7235	1	Left	-0.00059	29.590	493
7235	1	Right	-0.00049	30.520	627
7235	2	Left	-0.00055	29.540	515
7235	3	Left	-0.00049	30.510	630
7238	1	Left	-0.00077	28.010	337
7239	3	Left	-0.00056	29.290	487
7239	4	Left	-0.00089	27.620	295
7249	4	Right	-0.00058	26.910	262
7261	1	Right	-0.00085	28.020	378
7261	3	Right	-0.00079	28.390	408
7261	4	Right	-0.00093	27.930	360
7262	1	Right	-0.00076	28.420	416
7262	2	Right	-0.00065	29.350	502
7262	3	Right	-0.00065	29.060	486
7262	4	Right	-0.00077	28.570	422

Vehicle No.	Car Axle	Car Side	k (1/days)	Ylast (mm)	Life (days)
7263	1	Right	-0.00084	28.360	394
7263	2	Right	-0.00070	28.900	460
7264	1	Right	-0.00084	28.100	384
7264	2	Right	-0.00087	27.980	373
7264	3	Right	-0.00067	29.270	488
7265	1	Left	-0.00079	28.770	424
7265	2	Left	-0.00080	28.370	404
7265	4	Left	-0.00092	27.840	358
7296	2	Left	-0.00073	29.440	523
7316	1	Left	-0.00082	29.310	422
7316	2	Left	-0.00089	28.430	370
7316	3	Left	-0.00057	30.090	573
7316	4	Left	-0.00082	28.860	403
7317	1	Right	-0.00099	28.730	362
7317	2	Right	-0.00060	30.150	555
7317	3	Right	-0.00083	29.370	421
7317	4	Right	-0.00056	30.320	589
7318	1	Left	-0.00077	28.140	385
7318	1	Right	-0.00119	27.510	296
7318	2	Left	-0.00068	28.790	446
7318	2	Right	-0.00076	29.700	457
7318	3	Right	-0.00062	29.980	534
7318	4	Right	-0.00062	30.200	543
7319	1	Right	-0.00112	28.020	319
7319	2	Right	-0.00072	29.580	468
7319	3	Right	-0.00083	28.840	399
7319	4	Right	-0.00060	30.420	570
7320	1	Right	-0.00084	28.910	400
7320	2	Right	-0.00087	28.880	392
7320	3	Right	-0.00105	28.570	347
7320	4	Right	-0.00066	29.750	504
7355	4	Right	-0.00094	28.470	237
7371	1	Left	-0.00081	29.500	304
7372	1	Left	-0.00069	29.960	372
7372	2	Right	-0.00051	31.260	565
7372	3	Left	-0.00051	30.190	494
7373	1	Left	-0.00089	29.260	275
7419	3	Left	-0.00050	30.970	560
7419	4	Left	-0.00056	30.250	465
7446	2	Right	-0.00090	28.420	392
7446	4	Right	-0.00096	28.160	373
7447	2	Left	-0.00085	28.400	403
7447	3	Left	-0.00079	28.370	414
7447	4	Left	-0.00083	28.490	411

Vehicle No.	Car Axle	Car Side	k (1/days)	Ylast (mm)	Life (days)
7448	1	Left	-0.00085	28.360	401
7448	3	Left	-0.00076	28.640	437
7448	4	Left	-0.00081	28.480	415
7449	2	Left	-0.00082	28.280	404
7449	4	Left	-0.00076	28.720	439
7476	1	Right	-0.00081	30.150	341
7476	2	Right	-0.00083	30.050	327
7476	3	Right	-0.00077	29.920	343
7476	4	Right	-0.00082	30.160	338
7477	1	Left	-0.00077	30.210	357
7477	2	Left	-0.00077	30.070	349
7477	2	Right	-0.00042	31.580	695
7477	3	Left	-0.00054	31.060	532
7477	4	Left	-0.00073	30.410	380
7477	4	Right	-0.00042	31.640	701
7478	1	Left	-0.00080	30.260	347
7478	2	Left	-0.00058	30.310	453
7478	3	Left	-0.00082	30.320	343
7478	4	Left	-0.00075	30.360	370
7479	2	Left	-0.00083	27.940	240
7479	3	Left	-0.00069	28.960	327
7480	1	Left	-0.00085	30.360	336
7480	3	Left	-0.00075	30.250	366
7480	4	Right	-0.00042	31.430	689
7501	1	Left	-0.00052	30.160	495
7503	3	Left	-0.00053	30.410	506
7505	4	Right	-0.00057	29.840	545
7511	1	Right	-0.00062	29.310	488
7511	2	Left	-0.00069	28.420	413
7511	3	Left	-0.00072	28.190	390
7512	1	Right	-0.00062	29.050	475
7513	1	Right	-0.00067	28.730	435
7513	2	Left	-0.00073	28.150	385
7514	1	Right	-0.00058	29.540	525
7514	3	Right	-0.00062	29.020	473
7515	2	Left	-0.00067	29.160	459
7515	4	Left	-0.00063	29.340	484
7541	1	Right	-0.00106	27.450	322
7541	2	Right	-0.00077	28.860	432
7541	3	Right	-0.00087	28.450	388
7541	4	Right	-0.00074	28.980	447
7542	1	Right	-0.00088	28.360	383
7542	2	Right	-0.00081	28.250	393
7542	3	Right	-0.00078	28.690	421

Vehicle No.	Car Axle	Car Side	k (1/days)	Ylast (mm)	Life (days)
7542	4	Right	-0.00059	29.800	557
7545	1	Left	-0.00060	29.110	437
7545	2	Left	-0.00079	28.030	314
7545	2	Right	-0.00086	27.490	278
7547	2	Right	-0.00095	28.920	247
7548	4	Left	-0.00065	29.330	504
7550	2	Right	-0.00082	29.450	298
7550	4	Right	-0.00098	28.890	240
7551	1	Left	-0.00056	29.590	437
7552	1	Left	-0.00059	28.750	369
7552	3	Left	-0.00055	29.740	453
7555	2	Right	-0.00054	29.140	418
7558	1	Right	-0.00069	28.570	409
7560	1	Left	-0.00075	28.230	272
7565	2	Left	-0.00069	29.420	483
7565	3	Left	-0.00057	30.000	578
7565	4	Left	-0.00057	30.170	584
7567	2	Left	-0.00079	29.150	466
7568	3	Left	-0.00066	29.630	539
7568	4	Left	-0.00069	29.430	512
7570	1	Left	-0.00076	29.140	474
7570	2	Left	-0.00077	29.280	478
7570	3	Left	-0.00091	28.390	406
7570	4	Left	-0.00065	29.850	551
7572	4	Right	-0.00067	28.730	326
7574	2	Right	-0.00076	27.970	261
7574	4	Right	-0.00054	29.020	405
7575	1	Left	-0.00067	28.510	315
7575	3	Left	-0.00058	29.290	401
7576	1	Right	-0.00074	28.390	299
7576	2	Left	-0.00060	28.410	350
7576	3	Right	-0.00105	27.660	279
7576	4	Left	-0.00077	27.560	321
7576	4	Right	-0.00062	28.290	403
7577	1	Left	-0.00092	28.850	274
7578	1	Left	-0.00077	28.700	303
7578	1	Right	-0.00074	28.190	289
7579	2	Right	-0.00070	28.760	328
7579	3	Left	-0.00074	29.900	366
7579	4	Right	-0.00059	29.100	394
7580	1	Left	-0.00085	27.770	244
7580	2	Right	-0.00081	28.680	291
7580	3	Left	-0.00099	27.100	196
7580	4	Right	-0.00088	28.500	268

Vehicle No.	Car Axle	Car Side	k (1/days)	Ylast (mm)	Life (days)
7581	3	Left	-0.00085	28.830	267
7582	3	Left	-0.00057	30.710	480
7584	1	Left	-0.00078	29.150	298
7585	2	Left	-0.00070	26.860	224
7585	2	Right	-0.00066	26.590	218
7585	4	Left	-0.00058	28.210	339
7585	4	Right	-0.00056	27.520	303
7811	1	Right	-0.00068	29.560	487
7811	2	Right	-0.00060	29.730	539
7811	3	Left	-0.00075	28.330	405
7811	3	Right	-0.00093	28.190	358
7811	4	Right	-0.00068	29.440	483
7812	1	Right	-0.00071	29.340	467
7812	2	Right	-0.00068	29.600	492
7812	3	Right	-0.00062	29.920	537
7812	4	Right	-0.00064	29.840	524
7813	1	Right	-0.00089	28.340	372
7813	2	Right	-0.00057	30.110	574
7813	3	Right	-0.00069	29.460	480
7814	1	Right	-0.00081	28.460	394
7814	3	Right	-0.00097	28.470	362
7814	4	Right	-0.00068	29.160	469
7815	1	Left	-0.00057	30.250	589
7815	2	Left	-0.00095	28.190	355
7815	3	Left	-0.00055	30.180	595
7815	4	Left	-0.00099	28.360	354
7816	1	Left	-0.00069	30.050	529
7816	1	Right	-0.00073	28.820	455
7816	2	Left	-0.00089	28.810	412
7816	2	Right	-0.00080	28.890	435
7816	3	Left	-0.00064	29.910	544
7816	4	Left	-0.00090	28.860	411
7817	1	Right	-0.00083	28.870	428
7817	3	Right	-0.00079	29.970	487
7817	4	Left	-0.00070	28.890	468
7818	1	Right	-0.00089	29.010	418
7818	2	Right	-0.00061	30.260	578
7818	3	Right	-0.00067	30.240	546
7818	4	Right	-0.00065	30.650	578
7819	1	Right	-0.00092	29.030	413
7819	3	Left	-0.00084	28.560	412
7819	3	Right	-0.00097	28.990	401
7819	4	Right	-0.00062	30.440	587
7820	1	Right	-0.00082	29.360	450

Vehicle No.	Car Axle	Car Side	k (1/days)	Ylast (mm)	Life (days)
7820	2	Right	-0.00057	30.710	631
7820	3	Right	-0.00074	30.160	515
7820	4	Right	-0.00063	30.230	568
7821	1	Right	-0.00076	29.610	480
7821	2	Left	-0.00087	28.140	389
7821	2	Right	-0.00068	29.780	519
7821	3	Right	-0.00114	27.770	336
7821	4	Left	-0.00087	28.170	390
7821	4	Right	-0.00065	30.490	572
7849	1	Right	-0.00071	29.720	525
7849	4	Right	-0.00061	30.300	605
7850	1	Left	-0.00068	29.650	531
7850	4	Left	-0.00071	29.220	498
7851	2	Left	-0.00097	28.440	401
7852	2	Left	-0.00096	28.120	390
7853	2	Left	-0.00084	28.520	429
7853	4	Left	-0.00073	29.070	485
7854	4	Left	-0.00089	28.300	409
7860	1	Right	-0.00077	28.870	426
7860	3	Right	-0.00083	28.690	403
7861	2	Left	-0.00070	29.600	486
7861	4	Left	-0.00080	29.120	429
7862	2	Left	-0.00080	28.820	414
7862	4	Left	-0.00074	29.140	447
7863	2	Left	-0.00070	29.160	465
7863	4	Left	-0.00087	28.670	391
7864	2	Left	-0.00076	28.750	423
7864	4	Left	-0.00070	29.290	468
7865	2	Left	-0.00083	28.890	411
7865	4	Left	-0.00080	28.760	413
7877	1	Left	-0.00061	30.440	593
7877	2	Left	-0.00098	28.490	386
7877	3	Left	-0.00058	30.690	627
7877	4	Left	-0.00079	29.610	475
7878	1	Left	-0.00064	30.500	580
7878	2	Left	-0.00088	28.800	417
7878	3	Left	-0.00073	30.150	521
7878	4	Left	-0.00077	29.470	475
7879	1	Left	-0.00058	30.580	624
7879	2	Left	-0.00071	30.130	529
7879	3	Left	-0.00058	30.420	611
7879	4	Left	-0.00069	29.990	529
7880	1	Left	-0.00080	29.210	453
7880	2	Left	-0.00094	28.480	392

Vehicle No.	Car Axle	Car Side	k (1/days)	Ylast (mm)	Life (days)
7880	3	Left	-0.00058	30.670	626
7880	4	Left	-0.00069	30.410	549
7881	1	Right	-0.00067	30.040	541
7881	2	Right	-0.00066	30.480	567
7881	3	Right	-0.00069	30.110	534
7881	4	Right	-0.00065	30.310	566
7888	1	Right	-0.00053	30.650	637
7888	2	Right	-0.00051	31.160	687
7888	3	Right	-0.00062	30.550	569
7888	4	Right	-0.00055	30.450	610
7889	1	Right	-0.00076	29.740	463
7889	2	Right	-0.00057	30.640	604
7889	3	Right	-0.00057	30.760	613
7890	1	Right	-0.00063	30.130	538
7891	1	Right	-0.00073	29.750	478
7891	3	Right	-0.00062	30.520	568
7892	2	Left	-0.00077	29.510	451
7892	4	Left	-0.00077	29.360	443
7902	1	Left	-0.00052	29.610	454
7902	1	Right	-0.00053	28.710	396
7902	2	Right	-0.00080	28.540	280
7902	3	Right	-0.00069	29.050	338
7909	1	Right	-0.00112	27.720	310
7909	2	Right	-0.00058	30.470	586
7909	3	Right	-0.00087	29.080	400
7919	1	Left	-0.00082	28.930	288
7919	2	Left	-0.00049	29.150	450
7919	3	Left	-0.00069	29.470	358
7919	4	Left	-0.00050	29.120	444
7921	2	Right	-0.00059	29.620	403
7921	4	Right	-0.00070	29.170	328
7925	1	Left	-0.00095	28.710	248
7925	2	Left	-0.00071	28.260	286
7925	3	Left	-0.00086	29.430	295
7935	2	Right	-0.00069	29.040	346

ABOUT THE AUTHORS

Kyle Ebersole, MCE

Originally from Jackson, New Jersey, Mr. Kyle Ebersole is a graduate student at the University of Delaware. He is in his second year and will be graduating in June 2019 with his Master's Degree in Civil Engineering, with a concentration in Structural Engineering. Currently, Kyle is a graduate research assistant studying under Dr. Allan Zarembski in the Railroad Engineering and Safety Program. His research is focused around transit wheel wear analysis and wheel life forecasting, with applications of big data analytics. Upon graduation in June 2019, Kyle will begin working for SEPTA as an Engineer in their Management Rotational Program.

Previously, Kyle graduated Summa Cum Laude from Rowan University in May 2017, with his Bachelor's Degree in Civil and Environmental Engineering. Kyle is also a registered Engineer in Training in the state of New Jersey.

Allan M. Zarembski, Ph.D., P.E., Hon. Mbr. AREMA, FASME

Dr. Zarembski is an internationally recognized authority in the fields of track and vehicle/track system analysis, railway component failure analysis, track strength, and maintenance planning. Dr. Zarembski is currently Professor of Practice and Director of the Railroad Engineering and Safety Program at the University of Delaware's Department of Civil and Environmental Engineering, where he has been since 2012. Prior to that he was President of ZETA-TECH, Associates, Inc. a railway technical consulting and applied technology company, he established in 1984. He also served as Director of R&D for Pandrol Inc., Director of R&D for Speno Rail Services Co. and Manager, Track Research for the Association of American Railroads. He has been active in the railroad industry for over 40 years.

Dr. Zarembski has PhD (1975) and M.A (1974) in Civil Engineering from Princeton University, an M.S. in Engineering Mechanics (1973) and a B.S. in Aeronautics and Astronautics from New York University (1971). He is a registered Professional Engineer in five states. Dr. Zarembski is an Honorary Member of American Railway Engineering and Maintenance of way Association (AREMA), a Fellow of American Society of Mechanical Engineers (ASME), and a Life Member of American Society of Civil Engineers (ASCE). He served as Deputy Director of the Track Train Dynamics Program and was the recipient of the American Society of Mechanical Engineer's Rail Transportation Award in 1992 and the US Federal Railroad Administration's Special Act Award in 2001. He was awarded The Fumio Tatsuoka Best Paper Award in 2017 by the Journal of Transportation Infrastructure Geotechnology

He is the organizer and initiator of the **Big Data in Railroad Maintenance Planning Conference** held annually at the University of Delaware. He has authored or co-authored over 200 technical papers, over 120 technical articles, two book chapters and two books.

Joseph W. Palese, MCE, PE

Mr. Palese is a Senior Scientist and Program Manager of Railroad Engineering and Safety Program at the University of Delaware. He has over 28 years of experience in track component design and analysis, failure analysis and component life forecasting algorithm specifications, and development of inspection systems. Throughout his career, Mr. Palese has focused on acquiring and utilizing large amounts of track component condition data for planning railway maintenance activities.

Mr. Palese has a Bachelor's Degree of Civil Engineering, and a Master's Degree of Civil Engineering, both from the University of Delaware, along with a MBA from Rowan University. He is currently pursuing his PhD in Civil Engineering at the University of Delaware. He is a registered Professional Engineer in the state of New Jersey.